DISSERTATION

A STOCHASTIC MIXED INTEGER PROGRAM FOR MODELING WILDFIRE BEHAVIOR AND OPTIMIZING FIRE SUPPRESSION OPERATIONS

Submitted by

Erin Jean McCowen Belval

Department of Forest and Rangeland Stewardship

In partial fulfillment of the requirements

For the Degree of Doctor of Philosophy

Colorado State University

Fort Collins, Colorado

Spring 2014

Doctoral Committee:

Advisor: Yu Wei

Michael Bevers
Robin Reich
John Labadie

ABSTRACT

A STOCHASTIC MIXED INTEGER PROGRAM FOR MODELING WILDFIRE BEHAVIOR AND OPTIMIZING FIRE SUPPRESSION OPERATIONS

Wildfire suppression decisions combine multiple objectives and risk management to form a complex background against which decision makers attempt to determine efficient management actions in a short period of time. Their decisions are necessarily dynamic in nature as a sequence of random events unfolds at each fire. This dissertation presents a stochastic mixed integer program with full recourse to simulate spatially explicit fire behavior for a single fire representing a distribution of probable changes in behavior in response to weather changes. Suppression decisions and fire behavior respond dynamically to these weather events and to each other.

Initially, a deterministic mixed integer program is developed to explore how to integrate spatial fire behavior with suppression actions into a mathematical programming framework. The model uses a raster landscape. Fire behavior includes fire arrival time and fireline intensity at each cell and the minimum travel time path by which fire reached the cell. Spatially explicit fireline intensities and arrival times are dependent upon the fire spread paths, therefore fire suppression actions that change the minimum travel time path also change the fireline intensity and arrival time. Weather is modeled as constant. Test cases for the deterministic model provide examples of spatially explicit fire behavior and corresponding optimal suppression strategies for a variety of suppression levels.

Next, a stochastic mixed integer program is developed that expands upon the capabilities of the deterministic model. The stochastic model allows uncertain fire behavior to be simulated by referring to probabilistic weather decision trees. The fire behavior in the stochastic model interacts dynamically with both weather changes and suppression decisions. Constraints are included to characterize fire as ecologically beneficial or harmful based upon the fireline intensity, which allows the model to examine multiple policy objectives. A selection of

alternative policy objectives is modeled in test cases, including minimizing the total expected area burned, minimizing the expected area burned at an ecologically harmful fireline intensity, maximizing the expected area burned at an ecologically beneficial fireline intensity, and minimizing expected fireline production. Explicit nonanticipativity constraints ensure that the model produces suppression decisions that account for uncertainty in weather forecasts.

In the final model formulation, detailed fire control constraints are incorporated into the stochastic mixed integer fire growth and behavior program to model more realistic suppression decisions. These constraints account for spatial restrictions for fire crew travel and operations; for example, a crew's travel path must be continuous. Crew safety is also addressed; crews must keep a safety buffer zone between themselves and the fire. Fireline quality issues are accounted for by comparing control line capacity with fireline intensity to determine when a fireline will hold. The model lets crews work at varying production rates throughout their shifts, giving the model the flexibility to fit work assignments with the predicted fire behavior.

TABLE OF CONTENTS

Abstract ii

1 Introduction 1

1.1 Spatially Explicit, Dynamic Fire Growth and Behavior 3

1.2 Stochastic Programming Framework For Fire Growth 8

1.3 Suppression Constraints 11

2 Fire Growth Equations for a Deterministic Programming Framework 13

2.1 Introduction 13

2.2 Methods 16

2.2.1 Notation 16

2.2.2 Constraints 17

2.2.3 Objective Function 19

2.3 Results 20

2.4 Discussion 31

3 Fire Growth Equations for a Stochastic Programming Framework 33

3.1 Introduction 33

3.2 Methods 35

3.2.1 Notation 35

3.2.2 Constraints 37

3.2.3 Objective Functions 47

3.3 Results 47

3.4 Discussion 71

4 Fire Suppression Constraints for a Stochastic Programming Framework 73

4.1 Introduction 73

4.2 Methods 75

4.2.1 Notation 75
4.2.2 Constraints 76
4.2.3 Objective function 85
4.3 Results 86
4.4 Discussion 98

5 Future Work and Summary of Contributions 99

1 Introduction

Over the past decade wildland fire suppression costs have more than doubled in the United States (US). Appropriations from the US Congress for wildfire suppression averaged 2.9 billion dollars annually from 2001-2007, as compared to 1.2 billion from 1996-2000 (US GAO 2009a). This has led the US Government Accountability Office (GAO) to call repeatedly for the US Department of Agriculture Forest Service (the Forest Service) to develop cost effective firefighting strategies (US GAO 2009a). The GAO criticized all five firefighting agencies (the Forest Service and four agencies from the US Department of Interior: the Bureau of Land Management, the National Park Service, the Fish and Wildlife Service, and the Bureau of Indian Affairs) in 2007, stating "that officials in the field have few incentives to consider cost containment ... and that ... the lack of a clear measure to evaluate the benefits and costs of alternative firefighting strategies fundamentally hindered the agencies' abilities to provide effective oversight" (US GAO 2009b). In 2009, the agencies still had not adopted any measures to evaluate alternative firefighting strategies (US GAO 2009b).

Cost is only one of many issues forest managers must consider when fighting forest fires. Environmental values to consider include providing recreational opportunities, production of timber, protection of wilderness and wildlife, and providing high water quality (US GAO 2009a). Other values at risk in a fire can include residential houses, important infrastructure, high value cultural sites, and even lives of both the fire fighters and civilians. Wildfire suppression decisions combine multiple objectives and risk management to form a complex background against which decision makers attempt to determine efficient management actions in a short period of time.

In this dissertation, over the course of three developmental steps, I present a mathematical program to model a single wildfire's growth and the corresponding optimal fire suppression decisions. This model is capable of configuring optimal firefighting strategies and examining the implications of multiple objectives in a risk management framework. The goal of this work is to produce a working set of mathematical equations to simulate stochastic, spatially

explicit fire behavior that dynamically interacts with detailed fire suppression decisions. This chapter will introduce the reader to the problem I addressed, review the pertinent literature, identify the contributions of this work, and provide a broad overview of the modeling strategies used.

This dissertation is formatted so each chapter tests specific issues. Chapter 2 presents constraints for a mixed integer program that can model spatially explicit fire behavior on a raster landscape. Weather is assumed to be constant for the duration of the fire. In this chapter, suppression decisions are modeled using "control points." When a control point is placed in a flammable cell, that cell acts as a barrier to the fire. Test cases are examined using maps of the fire arrival times, spread directions, and fireline intensities at each cell. The initial test cases do not allow any suppression on the landscape in order to focus on properties of the simulated fire behavior. Varying numbers of control points are then added to show how efficiently allocated control points can control fire spread.

Chapter 3 builds on the fire behavior model from Chapter 2 by relaxing the assumption that weather is known and constant for the duration of a fire. The model uses multiple probabilistic weather forecasts with multiple weather changes using a stochastic branching weather tree to examine random variation in fire behavior. In Chapter 3, fire behavior responds dynamically to weather changes by assigning multiple sets of behavior parameters to each weather scenario. Control points are again employed as a simplified form of fire suppression to test if fire spread is reacting dynamically to suppression actions and if the model is efficiently allocating control points. The control points used in Chapter 3 are more nuanced than the control points in Chapter 2; in the stochastic model, control points can be allocated to a particular location in a particular decision stage, so the model can control both the location and the timing of suppression placement. The model is sensitive to changes in the objective function, so test cases are presented that provide examples of changes in optimal control point placements for different objective functions. Nonanticipativity constraints, which force the model to produce control point placements at the beginning of each decision

stage before the weather uncertainty is resolved, are introduced in this chapter and they highlight how the stochastic model can produce more robust solutions than its deterministic counterpart.

The control points used in Chapters 2 and 3 to test how fire behavior interacts with suppression decisions do not model key components of fireline production. Chapter 4 introduces a "control network" which can be seamlessly integrated with the fire behavior model from Chapter 3 to replace the control points. This control network accounts for spatial restrictions on fire crew movements, safety restrictions on fire crew actions, and issues related to fire behavior and fireline quality. Test cases focus on the response of the control network to different stochastic fire scenarios, demonstrating the effects of incorporating explicit nonanticipativity constraints into crew actions.

Throughout Chapters 2-4, the landscape used to produce results is held constant. I use a 6x6 raster grid to represent a small, flat, homogeneous landscape. The weather scenarios are also consistent throughout; two sets of fire parameters are used (a slower spreading fire and a faster spreading fire) and three major fire spread directions (northeast, north, and east). The parameters are based on simulations of a fire spreading through uniform grass and shrubs on flat ground in the Black Hills of South Dakota. For stochastic simulations, I assume all weather scenarios are equally likely.

Chapter 5 addresses the future work necessary to adapt this model to operational use including scaling the model up, solution times, additional fire behavior, and producing stochastic weather forecasts. In this proof of concept study, fire behaviors such as spotfires and reburns are not modeled.

1.1 Spatially Explicit, Dynamic Fire Growth and Behavior

Mathematical models have been used to support wildland fire decisions for many years. A fundamental part of this problem involves providing spatially explicit forecasts of fire growth and behavior. A large set of models that focus on predicting spatially explicit fire behavior

currently exist. These models predict rate of fire spread, fireline intensity, flame length, probability of crown fire, fuel consumption, etc (Andrews 2007). Typical parameters that must be specified to use these models include fuel characteristics (fuel type, spatial distribution, and moisture content), weather (surface wind speed, wind direction, min and max temperature, min and max humidity, precipitation, and cloud cover), and topography (elevation, slope and aspect) (Andrews 2007). Originally, fire behavior models predicted one dimensional fire behavior: i.e., the rate of spread in one direction and the fire behavior corresponding to that rate of spread (Rothermel 1972). These one dimensional fire predictions were extended into two dimensions by modeling fires as parametric shapes. Simple ellipses work particularly well to represent a single fire on a homogeneous landscape (Alexander 1985). These one dimensional and two dimensional models for a homogeneous landscape still underlie the fire models in use today, which are now capable of modeling two dimensional fire spread on a heterogenous landscape (Andrews 2007).

There are several types of model that have been used to simulate fire spread across a heterogeneous landscape. These models can be categorized into raster based or vector based; raster based models assume a landscape is discretized into homogeneous cells while vector based models draw information from points on the landscape. The raster based models assume fire spread characteristics can be calculated for each cell individually (Kourtz and O'Regan 1971). These heterogenous fire spread predictions are often based on the models originally developed for homogeneous landscapes (Andrews 2007). For example, cellular automata simulations are rule based modeling systems, where each cell on the landscape has a state (i.e, burned, unburned, burning). These states change based on the states of neighboring cells and the transition rates at which the cells change states are determined by the fire spread rates (Alexandridis et al. 2011). Minimum travel time (MTT) fire spread models, like cellular automata models, are based upon a raster landscape. Given an ignition on the landscape, MTT models test many different possible fire spread paths to each of the other cells on the landscape. Only the shortest possible spread time is recorded for each cell

(Kourtz and O'Regan 1971, O'Regan et al. 1976, Finney 2002). Rasterized landscapes are not required to model fire behavior on a heterogeneous landscape. For example, Huygens' wave principle is a commonly used method for predicting fire behavior that does not require a raster landscape (but can use one) in which a known fire perimeter is split into discrete points and from each of these points a new fire is propagated for a specified period of time. The fires simulated at each discrete point assume homogeneous conditions. The perimeters of each of the small fire footprints are then combined and smoothed to make one large fire footprint. If fire behavior predictions are desired further into the future, then the new fire footprint is again divided into many discrete points and the process repeats (Finney 2004).

Mathematical programs have been developed in the past for use as a decision support tools by fire managers. Of the mathematical programs that currently exist, most are quasi-spatial; they include spatial characteristics of the fire (for example, fire perimeter and/or area burned) but do not include explicitly spatial fire growth in the model. Many of these models examine dispatching and deployment decisions. For example, Parks (1964) built one of the first mathematical models to examine optimal fire suppression decisions, which determined optimal levels of suppression for initial attack on single fires. The only spatial information used in the model was fire area and rate of fire area growth. Wiitala (1999) also addressed optimal dispatch for initial attack but used a dynamic program that needed fire perimeters, rates of growth, and fire areas as the spatial components of fire, but also did not use spatially explicit information. Donovan and Rideout (2003) built a deterministic integer programming model to determine the optimal set of resources that should be dispatched to a single fire for initial attack while minimizing the cost of the resources plus the damage from the fire. Their model also uses fire perimeter and area burned but, again, does not include explicitly spatial fire growth. An extension of this model is presented by Hu and Ntaimo (2009). They integrate Donovan and Rideout's dispatching model into a spatially explicit stochastic simulation of fire growth and fireline construction. A daily deployment and dispatching optimization model was developed by Haight and Fried (2007) using a scenario

based standard response model which was used to examine tradeoffs between the number of suppression resources available and the number of fires that did not get a standard response. The spatial data needed in the model is limited to fire perimeter, which is used in determining if a fire escapes initial attack or not. Kirsch and Rideout (2003) developed a mixed integer programming model to examine the tradeoffs between initial attack effectiveness and budget. They simulate multiple fire ignitions and optimize containment decisions for each fire while minimizing the value of the area that burns. Again, the model only includes quasi-spatial information (Kirsch and Rideout 2003).

Another fire suppression problem that has been addressed by the use of mathematical programming is optimal air tanker location assignments. Two mixed integer programs were developed by Hodgson and Newstead (1978) to find the optimal placement of air tanker bases in Alberta, the first maximizing the number of fires within range of each base and the second minimizing the mean distance between fires and the bases. No spatial information about single fires was used except the distance between the fire and the air bases. Chow and Regan (2011) addressed a similar problem as Hodgson and Newstead (1978); they wanted to determine where to station air tankers for initial attack availability. Their chance constrained dynamic relocation problem also only required spatial information about the distance between the fires and bases.

Some mathematical models have been constructed to incorporate explicitly spatial fire behavior. Hof et al. (2000) built a mixed integer program to optimize suppression decisions to slow fire headed towards a high value area of land. Using a gridded landscape, the goal of the program is to maximize the amount time before fire reached the protected area. The constraints smallest possible fire arrival time at each cell. These constraints only calculate fire arrival time correctly because they work counter to the objective function; the goal is to slow fire and the constraints force fire to arrive at the fastest possible time for all binding burning paths. However, the fire arrival times may not be calculated correctly for non binding paths. Another example of MTT fire arrival times being embedded in an mixed integer program is

presented by Wei et al. (2011). They built a mixed integer program to optimize suppression placement decisions on large fires. Their fire arrival time constraints were based on the same assumptions as Hof et al. (2000) and for their suppression problem the incorrect arrival times for non binding fire spread paths was an issue. To adjust any incorrect fire arrival times the optimization program was run twice, once to get optimal suppression placement and second to correct the non binding arrival times. The model built by Wei et al. (2011) minimizes the value lost due to the fire. Neither of the models built by Hof et al. (2000) or Wei et al. (2011) track any spatially explicit fire behavior beyond fire arrival time.

This dissertation will present two models of fire spread, one deterministic and one stochastic. Both models track spatially explicit fire behavior which interacts dynamically with suppression actions. As a significant improvement on Hof et al. (2000) and Wei et al. (2011), both the deterministic and stochastic fire behavior models presented in this dissertation track exactly which paths between cells produce the MTT spread paths. Knowledge of the MTT spread paths allows for accurately calculating the fireline intensity and the detrimental or beneficial effect of fire at a specific location on a landscape.

Fireline intensity is a fire behavior characteristic that informs managers how much heat a fire releases per unit length of fire perimeter per unit time (for example, BTU/ft/sec). This characteristic can be used as a proxy for several important factors in fire management. For example, fireline intensity can be related to the likelihood of fire crossing a fireline (Hirsch et al. 1998) or how long it takes to build a section of fireline (Holmes and Calkin 2013). Therefore, tracking fireline intensity can greatly expand the accuracy, realism, and possible uses of a mathematical program that models fire behavior. Because both mathematical programs presented in this dissertation explicitly track fire spread paths, they can also track fireline intensity.

The capability of the models presented in this dissertation to track spatially explicit fire behavior that interacts with landscape features and suppression control points is primarily examined in Chapter 2. Chapter 3 builds upon the model in Chapter 2 and relies on the

spatially explicit, dynamic fire behavior, but does not focus on presenting and examining the model's fire behavior prediction capabilities. Rather, Chapter 3 focuses on the extra dynamic aspect of fire behavior prediction added by modeling stochastic weather scenarios.

1.2 Stochastic Programming Framework For Fire Growth

First proposed by Dantzig in 1955, stochastic programming has become a standard risk management tool (Dantzig 2002). Stochastic programming is an extension of linear programming that seeks to incorporate uncertainty into the decision making process. A stochastic program is typically organized into two or more decision stages (Birge and Louveaux 1997). Each stage of the problem involves decisions that must be made before the outcomes of uncertain events are known and these earlier decisions influence the decisions made in later stages. Stochastic programming models enforce the condition that earlier decisions must be consistent across multiple future scenarios. This property is called "nonanticipativity," i.e., the program is not allowed to anticipate the outcome of the unknown events. The follow up decisions, made once the outcome of the uncertainty is known, are called recourse decisions. The ability to model nonanticipative and recourse decisions produces better quality early stage decisions than a deterministic program, especially in cases where different outcomes may dramatically influence the first stage decisions. Stochastic programs may be formulated using probabilistic scenarios that represent the range of uncertainty in the problem's parameters (Birge and Louveaux 1997).

Predicting fire behavior depends heavily on weather forecasts, which are not known with certainty. Fire suppression actions must be taken before future fire behavior is known. These suppression actions must be successful regardless of the actual manifestation of fire behavior. Therefore, the initial assignment of fire suppression resources can be viewed as the first stage decisions in a stochastic program. Follow up suppression actions can be viewed as recourse decisions. Designed properly, a stochastic programming model should simulate stochastic fire growth, suppression tactics, and the interaction between the suppression decisions and

fire growth while optimizing fire suppression strategies to meet a manager's stated goals. In order to produce such a model, constraints must be developed that can predict stochastic fire behavior.

Stochastic fire behavior has been the subject of numerous studies. For example, FSPro, which is one of the fire growth simulators supported by the Forest Service, allows fire managers to examine stochastic fire growth (Andrews 2007). FSPro uses stochastic weather streams to create probabilistic fire footprints. A time series process is used to generate temporally correlated weather predictions. Fire behavior is then calculated for thousands of different weather scenarios (using an MTT algorithm) and the results of these scenarios are compiled to make probabilistic fire footprints (Finney et al. 2011). Boychuk et al. (2009) designed a continuous time Markov chain on a spatial lattice to compute fire spread probabilistically. Their fire behavior predictions include growth due to spotting, which is modeled as a random process that depends on three main factors: firebrand production; length the firebrand burns (exponential distribution); and if the firebrand does land on fuel, whether the fuel catches fire or not (Bernoulli distribution). Stochastic fire spread rates are calculated for each cell using random draws from an exponential distribution (Boychuk et al. 2009). Alexandridis et al. (2011) developed another example of a model that calculates stochastic spread rates independently for each cell on a raster landscape. This lattice based cellular automata model makes stochastic fire spread predictions using the probability of fire transmission between cells. This probability is developed based upon vegetative density, vegetation type, wind field characteristics, slope, vegetation moistures, and vegetation height. Spotting is added using the combination of a Poisson variable that determines when spotting takes place and a conditional probability that a cell will ignite given that spotting does take place. Alexandridis et al. (2011) include a simulation of air tanker suppression tactics in their model. Air attacks are modeled using a Poisson distribution determining if an air attack takes place on a cell and the probability that fire will be extinguished in a cell if an air attack does indeed take place. The DEVS-FIRE model developed by Ntaimo et al.

(2004) is also cellular and calculates stochastic spread rates between cells. The spread rates are made stochastic by allowing uncertain parameters to be drawn from arbitrary probability distributions. A totally different type of model is presented by Mandel et al. (2006); they developed a wildfire growth model comprised of coupled differential equations based on balance equations for energy and fuel. An ensemble Kalman filter integrates these equations with real data. This data assimilation method incorporates data in real time and is capable of achieving accurate results faster than real time, even with erroneous initial ignition placement.

Of all the stochastic fire spread models listed above, only one has been used in a stochastic program to optimize suppression resource assignments. Ntaimo et al. (2013) built an integrated fire simulation-optimization routine that simulates spatially explicit stochastic fire growth, which is then used in a two stage stochastic model. Deployment decisions are modeled as the first stage decisions and dispatch is modeled as the second stage decisions. Suppression tactics are not spatially optimized and there is no interaction between fireline production and fire growth. The model developed by Ntaimo et al. (2013) was built to optimize deployment decisions. My model will focus on a different part of the fire suppression problem: optimizing spatially explicit suppression decisions on a single fire.

A set of stochastic programming constraints is developed in Chapter 3 that allows fire behavior predictions to respond to weather changes within a weather scenario. These constraints are also capable of modeling probabilistic fire behavior. The constraints allow the fire behavior to dynamically interact with suppression actions, so that the stochastic fire behavior can be seamlessly integrated with fire suppression constraints. The fire suppression constraints that incorporate multiple aspects of fireline production are then developed in Chapter 4.

1.3 Suppression Constraints

Models that examine fire suppression are also important for fire managers. While both fire growth and fireline construction models play an important role in wildfire management, they provide more nuanced information when they can interact with each other.

Of the fire suppression optimization models that currently exist, very few account for the interaction between fireline production and fire growth. Parks (1964), Donovan and Rideout (2003), and Kirsch and Rideout (2003) do not account for the interaction between fire growth and fireline production at all. Hu and Ntaimo (2009) do account for the interaction between fireline production and fire growth, but in simulation program rather than a mathematical program. Wei et al. (2011) does account for the interaction between fire growth and fire suppression but is not stochastic.

Other models that are not mathematical programs have been built to model fire containment. Most notably, Fried and Fried (1996) developed a simulation algorithm to explicitly account for the interaction between fireline production and fire growth, i.e, that the fire growth is hampered by fireline production. Their model has been used in several operational programs including CFES (a fire suppression budgeting model for California) and FPA (a fire suppression budgeting model for the US) (Fried and Fried 2010). While the model developed by Fried and Fried (1996) does account for the interaction between fireline production and fire growth, it is typically implemented in a quasi-spatial manner, where the fire is assumed to take the shape of an ellipse and burns on a homogeneous landscape (Fried and Fried 2010). More recently, HomChaudhuri et al. (2010) developed a genetic algorithm for placing wildfire suppression on a landscape. They determine a parametric shape for the containment line and then use a simulation-optimization framework to solve for the best locations for anchor points and the best path for the fire crew to take to connect the anchor points.

Another important factor in fire suppression research is quantifying fireline production rates. The most recent update of the standard crew production rates used by the Forest Service was provided by Broyles (2011). Broyles (2011) directly observed fire crews to obtain

new estimates of fireline production rates. Nine of the of the thirteen fuel models were assigned a value for the production of fireline in direct attack and indirect attack. Other research to quantify fireline productions rates includes Fried and Gilless (1989) and Hirsch et al. (1998), who used expert option surveys to determine fireline production rates. Recently, Holmes and Calkin (2013) attempted to quantify econometric relationships between fireline production rates with the level of suppression input using data gathered from large wildland fires in the US in 2008. While these are important studies that can help parameterize fire suppression models, they do not examine the spatially explicit interactions between fireline production and fire behavior.

None of the previous studies integrate explicitly spatial, stochastic fire behavior with an explicitly spatial suppression decisions that account for crew movement, crew safety, line production, and line quality. The deterministic and stochastic fire behavior models presented in Chapters 2 and 3 integrate suppression decisions using "control points" which model the placement of suppression resources on the landscape. These control points are used to test fire behavior interactions with suppression decisions. A more advanced model of suppression, called a "control network," is introduced in Chapter 4. The control network models suppression placement, ensuring that crews move on the landscape in a continuous path. Suppression timing is also modeled; the constraints require the suppression activities to be finished in a cell before the fire reaches that cell. Crew safety is accounted for using a variable safety buffer, which the crews must keep between them and the fire. Lastly, constraints ensure that the quality of fireline is high enough to withstand the fireline intensity or suppression will not be successful. The control network provides a nuanced and realistic model for suppression decisions which can be integrated with the stochastic fire spread model.

2 Fire Growth Equations for a Deterministic Programming Framework

2.1 Introduction

In this chapter I present a set of equations to model fire behavior in a mixed integer programming framework. Developing a set of deterministic fire behavior constraints allows mathematical concepts to be examined in a simpler context before extending them to a more complex stochastic environment. Many of the equations developed for the deterministic model carry over to the stochastic model.

There are three main components that determine fire behavior: the landscape topography (elevation, slope and aspect), the fuels on the landscape (fuel type, spatial distribution, and moisture content), and the weather (surface wind speed, wind direction, min and max temperature, min and max humidity, precipitation, and cloud cover). All three of these components of fire spread are incorporated into one set of fire behavior parameters and thus differing weather conditions appear in the model as differing fire behavior parameters. While the stochastic model presented in Chapter 3 allows variable weather probabilistic fire behavior parameters over the course of a fire, the model developed in this chapter assumes only one set of fire behavior parameters and assumes that the weather is constant for the entire length of the fire.

The constraints in the model can be categorized into three main groups: spatial relationships, fire arrival time calculations, and fireline intensity calculations. The constraints that define spatial relationships determine where fire is allowed to spread throughout the landscape. The landscape data is discretized into homogeneous square cells. A node is located at the center of each cell and fire can spread from node to node based on the spatial relationships between the cells (see Figure 2.1). These relationships follow the example of previous studies (e.g. Alexandridis et al. 2011, Ntaimo et al. 2004) as they allow fire to spread between cells that share an edge or a vertex. I based this work on raster data because most spatial data currently being used in fire management is in raster form; however, the model

itself is not dependent on using raster based data and the landscape could be divided into cells shaped as any regular polygon. For example, hexagonal or triangular cells could be used. The area within each cell is assumed to be homogeneous with respect to fuels and topography so fire is assumed to spread at a constant rate across each cell.

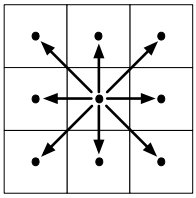

Figure 2.1: The node associated with each raster cell is assumed to be connected to the nodes of neighboring cells with which it shares an edge or vertex. This image shows an example using square raster cells (as was used in the testing of this model).

The fire arrival time constraints in this model are based on minimum travel time (MTT) concepts. When fire is traveling over a landscape, it often has several routes that it can take to reach a cell and it may be traveling along multiple routes simultaneously. Typically fire managers are most interested in the first time fire arrives at a node. This is reflected in MTT algorithms, which assume fire always takes the fastest possible path and each node receives fire from at most one neighboring node, thus, MTT models are only concerned with the first time fire arrives at each node. MTT algorithms are computationally efficient and have been used in fire spread simulations in the past (Finney 2002). While other MTT models can examine multiple paths from neighbors further away than the nodes that border each other (e.g. Finney 2002), I only examine fire spread from neighbors that share an edge or vertex in this study.

Fire arrival time is not the only fire behavior of interest to fire managers. For example, fireline intensity predicts how much heat will be released by the fire over a unit length per unit time, i.e., how many BTU will be released by one foot of fireline per second. The constraints that calculate fireline intensity in this model consider the direction that the fire is traveling when reporting the fireline intensity. For example, a fire going down a hill is likely

to be less intense than a fire going up the same hill, and a fire moving the same direction as the wind is likely to be more intense than a fire moving against the wind. These constraints become important when multiple objectives like safety, line quality, and ecological objectives are incorporated into the model.

Control points are incorporated into the model to test fire behavior response to control activities. If a control point is placed in a node, then the node becomes nonflammable. Therefore, nonflammable nodes and nodes with control points in them act identically in the model, except that nonflammable nodes are predetermined during the model parameterization process while control point locations are determined in the model's optimal solution. Control points exist in this chapter as a simple way to test the response of fire behavior to control activities. A control network incorporating more realistic fire suppression considerations beyond individual control points is not developed until Chapter 4.

An optimal solution to the mathematical optimization program will report the fire arrival times and fireline intensities for each node, along with the fire spread directions. Fire growth is calculated independently of the objective function. That is, the constraints form a convex hull suitable for use with objective functions that treat fires as either desirable or undesirable. This is important because fire behavior does not change depending on a manager's goals, rather it changes because of actions the fire manager chooses to take. Thus, the fire behavior can be changed only by suppression actions, which must be guided by various objective functions. In this model, if suppression resources are allocated to a node by the optional solution selecting that node as a control point, then that node is no longer able to spread fire to its neighbors. There is no time limit for fire growth predictions in this model; either the fire is successfully contained by surrounding all burning nodes with suppression resources or it escapes off at least one edge of the landscape.

2.2 Methods

2.2.1 Notation

The notation used in the model is presented below. In this dissertation, capital Arabic letters are used to represent decision variables, lower case Arabic and Greek letters indicate parameters, and capital Greek letters represent sets. The only exception to this is "big M," which is a standard parameter used in logic constraints to force if-then scenarios to hold.

Decision Variables:

D_i	binary indicator: $D_i = 1$ indicates node i burned
Y_i	binary indicator: $Y_i = 1$ indicates a control point has been placed in node i
$B_{j,i}$	binary indicator: $B_{j,i} = 1$ indicates that the MTT travel path for fire spreading into node i was from node j
F_i	fire arrival time in node i
I_i	fireline intensity in node i

Parameters:

n_i	number of cells bordering node i
b_{ji}	amount of time it takes fire to spread from cell j to node i
κ_{ji}	intensity of fire in node i if fire spreads from node j to i
κ_i	intensity of fire in node i if node i contains an ignition point
x_i	binary indicator that node i contains an ignition point
ξ_i	binary indicator that node i is nonflammable
f_i	ignition time for node i (only available if $\xi_i = 1$)
M	a relatively large number ("Big M")
Ω_i	the set of cells from which fire can spread to cell i

Other:

Ω_i	the set of nodes from which fire can spread to node i

2.2.2 Constraints

Spatial Relationship Constraints

The four constraints defining the spatial connections between the nodes are listed below.

$$D_i \leq 1 - \xi_i \qquad \forall \quad i \tag{2.1}$$

$$D_i + Y_i + \xi_i \geq \frac{1}{n_i} \sum_{j \in \Omega_i} D_j \qquad \forall \quad i \tag{2.2}$$

$$\sum_{j \in \Omega_i} B_{ji} = D_i - x_i \qquad \forall \quad i \tag{2.3}$$

$$B_{ij} \leq D_i \qquad \forall \quad i, j \in \Omega_i \tag{2.4}$$

Equation 2.1 allows each node i to burn if node i is flammable but never allows node i to burn if node i is nonflammable (if a cell is non-flammable then the parameter ξ_i is set to one). If node j (a neighbor to node i) burns, then node i must burn unless a control point has been located in node i or node i is non flammable (Equation 2.2). If node i burns and there was no ignition point at the node, then Equation 2.3 ensures that node i be ignited by exactly one neighboring node. Equation 2.4 guarantees that a node i can only ignite a neighbor if node i is on fire.

Fire Arrival Time Constraints

The following equations act as MTT constraints: the program is parameterized with the time it takes fire to spread from all nodes into each of their neighbors and can consequently calculate all the possible arrival times for each node. The program must choose the earliest fire arrival time as the only fire arrival time that it records, and the earliest spread time the determines the MTT spread path. This fire arrival time determines the fastest spread path, which is also the only spread path recorded for the fire.

The three fire arrival time constraints are shown below:

$$F_i = f_i \qquad \forall \quad \{i|x_i = 1\} \tag{2.5}$$

$$F_i \leq F_j + b_{ji} + M(1 - D_j) \qquad \forall \quad i, j \in \Omega_i \tag{2.6}$$

$$F_i \geq F_j + b_{ji} - M(1 - B_{ji}) \qquad \forall \quad i, j \in \Omega_i \tag{2.7}$$

Equation 2.5 forces the fire arrival time of nodes that contain an ignition to be equal to the ignition time. Since the only fire arrival time of interest is the first time that the node is ignited, Equation 2.6 sets the upper bound of the fire arrival time to the earliest possible fire arrival time. If Equation 2.6 is binding for cells i and j, then fire must have arrived at node i from node j. While Equation 2.6 forces the fire arrival time to less than or equal to the smallest possible time, Equation 2.7 works with Equation 2.6 to ensue the fire arrival time is equal to the smallest possible arrival time. When binding, these two equations work together to calculate the exact fire arrival times for nodes that burn, otherwise they are never binding. Thus, the fire arrival time in cells that do not burn is set arbitrarily by the solution algorithm. The arbitrarily set fire arrival times are acceptable results because the output of the model identifies cells that do not burn.

Fireline Intensity Constraint

$$I_i = \sum_j \kappa_{ji} B_{ji} + \kappa_i x_i \qquad \forall i \tag{2.8}$$

Equation 2.8 determines the fireline intensity of the fire in each cell. Therefore, the intensity in the cell is not only determined by the fuel and terrain in the cell itself, but also the MTT spread path. For example, this model may give a different fireline intensity if the fire is moving up or down a hill. Modeling fireline intensity in a dynamic fashion is a key contribution of this model. The simulation models currently used in the US do not report fireline intensity in this fashion: rather, they report the maximum fireline intensity possible.

Modeling fireline intensity in this fashion allows for future extensions of the model to use fireline intensity to create firefighter safety constraints and examine ecological objectives. It also allows suppression actions to be based on lowering fireline intensity rather than solely containing the fire. The ability to base modeled suppression actions on predicted fireline intensity is novel and will allow for the optimization of ecological fire objectives. It will also help determine if a control action is safe for fire crews and if a fireline is of high enough quality to stop the fire.

2.2.3 Objective Function

None of the constraints in Section 2.2.2 rely on an objective function to work properly. If no suppression is allowed on the landscape (i.e., $\sum_i Y_i = 0$), the solution will always be the same, regardless of the objective function. The robust nature of these fire behavior constraints allows for flexibility in the objection function design. Thus, the objective function can be chosen to examine any policy objectives. The ability to create objective functions that reflect different policies is a critical strength of the model, as examining different weighting schemes and different goals should help a manager determine how differing priorities translate into different suppression strategies.

For initial testing I used the following objective function.

$$\text{Min } Z = \sum_i D_i + \sum_i 0.1 Y_i \tag{2.9}$$

This objective function minimizes the area burned and the amount of suppression assigned, but weights one burned node to be ten times more undesirable than one node with suppression so that the fire is always controlled if possible. However, including suppression in the objective function ensures that the program has an incentive to put controls only in cells where they will accomplish something. This objective function treats all fire on the landscape is bad. In order to model fire that achieves policy objectives other than minimizing area

burned (i.e., multi-objective fires) the model's objective function will need to be adjusted. More complex objective functions are examined in Chapters 3, 4, and 5.

2.3 Results

Recall that in these test cases the landscape is homogenous; i.e., in each landscape, the fire spread parameters and the fireline intensity parameters are the same for all nodes. These simplified 6x6 node landscapes are big enough to show the details of the model solutions and small enough to keep the model from running into size issues. Model size issues will be discussed in Chapter 5.

The parameters used to obtain these results are based on a FlamMap simulation of a fire in fuel type 122 (moderate load, dry climate grass shrub) with wind speeds between 10-15 miles per hour in a low fuel moisture scenario (Scott and Burgan 2005). FlamMap calculates fire spread rates for every cell of a landscape based on Rothermel's equation and maximum fireline intensity based on Byram's fireline intensity (Finney 2004). FlamMap outputs include the major fire spread direction in each cell, the parameters of the ellipse that describes the fire shape, and the maximum fireline intensity. The eight fire spread directions of interest are shown in Figure 2.3a. Figure 2.3b shows two neighboring cells and the angles between the major spread direction and the spread direction of interest. Using the angles between the major spread direction and the actual direction of interest and the ellipse parameters that describe the shape of the fire in each cell, the rate of spread between all neighboring nodes can be calculated. This rate of spread can then be translated into the amount of time that it takes fire to spread from a node into each of its neighboring nodes. For more detail on these calculations, see Wei et al. (2011).

The fireline intensity parameters can also be derived from FlamMap output. Fireline intensity is calculated as $I = H\omega r$, where I is the fireline intensity (BTU/ft/sec, also called Byram's fireline intensity), H is the fuel heat of combustion (BTU/lbs/sec), ω is the weight of fuel consumed per unit area in the active flaming zone (lbs/ft^2), and r is the rate of spread

a.

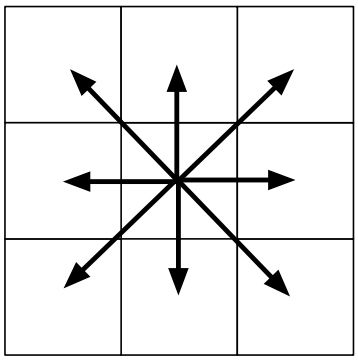

b.

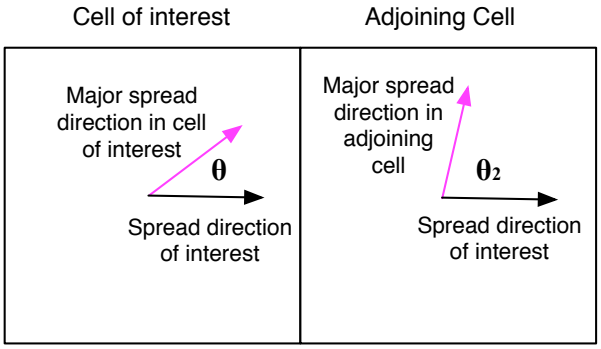

Figure 2.2: The image on the left shows all the possible fire spread directions and the image on the left shows how the rate of spread for the major spread direction is converted into a rate of spread in one of the possible fire spread directions that the model can accommodate.

(ft/sec). Because one of FlamMap's outputs is the fireline intensity for the maximum rate of spread and fireline intensity is directly proportional to rate of spread, I calculate the fireline intensity in the direction of interest as follows, given fire spreading from cell j to neighboring cell i:

$$\begin{aligned} I_i &= \text{fireline intensity for the maximum rate of spread in node } i \\ \kappa_{ji} &= \text{intensity of fire in cell } i \text{ if fire spreads from node } j \text{ to } i \\ R_i &= \text{maximum rate of speed in node } i \\ ROS_{ji} &= \text{actual rate of speed from node } j \text{ to node } i \end{aligned}$$

$$\kappa_{ji} = \left(\frac{I_i}{R_i} + \frac{I_j}{R_j} \right) \frac{ROS_{ji}}{2} \tag{2.10}$$

The calculation of parameters and the formulation of the constraint matrices and the objective function to create a mixed integer linear program (MILP) was performed in Microsoft Visual Studio using Visual Basic. The MILP was then imported into CPLEX 12.2 (a software program the contains a callable library of solution algorithms for mathematical problems) where it were solved using the default mixed integer program parameter settings. All of the test cases in this chapter could be built and solved in less than 10 seconds on a

Table 2.1: The "southwest winds scenario" set of fire behavior parameters for the deterministic mixed integer programming model. This set of parameters assumes fuel model 122 with low fuel moisture and 10 mph winds coming from the southwest.

Southwest Winds Scenario Characteristic	Value
Major Spread Direction	Northeast (45 degrees)
Max ROS	25 ft/min
Ellipse B	17.5 ft/min
Ellipse C	2.21 ft/min
Max Fireline Intensity	225.26 BTU/ft/sec

Table 2.2: The "south winds scenario" set of fire behavior parameters for the deterministic mixed integer programming model. This set of parameters assumes fuel model 122 with low fuel moisture and 10 mph winds coming from the south.

South Winds Scenario Characteristic	Value
Major Spread Direction	North (0 degrees)
Max ROS	25 ft/min
Ellipse B	17.5 ft/min
Ellipse C	2.21 ft/min
Max Fireline Intensity	225.26 BTU/ft/sec

2012 Macbook Pro through Parallels Desktop 6 with 3 GB of available RAM.

I used two sets of weather parameters to build the test cases presented in this chapter. On a homogeneous, flat landscape, the wind directions correlate directly with the major rate of spread, so a major spread direction of north means the winds must be coming out of the south. The first set of weather parameters assumes winds are out of the southwest at 10 miles per hour. This set of parameters will be referred to as the "southwest winds scenario" in the following discussion. The second assumes winds are out of the south, also at 10 miles per hour, and will be referred to as the "south winds scenario" in the discussion. Tables 2.1 and 2.2 show the values used to parameterize the model using the southwest winds scenario and the south winds scenario, respectively.

The results of the test cases are shown using three separate maps. The first map, labeled "a" in each set, shows the fire arrival times for each node. The second map, labeled

"b" in each set, shows the fire spread patterns: each arrow indicates the MTT path from which the fire arrived at each node, i.e., from which node did fire spread into the node containing the arrow. The third map, labelled "c" in each set, shows the fireline intensity at each node. Note that all the maps use the convention that north is the top of the map.

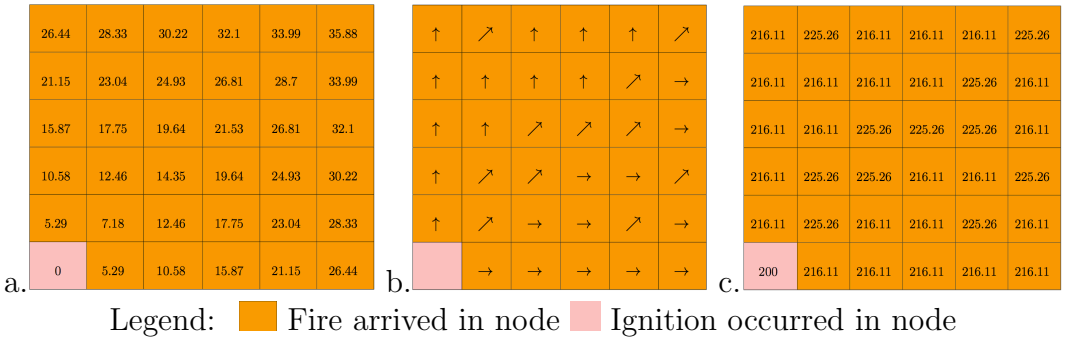

Figure 2.3: Fire arrival time (a), spread directions (b) and fireline intensities (c) for the southwest winds weather scenario.

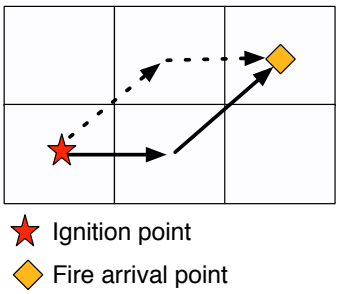

Figure 2.4: An example of two possible MTT spread paths that could result in a tie on a homogeneous landscape.

The first test case is shown in Figure 2.3. This test case used the southwest wind weather parameters and the fire behavior reflects these parameters. The ignition occurred in the southwest corner. Fire then moves fastest and has the highest fireline intensity spreading from southwest to northeast. The fire behavior should be symmetrical with respect to the diagonal running from southwest to northeast as well; for example, the fire behavior in the northwest and southeast corners ought to be identical. The fire arrival times (Figure 2.3a) do show this symmetry. However, the spread paths and fireline intensity (Figures 2.3b and 2.3c) are not exactly symmetrical. These anomalies are due to multiple possible MTT

paths. Figure 2.4 shows an example of how two fire spread paths can give equal fire arrival times; this example demonstrates how moving southwest and then west would take the same amount of time as moving west first and southwest second. The solution algorithm simply breaks these ties randomly, which leads to the non-symmetries we observe in the choice spread paths. Because the fireline intensity is dependent upon the spread path, the random choice of spread path gives non symmetrical fireline intensity as well. In the example in Figure 2.4, if the winds were out of the southwest, the spread path shown by the dotted line would give a lower fireline intensity for the fire arrival point than the spread path shown by the continuous line. Since fireline intensity may be used to determine safety or ecological objectives, having the solution algorithm breaking these ties randomly is not desirable, but even worse would be a scenario in which the solution algorithm could exploit these multiple MTT paths to produce a "better" result, for example, choosing the path with the lowest fireline intensity. While acknowledging this potential issue is important, it only occurs on exactly homogeneous landscapes. Any slight variation over the landscape removes these ties. Because very few landscapes are exactly homogeneous, I anticipate this issue causing very few problems if the model is used operationally. For homogeneous landscapes, the ties could be broken using very small random perturbations of the fire spread time parameters such that the ties are broken randomly by the model user, rather than by the solution algorithm. These perturbations could also be chosen systematically in order to ensure the highest possible intensity or any other worst case scenario fire behavior. To make the test cases examined in this chapter easier to compare, I chose to randomly vary the fire spread parameters over the test case landscape, holding these random perturbations constant across each test case, to ensure that the spread paths and fireline intensities would be consistent throughout the test cases. The post-perturbation test case corresponding to the results from Figure 2.3 is shown in Figure 2.5.1. Note that while some of the spread paths have changed, along with the corresponding fireline intensities, the fire arrival times remain exactly the same.

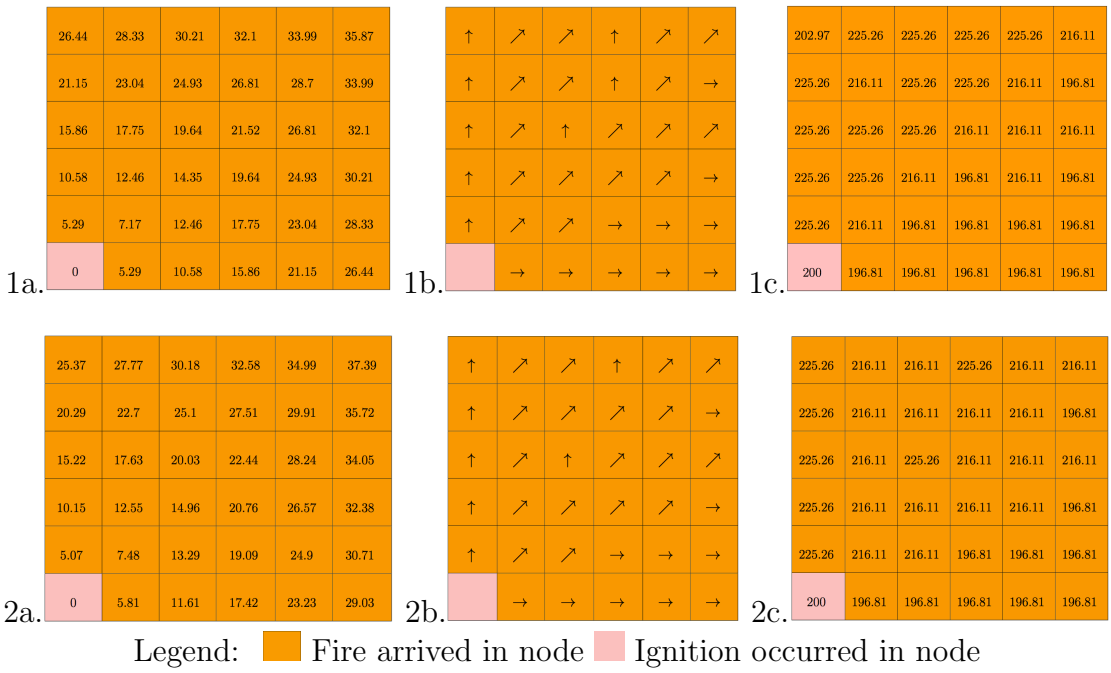

Figure 2.5: Fire arrival time (a), spread directions (b) and fireline intensities (c) for the southwest winds weather scenario with random perturbations to break MTT path ties (1), and the south winds weather scenario with random perturbations to break ties (2).

The test case shown in Figure 2.5.2 shows results that used the south winds parameters instead of the southwest winds parameters. The change in major spread direction is reflected in the faster spread in the northerly direction; for example, fire arrives at the northwest corner several minutes before arriving at the southeast corner. Fireline intensity is higher where fire spreads from south to north than where fire spreads to the west. Because the ignition point is in the southwest corner, the resulting maps are not expected to show the same symmetry in fire arrival times as the results in Figures 2.3 and 2.5.1, however, there are still possible MTT path ties broken by the same perturbations that were used for the results in Figure 2.5.1.

The results in Figure 2.5 show the model responding the differing fire behavior. The following test cases will focus on testing that the model can respond to different landscape conditions. For the rest of the test cases in this chapter, only the southwest winds weather scenario is used for parameterization. The random perturbations that break minimum fire travel time paths stay constant throughout all the test cases.

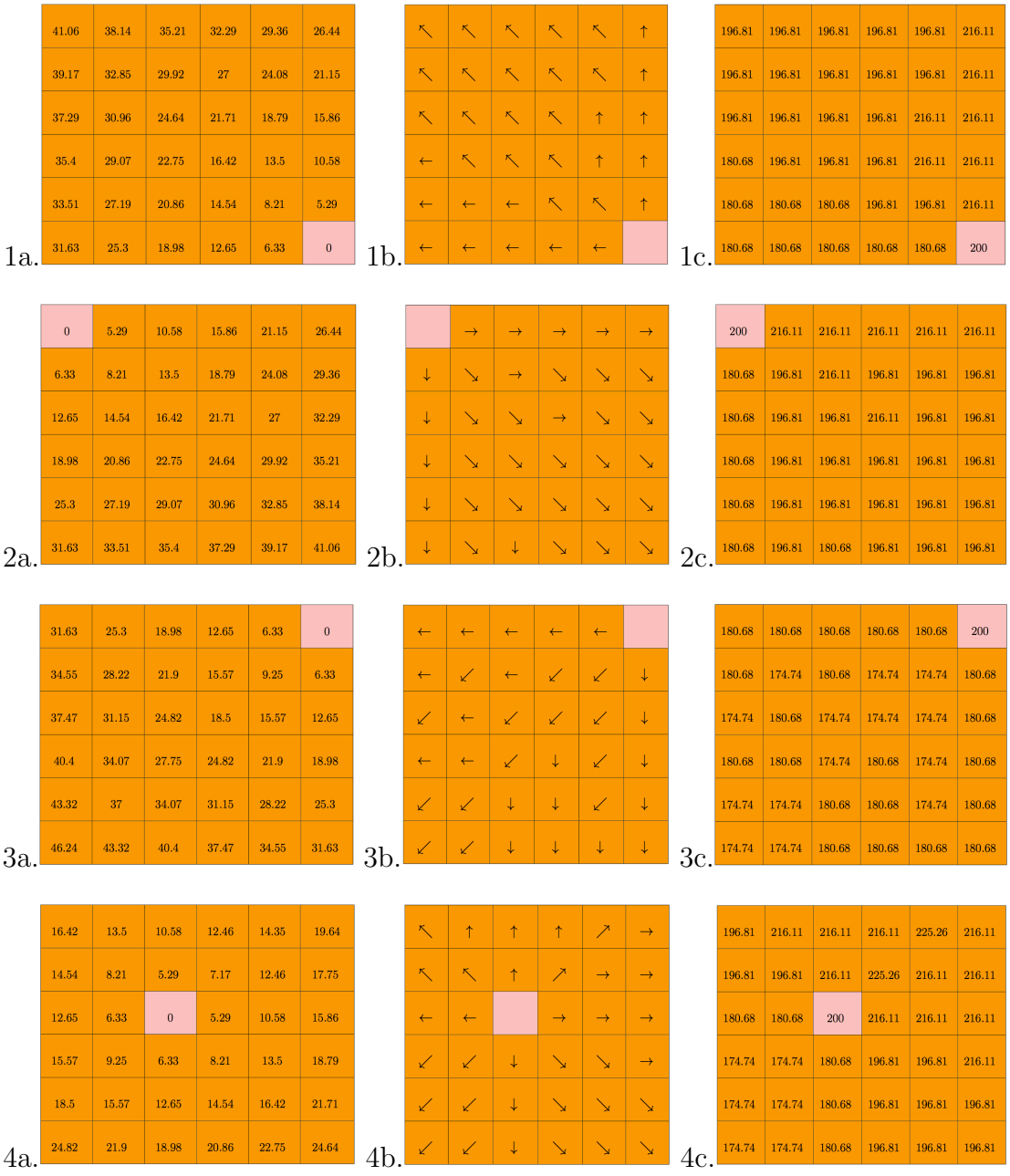

Figure 2.6: Fire arrival time (a), spread directions (b) and fireline intensities (c) for the southwest winds weather scenario with an ignition in the southeast corner (1), an ignition in the northwest corner (2), an ignition in the southeast corner (3), and ignition in the center of the landscape (4).

The test cases in Figure 2.6 show that placement of the ignition point does not affect fire behavior predictions. Each of the four test cases has a different ignition point, but they all share the same southwest winds weather. Since the wind is coming from the southwest, fire arrives at the same time in the northwest corner for the results in Figure 2.6.1a as it does in the southwest corner in Figure 2.6.2a. The fire also arrives at the same fireline intensity in both those nodes. Similarly, the fire behavior is exactly the same in the west-most column shown in Figure 2.6.2a and the east-most column in Figure 2.6.3a. When the ignition point is moved in to the center of the landscape, the fire behavior to the northeast of the ignition point is identical to the fire behavior in Figure 2.5.1., the fire behavior to the northwest matches with Figure 2.6.1, the fire behavior to the southeast matches with Figure 2.6.2, and the fire behavior to the southwest matches withFigure 2.6.3. Any anomalies in spread pattern or intensity are due to the perturbations that break the MTT path ties, as they stay constant on the landscape, regardless of where the ignition point is moved.

Figure 2.7 shows results in which the model propagates fire from multiple ignition points and the fire spreads around non flammable nodes. The spread paths are particularly informative in these test cases. The results in 2.7.1 show that the MTT paths can come from more than one ignition point. If a fire were discovered after it had spread to several nodes, the model would have no trouble using multiple ignition points to represent the fire footprint at discovery. In Figure 2.7.2, fire spreads from two ignition points around a non flammable barrier. The winds are from the southwest, so the fire spreads faster getting to the north side of the barrier than while moving from north to south after getting around the barrier. This behavior is opposite of the fire behavior produced when spreading around the south side of the barrier: the fire moves more slowly when spreading towards the south end of the barrier and then speeds up when moving from the south side of the barrier toward the north. The differing behaviors do produce consistent results: the fire arrives at exactly equal times in the center of the two east most columns, which is to be expected given that fire spreading around either side of the barrier must go an equal distance north and south. Figure 2.7.3

shows that the model can predict fire behavior from multiple, separate ignitions and can produce spread paths that move around multiple non flammable islands. These complex fire spread patterns shown in Figure 2.7 demonstrate that the model can simulate fire behavior over numerous landscape and initial fire conditions.

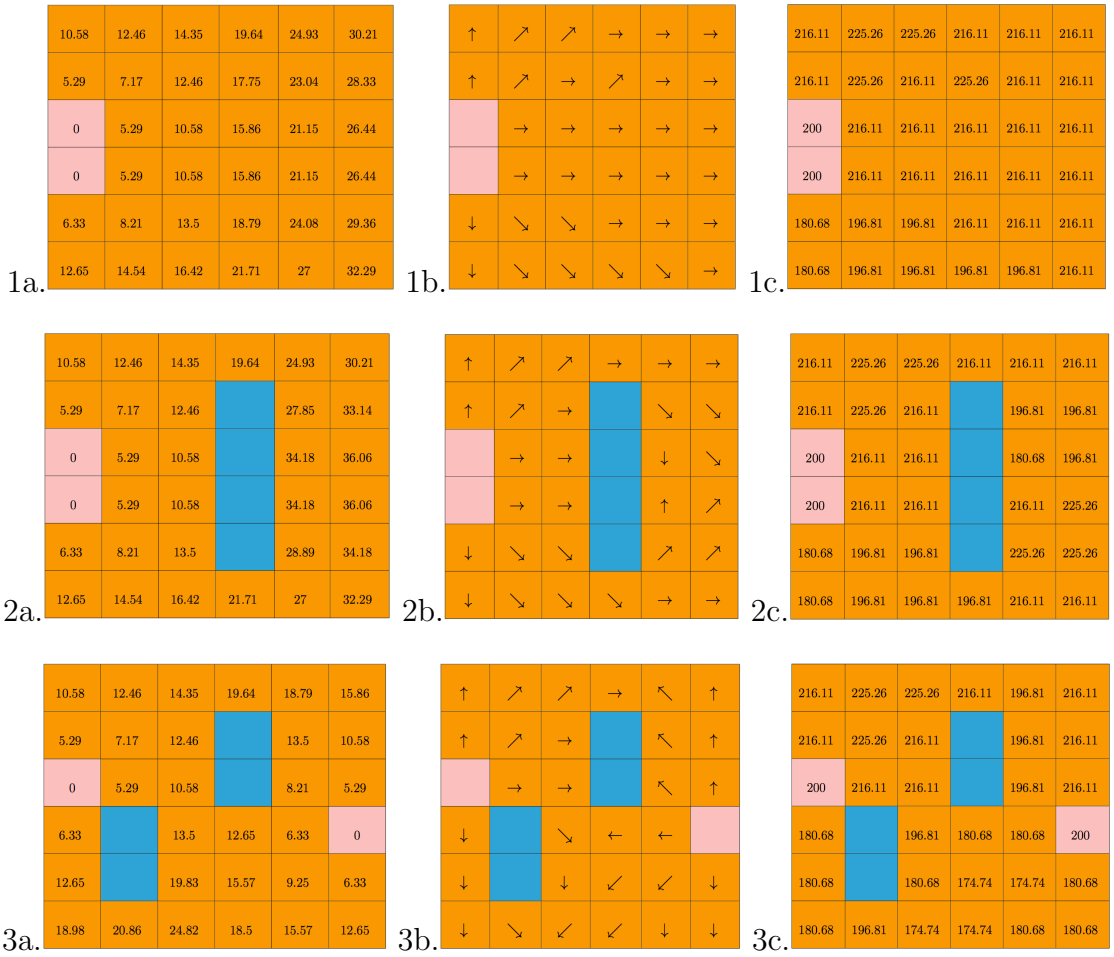

Figure 2.7: Fire arrival time (a), spread directions (b) and fireline intensities (c) for the southwest winds weather scenario with two ignition points (1), two ignition points and a nonflammable barrier (2), two ignition points and two nonflammable islands (3).

The results in Figure 2.8 demonstrate the first instances of fire behavior interacting with control points. Control points differ from the nonflammable cells because the program can choose to place the control points anywhere on the landscape, depending on the program's objective function. However, once the decision of where to place to control points is made,

they act exactly the same as non flammable nodes. As mentioned in Section 2.2.3, the results in this chapter only examine how control points are placed when the goal is to minimize fire on the landscape using the fewest control points possible. In the Figure 2.8.1, unlimited control points were allowed, but only three control points were needed to contain the fire to only the cell in which the ignition occurred. Note that while this test case shows the model "containing" the fire, it also highlights a problem with using small landscapes. If the model can use the edge of the landscape as a containment boundary, it will. While some landscapes may allow for this (for example, if two of the edges of the landscape are roads), it may not be acceptable for others. The necessity of providing the model with a large landscape in order to completely contain a fire, unless the edges of the landscape can be considered non flammable, is evident in all of the examples in Figure 2.8.

Figure 2.8.2 shows a slightly different ignition point than in Figure 2.8.1 and adds two non flammable nodes to the landscape. The model is allowed five control points which it uses to trap the fire against the southwest corner of the landscape, only allowing two nodes to burn. Because the model is allied to place five control points on the landscape, the fire has no incentive to connect the control points to the non flammable nodes. In Figure 2.8.3 the number of control points is reduced from five to four and the model can no longer confine the fire to the southwest corner. Therefore, the control points are connected to one of the non flammable nodes in order to save the four nodes in the northeast corner. Because the control points exploit the nonflammable node in the center of the landscape, the model saves three more cells than it would have without the nonflammable node. In the test case shown in the Figure 2.8.4, the model is still allowed only four control points, but another nonflammable node is added to the center of the landscape. The model is able to take advantage of this to save all twelve nodes on the east side of the landscape. All four of these test cases show the model efficiently using fire suppression resources to achieve the goal of minimizing fire on the landscape. I did not show results where fire spreads around any control points because in regards to fire behavior, control points act exactly the same as nonflammable nodes.

Figure 2.8: Fire arrival time (a), spread directions (b) and fireline intensities (c) for the southwest winds weather scenario with three nodes of suppression allowed (1), five nodes of suppression allowed (2) and four nodes of suppression allowed (3 and 4).

2.4 Discussion

This chapter introduces a deterministic mixed integer programming model that predicts fire behavior across a landscape given a constant weather scenario. Results showed the fire behavior reacting to differing weather scenarios (Figure 2.5), differing ignition points (Figure 2.6), nonflammable barriers (Figure 2.7), and control points (Figure 2.8). In these results, constraints simulating explicitly spatial fire behavior reacted dynamically to optimal suppression activities.

However, the model still has some weaknesses. This framework does not allow for prediction of fire behavior using more than one set of weather parameters. If the weather changes, the model would have to be run in an iterative fashion in order to use the different sets of weather parameters (e.g. Finney 2004, 2006). Current fire behavior prediction software is capable of using a weather stream to simulate fire behavior under changing weather conditions. Given how dramatically weather changes can effect fire behavior, this restriction is a major weakness of this model.

An additional weakness is that the suppression decisions this model supports are quite simplistic. While modeling control points does allow the fire behavior to dynamically interact with suppression decisions, it fails to take into account many important facets of suppression. Control points only allow for the location of suppression to be determined. They do not allow for the importance of the timing of the control actions, i.e., can the actions be completed before the fire reaches a node. They also fail to address safety concerns for fire crews and possible access issues. Modeling suppression using control points as implemented here assumes that if control is placed in a node, then the node becomes nonflammable. This assumption is driven by the standard definition of control: that a fire is under control once it is surrounded by fireline. This definition of control has been used by multiple researches (e.g. Donovan and Rideout 2003, Fried and Fried 1996). However, if fireline is not robust enough, the fire may jump the line. Therefore, this definition of control may not reflect actual fireline quality issues adequately.

Because this model is an integer program, large landscapes present exponentially more difficult models for mathematical programming methods to solve. Specifically, the branch and bound solution algorithm has a much larger decision space to cover and therefore the algorithm runs much slower on a large landscape. Scaling the model up so that it can handle a large landscape presented issues on its own and work on that problem is presented in Chapter 5.

Despite the weaknesses identified above, the deterministic model is a step forward in modeling fire spread and suppression. This formulation is one of very few models to successfully incorporate explicitly spatial, dynamic fire spread into a mathematical programming framework. The inclusion of fireline intensity in addition to fire arrival times provides many options for further extensions of the model. For example, it could be used to help determine if fire is ecologically beneficial or harmful. Fire behavior results can also be incorporated into safety constraints and may help determine if the fireline produced is robust enough to withstand the arriving flame front. While the suppression modeled is simplistic, it does demonstrate that mathematical programming can produce optimal suppression decisions that interact dynamically with fire behavior.

The next step in building a model that integrates spatial fire spread and suppression decisions is to build a model that allows for multiple sets of weather parameters. The next chapter introduces a stochastic programming model that predicts fire behavior using multiple probabilistic weather streams.

3 Fire Growth Equations for a Stochastic Programming Framework

3.1 Introduction

Of the three components that influence fire behavior (landscape characteristics, fuels, and weather), only the weather is variable over the short-term. Fuels may change on a long-term scale, but are unlikely to change over the course of a fire, except for moisture content which is weather driven. The fuel consumption that occurs once the fire arrives alters the fuels, but most fire behavior models, including this one, are concerned only with the fuel available when the fire is first ignited. Landscape characteristics are even less likely than fuels to change over the course of a fire. While the deterministic model presented in Chapter 2 only allowed for one set of fire behavior parameters, the stochastic model developed here allows for variable weather and numerous weather scenarios that produce more than one set of fire behavior parameters over the course of a fire.

Fire containment requires decisions to be made while weather predictions are still imperfect. In this chapter, the deterministic mixed integer program from Chapter 2 is adapted to add multiple weather streams to the model so as to allow potential weather changes to drive decisions, just as they would in an actual fire suppression situation. The framework developed in this chapter provides the fire behavior equations that can be used as constraints in a multi-stage stochastic mixed integer program. Control points are used again to examine fire behavior response to suppression decisions. A more sophisticated control network is developed in Chapter 4.

The first step in building the model is to gather a set of probabilistic weather predictions for the landscape of interest. These predictions can be visualized as a stochastic decision tree. An example of a set of weather predictions is shown in Figure 3.1. The separate branches on the tree will be referred to as "sub scenarios," each of which represents one set of weather parameters. When the weather changes, a new branch must be formed with the new set of parameters. A sequence of sub scenarios over time form one continuous weather stream,

which will be referred to as a "weather scenario". In this model the scenario tree can be built to reflect uncertainty in both when and how the weather will change, thus, a sub scenario may last any amount of time. When a weather changing event occurs, new branches are formed to reflect how the weather is likely to change. The number of sub scenarios for each weather scenario is equivalent to the number of times the weather is expected to change. Any change in the weather must be modeled as a new sub scenario, so if, for example, a diurnal change is expected to occur then there must be a sub scenario that reflects both the weather before the change and the weather after. The weather predictions must cover the planning horizon for the modeled fire event. The statistical process of building a weather scenario tree has been left for future work, but is discussed further in Chapter 5.

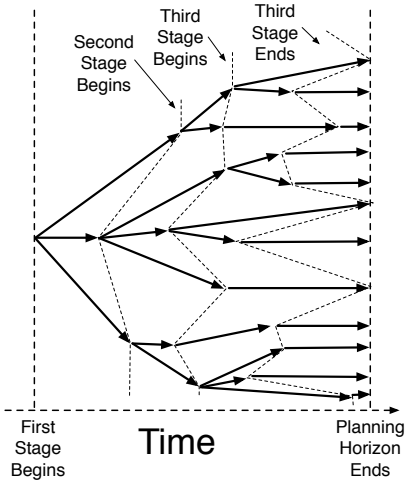

Figure 3.1: An example of a weather scenario tree with the sub scenarios lasting different lengths of time for each scenario.

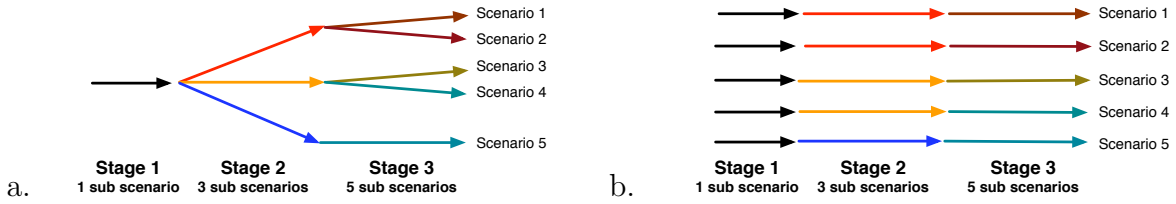

Figure 3.2: a. An example of a stochastic weather tree. b. The stochastic weather tree from (a) broken up into its deterministic equivalent problems.

Most stochastic programs can be broken down into one or more "deterministic equivalent" programs, with each scenario making up one deterministic program. This is shown in Figure 3.2. The first stage of the weather tree in Figure 3.2 is shorter than the other two; weather sub scenarios may not all last the same amount of time. The deterministic equivalent problems for the stochastic fire spread model do not look like the deterministic program presented in Chapter 2 because the model presented in Chapter 2 does not have a way to include weather changes. The weather is allowed change over time in the deterministic equivalent of the stochastic model presented here.

The fire growth equations below are designed for a multi-stage stochastic integer programming model with full recourse (Birge and Louveaux 1997). The random parameters in the model are the possible fire spread rates between nodes and the corresponding fireline intensities, which are calculated using variable weather. Exact fire arrival times and fireline intensities are calculated regardless of the objective function.

Just as in Chapter 2, fire growth is modeled as movement of fire between nodes. In the test cases, I used raster data organized into square cells with each raster cell representing a homogeneous landscape condition. A node represents each cell and fire can spread from node to node (see Figure 2.1 in Section 2.1). This model follows the example of several previous studies (e.g. Alexandridis et al. 2011, Ntaimo et al. 2004) and allows fire to spread between cells that share an edge or a vertex. As mentioned in Chapter 2, this is convenient as raster data are commonly used in fire management.

3.2 Methods

3.2.1 Notation

As in Chapter 2, lower case Arabic and Greek letters represent parameters, upper case Greek letters represent sets, and upper case Arabic letters represent decision variables. The following notation indicates indices and sets:

i index for the nodes

Ω_i set of all nodes that neighbor to node i

j index for a neighboring node to node i (element of Ω_i)

q index for a weather scenario of interest

Φ_q set of sub scenarios within weather scenario q

m index for the sub scenarios of weather scenario q (element of Φ_q)

q_m index for the sub scenario m from scenario q

Λ_{q_m} set of all sub scenarios that follow sub scenario q_m

The parameters used in the formulation of the model are listed below. These must be calculated before the optimization algorithm is run.

t_{q_m} the length of time sub scenario m lasts for sub scenario q (note that this model assumes all q_1 start at $t_0 = 0$)

n_i number of nodes that border node i (number of elements in Ω_i)

g_i threshold that determines at which intensity fire in cell i becomes harmful

κ_{j,i,q_m} intensity of fire at node i if fire spreads from node j to node i arriving during sub scenario q_m

κ_{i,q_m} intensity of fire at node i if the ignition point occurs at node i in sub scenario q_m

x_{i,q_m} binary indicator that an ignition point occurs at node i during sub scenario q_m

f_{i,q_m} the ignition time corresponding to ignition x_{i,q_m}

$d_{j,i}$ the distance between the centers of node j and node i

r_{j,i,q_m} the rate at which fire could spread from node j to node i in sub scenario q_m

ξ_i takes a value of 1 if node i is non-flammable, 0 otherwise

M a large number that forces the logic constraints to work ("Big M")

The decision variables in the model are listed below. Note that all decision variables have an implicit lower bound of zero.

D_{i,q_m} binary indicator that fire arrived at node i during sub scenario q_m

$D_{i,q_{\tilde{m}}}$ binary indicator that fire arrived at node i in scenario q after the end of the planning horizon

$F_{i,q}$ fire arrival time at node i for scenario q

$\mathrm{I}_{i,q}$ fireline intensity at node i for scenario q

B_{j,i,q_m} binary indicator that fire arrived at node i for the first time in sub scenario q_m and was ignited by node j

$G_{i,q}$ binary indicator that node i burned below intensity threshold g_i for scenario q

$H_{i,q}$ binary indicator that node i burned above intensity threshold g_i for scenario q

Y_{i,q_m} binary indicator that a control point was placed in node i at the beginning of sub scenario q_m

T_{j,i,q_m} time fire could have traveled from node j to node i during sub scenario q_m

TT_{j,i,q_m} total time fire has traveled from node j to node i at the end of sub scenario q_m

L_{j,i,q_m} potential distance fire could have traveled from node j to node i during sub scenario q_m

TL_{j,i,q_m} total potential distance fire could have traveled from node j to node i at the end of sub scenario q_m

A_{j,i,q_m} takes a value of 1 for the first time $TL_{j,i,q_m} \geq d_{j,i}$, else 0

3.2.2 Constraints

The constraints in this stochastic model parallel deterministic constraints in Chapter 2: one set of constraints governs the spatial relationships between nodes, a second set uses MTT methods to track fire arrival times, and a third set calculates fireline intensity. While the spatial relationship constraints remain very similar to their counterparts in the deterministic

model, the fire arrival time equations had to be changed to accommodate the stochastic weather parameters. These changes expanded the set of fire arrival time constraints, which now track fire spread times and distances as well as fire arrival times. The last major change from the deterministic model is the addition of constraints that determine whether fire is beneficial or harmful to a cell based on the fireline intensity at that cell's node. This allows the model to represent ecological objectives.

Spatial Relationship Constraints

Equations 3.1, 3.2, 3.3, and 3.4 define the spatial relationships between the nodes in the landscape.

$$1 - \xi_i \geq \sum_{m \in \Pi_q} (D_{i,q_m} + Y_{i,q_m}) \quad \forall i, q \tag{3.1}$$

$$\sum_{m \in \Pi_q} (Y_{i,q_m} + D_{i,q_m}) + c_i \geq \frac{1}{n_i} \sum_{j \in \Omega_i} \left(\sum_{m \in \Pi_q} D_{j,q_m} \right) \quad \forall i, q \tag{3.2}$$

$$\sum_{j \in \Omega_i} B_{j,i,q_m} = D_{i,q_m} - x_{i,q_m} \quad \forall i, q, m \in \Phi_q \tag{3.3}$$

$$B_{i,j,q_m} \leq \sum_{k=1}^{m} D_{i,q_k} \quad \forall i, j \in \Omega_i, q, m \in \Phi_q \tag{3.4}$$

Equation 3.1 allows each node i to burn only once per scenario if node i is a flammable cell but never allows node i to burn if node i is nonflammable or if a control point has been place in node i (if a cell is non-flammable then the parameter ξ_i is set to one). Equation 3.2 forces node i to burn in scenario q if node i has a neighbor j that burns in scenario q, unless a control point has been placed in node i. The right hand of Equation 3.2 indicates all of the possible sub scenarios in which each neighbor j can burn in scenario q. If no neighbors burn, then the right hand side of Equation 3.2 is zero and cell i does not burn. If at least one neighbor burns, then the right hand side of Equation 3.2 is greater than zero but less than or equal to one, forcing cell i to burn. The left side of Equation 3.2 will be one if node

i burns during some sub scenario m in scenario q and zero otherwise. Equation 3.3 enforces the condition that if node i burns and cell i did not contain an ignition then the fire must have come from some neighboring node j. The last of the spatial equations (3.4) ensures that fire cannot spread from node i to node j unless node i is burning.

At the end of a scenario, if any unburned nodes exist with neighbors that have burned, then Equation 3.2 will be violated and the model will be infeasible. To avoid this, after the weather scenario tree is built a final sub scenario is added to the end of each scenario. This sub scenario is denoted by $q_{\tilde{m}}$. Note that $q_{\tilde{m}}$ is a member of Φ_q, the set of all sub scenarios that create scenario q. The predictions of fire growth from sub scenario $q_{\tilde{m}}$ will be considered outside the boundary of the problem, although any cell that burns within sub scenario $q_{\tilde{m}}$ would be at risk of burning after the end of the planning horizon. No suppression actions will be considered in this sub scenario.

Potential Fire Travel Time Constraints

The deterministic model in Chapter 2 did not need to track the amount of time fire traveled along each possible MTT path; the time was set by the rate of spread between nodes. However, now that time is divided into sub scenarios, fire may take more than one sub scenario to travel from a node into its neighbor. Each spread path may need to be calculated using more than one rate of spread parameter because the rate of spread changes with the weather. Therefore, in order to accurately calculate fire arrival times over changing weather conditions, the model must track both the length of time fire takes to spread from each node to its neighboring nodes and the distance that fire travels in each sub scenario. The following section addresses the spread distance.

Two related decision variables indicate the amount of time that fire has been spreading from node j to cell i in sub scenario q_m. The first, T_{j,i,q_m}, is the maximum amount of time that fire could potentially be spreading from j to i during sub scenario q_m. The second of these decision variables is TT_{j,i,q_m}, a bookkeeping decision variable which is simply the sum

of all the preceding T_{j,i,q_m} and indicates the total time that fire has been spreading from node j to node i from the beginning of scenario q through the end of sub scenario q_m.

$$T_{j,i,q_m} \leq M \sum_{k=1}^{m} D_{j,q_k} \quad \forall i,j \in \Omega_i, q, m \in \Phi_q \tag{3.5}$$

$$T_{j,i,q_m} \leq \left(\sum_{k=1}^{m} t_k \right) - F_{j,q} + M(1 - D_{j,q_m}) \quad \forall i,j \in \Omega_i, q, m \in \Phi_q \tag{3.6}$$

$$T_{j,i,q_m} \geq \left(\sum_{k=1}^{m} t_k \right) - F_{j,q} - M(1 - D_{j,q_m}) \quad \forall i,j \in \Omega_i, q, m \in \Phi_q \tag{3.7}$$

$$T_{j,i,q_m} \leq t_{q_m} + M\left(1 - \sum_{k=1}^{m-1} D_{j,q_k}\right) \quad \forall i,j \in \Omega_i, q, m \in \Phi_q | m > 1 \tag{3.8}$$

$$T_{j,i,q_m} \geq t_{q_m} - M\left(1 - \sum_{k=1}^{m-1} D_{j,q_k}\right) \quad \forall i,j \in \Omega_i, q, m \in \Phi_q | m > 1 \tag{3.9}$$

$$TT_{j,i,q_m} = \sum_{k=1}^{m} T_{j,i,q_k} \quad \forall i,j \in \Omega_i, q, m \in \Phi_q \tag{3.10}$$

If fire has not yet reached node j by the end of sub scenario q_m, then fire cannot be spreading from cell j to cell i at all during sub scenario q_m. Equation 3.5 sets the potential time that the fire is able to travel from cell j to node i during sub scenario q_m to zero if fire has not arrived at node j by the end of sub scenario q_m. If fire reaches node j during sub scenario q_m, then fire can potentially be spreading from j to i only during the part of the sub scenario that follows fire arriving at node j. Equations 3.6 and 3.7 set the time fire is able to travel from cell j to node i during sub scenario q_m to be the time at the end of the sub scenario minus the time fire arrived at node j. If fire has reached node j before the beginning of sub scenario q_m then fire can potentially be spreading from node j to node i during the entirety of the sub scenario and the potential time fire is able to travel from cell

j to node i during sub scenario q_m should be set to the entire length of the sub scenario. Equations 3.8 and 3.9 set the time fire has potentially traveled from cell j to node i during sub scenario q_m equal to t_{q_m} given that sub scenario q_m begins after fire has arrived at node j. Equation 3.10 sums the potential time that fire has been able to spread from node j to node i in the current and preceding sub scenarios to determine the total potential fire spread time from node j to node i at the end of sub scenario q_m.

Potential Distance Fire Can Travel Constraints

$$L_{j,i,q_m} = r_{j,i,q_m} T_{j,i,q_m} \quad \forall i, j \in \Omega_i, q, m \in \Phi_q \tag{3.11}$$

$$TL_{j,i,q_m} = \sum_{k=1}^{m} L_{j,i,q_k} \quad \forall i, j \in \Omega_i, q, m \in \Phi_q \tag{3.12}$$

Once the amount of potential fire spread time from node j into node i during sub scenario q_m is known (set by Equations 3.5, 3.6, 3.7, 3.8, and 3.9), then the potential distance that the fire could have traveled from node j to node i during sub scenario q_m can be calculated using Equation 3.11. Equation 3.11 is simply a standard physics equation: distance (L_{j,i,q_m}) equals rate (r_{j,i,q_m}) multiplied by time (T_{j,i,q_m}). The rate of spread can be calculated using any fire spread model. As fire spread models become more sophisticated and accurate, the rate parameter can be calculated using the most accurate spread model available. Equation 3.12 is analogous to Equation 3.10; it determines the total potential distance that fire spreading from node j to node i could have gone by the end of sub scenario q_m.

Fire Arrival Time Constraints

These MTT constraints are similar to the MTT constraints presented in Chapter 2, but had to be modified in order to use multiple weather parameters. The same concepts hold: each node receives fire from the fastest possible fire spread path. However, the spread paths may now take more than one sub scenario to complete. For example, a node may start spreading fire into its neighbor in the one sub scenario but the fire does not reach the

neighboring node until the next sub scenario or later. Equations 3.5-3.12 inform the model of the distance that the fire travels in each sub scenario. The MTT travel time equations must then determine how much further the fire needs to go, the amount of time that would take given the weather in the second sub scenario, and whether or not fire actually does arrive in the second sub scenario. The following equations achieve all of these objectives.

$$F_{i,q} = f_{i,q_m} \quad \forall\{i|x_{i,q_m} = 1\} \tag{3.13}$$

$$TL_{j,i,q_m} \leq d_{j,i} + M\sum_{k=1}^{m}(A_{j,i,q_m} + Y_{i,q_m}) \quad \forall i,j \in \Omega_i, q, m \in \Phi_q \tag{3.14}$$

$$F_{i,q} \leq F_{j,q} + TT_{j,i,q_{m-1}} + \frac{d_{j,i} - TL_{j,i,q_{m-1}}}{r_{j,i,q_m}} + M(1 - A_{j,i,q_m}) \quad \forall i,j \in \Omega_i, q, m \in \Phi_q \tag{3.15}$$

$$F_{i,q} \geq F_{j,q} + TT_{j,i,q_{m-1}} + \frac{d_{j,i} - TL_{j,i,q_{m-1}}}{r_{j,i,q_m}} - M(1 - B_{j,i,q_m}) \quad \forall i,j \in \Omega_i, q, m \in \Phi_q \tag{3.16}$$

$$TT_{j,i,q_0} = 0 \quad \forall i,j \in \Omega_i, q \tag{3.17}$$

$$TL_{j,i,q_0} = 0 \quad \forall i,j \in \Omega_i, q \tag{3.18}$$

If an ignition point occurs at node i then the fire arrival time for node i is set *a priori* by Equation 3.13. Otherwise Equations 3.14, 3.15, and 3.16 work together to set the fire arrival time. The auxiliary variable A_{j,i,q_m} indicates the first sub scenario q_m in which the distance the fire has traveled from node j to node i has exceeded the distance between the nodes. During the sub scenarios in which the distance the fire has traveled is less than or equal to the distance between the nodes and sub scenarios in which a control point has been placed in node i either in that sub scenario or a previous sub scenario, Equation 3.14 is never binding, so the auxiliary variable can be zero and Equation 3.15 will be non-binding. However, Equation 3.14 requires that the auxiliary variable take a value of one in the first sub scenario q_m in which the distance the fire has traveled from node j to node i is greater than

the total distance between the nodes. This activates Equation 3.15, which could become binding. Equation 3.16 forces the fire arrival time to be as large as the smallest possible arrival time and thus forces the program to choose to ignite node i from the node j that gives the smallest fire arrival time for node i. At the beginning of the first sub scenario ($m = 1$), the fire has not traveled any distance from j to i, therefore Equations 3.17 and 3.18 are necessary to set the total time and total distance traveled from node j to node i to zero. The distance fire has traveled from node j to node i may end up being significantly larger than the distance between nodes j and i, but this does not have any effect on the model; once the earliest possible fire arrival time is set for node i then the times and distances that fire has traveled from all of the neighbors no longer matter.

$$F_{i,q} \geq \sum_{k=1}^{m} t_{q_k} - M\left(\sum_{k=1}^{m} D_{i,q_k}\right) \quad \forall i, q, m \in \Phi_q \tag{3.19}$$

$$F_{i,q} \leq \sum_{k=1}^{m} t_{q_k} + M\left(1 - \sum_{k=1}^{m} D_{i,q_k}\right) \quad \forall i, q, m \in \Phi_q \tag{3.20}$$

Equations 3.19 and 3.20 link the time fire arrives in node i to the sub scenario in which the node is ignited. Given a fire arrival time for a node i in scenario q ($F_{i,q}$), Equations 3.19 and 3.20 force the model to correctly pick the decision variable indicating in which sub scenario the node burned (D_{i,q_m}) that matches the fire arrival time. Until the occurrence of the sub scenario in which fire arrives, Equation 3.19 ensures that node i cannot burn. Once the sub scenario in which the fire arrives occurs, then Equation 3.20 forces the decision variable indicating node i burned in sub scenario q_m to be one.

Fireline Intensity Constraints

The constraints outlined above are a complete set of fire growth equations and solved together will give a prediction of when fire will arrive at each node in a landscape. However, as in Chapter 2, fireline intensity calculations are also included in the set constraints. Fireline

intensity may be used as a proxy to determine if a fire is harmful or beneficial to an ecosystem and to determine if it is safe to send suppression resources to a node. Fireline intensity is highly dependent on which path fire takes and so the fireline intensity of node i is dependent upon which node j ignited node i and in which sub scenario node i was ignited.

$$I_{i,q} = \sum_{m \in \Phi_q} \left(\kappa_{i,q_m} x_{i,q_m} + \sum_{j \in \Omega_i} \kappa_{j,i,q_m} B_{j,i,q_m} \right) \qquad \forall i, q \tag{3.21}$$

The fireline intensity at which a node burned is set using Equation 3.21. All the possible fireline intensities at which node i could burn given that fire spread from node j in sub scenario q_m are calculated before the optimization model is run (κ_{j,i,q_m}). These parameters are multiplied by the binary variables indicating which node j ignited node i, so when the binary variable is one (which only happens once per scenario), the fireline intensity is set properly.

Fire policy in the US requires fire managers to consider multiple objectives (Calkin et al. 2011). For example, in areas that benefit from being burned, the fire might be monitored but not actively suppressed, whereas in areas where fire threatens structures or other values at risk, the fire might be actively suppressed. Each node on the landscape is assigned a threshold that determines at what fireline intensity the fire becomes harmful. For cells with structures or other values (habitat for endangered species, etc), the threshold at that node can be set to zero, indicating that any fire in that cell is harmful and should be avoided. For cells that could benefit from low severity fire, the threshold can be set to reflect the highest intensity that would benefit the ecosystem. If high severity fire would be beneficial, this threshold can be set very high. The following equations only demonstrate one threshold for each node, but the constraint set could be modified to include more than one threshold parameter (e.g., one threshold to indicate at which fireline intensity fire becomes moderately harmful, one threshold to indicate at which intensity fire becomes very harmful, and one threshold to indicate if it is safe for suppression crews to be actively working in or near the

cell). Including these thresholds in the model allows the objective function to reflect multiple objective policies.

$$G_{i,q} + H_{i,q} \leq \sum_{k=1}^{\tilde{m}-1} D_{i,q_k} \quad \forall i, q \tag{3.22}$$

$$I_{i,q} \leq g_i + M\left(H_{i,q} + (1 - \sum_{k=1}^{\tilde{m}-1} D_{i,q_k})\right) \quad \forall i, q \tag{3.23}$$

$$I_{i,q} \geq g_i - M\left(G_{i,q} + (1 - \sum_{k=1}^{\tilde{m}-1} D_{i,q_k})\right) \quad \forall i, q \tag{3.24}$$

Equation 3.22 makes sure that fire in node i must be classified as either beneficial or harmful if node i burns within scenario q before the final sub scenario $\tilde{m}$. When the fireline intensity is above the threshold, then fire must be classified as harmful in order to make Equation 3.23 feasible. Similarly, when the fireline intensity is below the threshold, then fire must be classified as beneficial in order to make Equation 3.24 feasible. Note that Equations 3.22, 3.23, and 3.24 do not allow a beneficial or harmful designation for a node if it burns in the final sub scenario ($q_{\tilde{m}}$) because it is outside the problem boundaries.

Nonanticipativity and Decision Timing

When fire managers make suppression decisions, they do not know what weather scenario is going to occur. Instead they must ensure that their decisions are "good," for any weather scenario that might reasonably occur. This is called a nonanticipative decision; the manager cannot anticipate which weather scenario will happen, and their decisions must reflect this. One of the advantages of stochastic programming is that decisions the model makes can be forced to obey nonanticipativity constraints. The decisions modeled in Chapter 2 were anticipative; the model knew what the future weather would be when the control points were placed.

Decision points are determined after the weather decision tree is formed. If the deci-

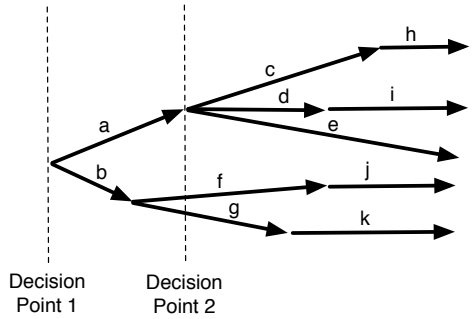

Figure 3.3: A weather scenario tree with decision points added.

sion points do not correspond to a weather change for a scenario, then a decision point may force some sub scenarios to be split in to two separate sub scenarios with the same weather parameters. Figure 3.3 shows a weather scenario tree that has the decision points superimposed. All suppression actions determined at decision point one (and therefore occur between decision point one and decision point two) must be the same. Depending on the weather outcome, there are three possible recourse decisions, which will reflect whether the weather actually followed sub scenario a, sub scenarios b and f, or sub scenarios b and g. The recourse decisions do not need to be the same, but for recourse decision a, the actions happening after decision point two must be the same for sub scenarios c, d, e, h, and i. Similarly, the recourse decisions for b-f and for b-g must hold for the second half of f and g and for all of sub scenarios j and k. While no changes are necessary for sub scenarios c, d, and e, sub scenarios f and g both must form two new sub scenarios at decision point two.

$$Y_{i,q_k} = Y_{i,q_m} \quad \forall i, q_m \text{ and } q_k \in \Lambda_p, p \in \{0, ..., \tilde{m} - 1\} \tag{3.25}$$

Equation 3.25 ensures that if sub scenarios q_k and q_m branch from the same previous sub scenario, then their suppression control placements must be equal.

3.2.3 Objective Functions

Several different objective functions were used to test this model.

$$\text{Min } Z = \sum_{q} \Pr[q] \sum_{k \in \Phi_q} \sum_{i} D_{i,q_m} \tag{3.26}$$

$$\text{Min } Z = \sum_{q} \Pr[q] \sum_{i} (1.75 B_{i,q} - G_{i,q}) \tag{3.27}$$

$$\text{Min } Z = \sum_{q} \Pr[q] \sum_{i} B_{i,q} \tag{3.28}$$

Equation 3.26 minimizes total expected burned area (both during the planning horizon and after the planning horizon is over). Equation 3.27 minimizes the expected number of nodes that burn at a harmful intensity while also maximizing the expected number of nodes that burn at a beneficial intensity, again, weighted by the probability that scenario q occurs. The nodes that burn at a harmful intensity are weighted to be more important than those that burn at a beneficial intensity. Equation 3.28 minimizes the expected number of nodes that burn above the intensity threshold. I chose not to include any incentive to use suppression efficiently because the test cases I examined all had scarce enough suppression resources that the model was forced to use the resources efficiently without having control points in the objective function.

3.3 Results

Three sets of wind directions (which correspond directly to major spread direction on flat homogeneous landscapes) and two sets of fire shapes are used for fire growth and behavior parameters in the test cases that follow. The two sets of fire shape parameters are listed in Tables 3.1 and 3.2. The winds can come from the southwest, the west, or the south. The parameter sets will be referred to by fire shape and the wind direction (for example, fast southwest winds or slow west winds). These are consistent with the two sets of weather

Table 3.1: The "fast" set of weather parameters used to test the deterministic mixed integer programming model. This set of parameters is based upon fuel model 122 on a low fuel moisture day with 15 mph winds.

Fast Winds Characteristic	Value
Max ROS	39 ft/min
Ellipse B	25.5 ft/min
Ellipse C	4.16 ft/min
Max Fireline Intensity	348.94 BTU/ft/sec
Intensity Threshold	215 BTU/ft/sec
Possible Major Spread Directions	Northeast (45), North (0), or East (90)

Table 3.2: The "slow" set of weather parameters used to test the deterministic mixed integer programming model. This set of parameters is based upon fuel model 122 on a low fuel moisture day with 10 mph winds.

Fast Winds Characteristic	Value
Max ROS	12.5 ft/min
Ellipse B	17.5 ft/min
Ellipse C	2.21 ft/min
Max Fireline Intensity	225.26 BTU/ft/sec
Intensity Threshold	215 BTU/ft/sec
Possible Major Spread Directions	Northeast (45), North (0), or East (90)

parameters used in Chapter 2. The parameter set called "southwest winds" in Chapter 2 is now called the "slow southwest winds" parameter set and the parameters referred to as "south winds" are now the "slow south winds" parameters. For most of the examples, 215 BTU/ft/sec (about 6 ft flame lengths) was used as the fireline intensity threshold; those examples with a different threshold are noted in the text. Unless otherwise explicitly noted, the objective function used for the tests is Equation 3.26 and the probabilities of all scenarios are assumed to be equal. A fireline intensity threshold of 215 BTU/ft/sec is used to determine if fire is beneficial or harmful unless otherwise noted.

The test cases in this chapter are presented in a similar format to Chapter 2. Color gradients have been added to show additional information about sub scenarios and fireline intensity. In the fire arrival time maps (labeled "a") and the fire spread pattern maps

(labeled "b"), each gradient darker indicates fire arrival one sub scenario later. In the fireline intensity maps (labeled "c"), yellow indicates that the fireline intensity was under the intensity threshold (i.e., is designated as beneficial) while red indicates that the fireline intensity was over the intensity threshold (is harmful).

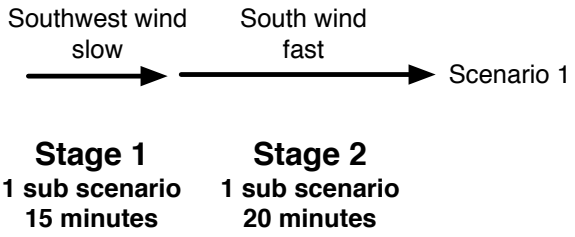

Figure 3.4: The weather scenario tree used to parameterize the results shown in Figure 3.5.

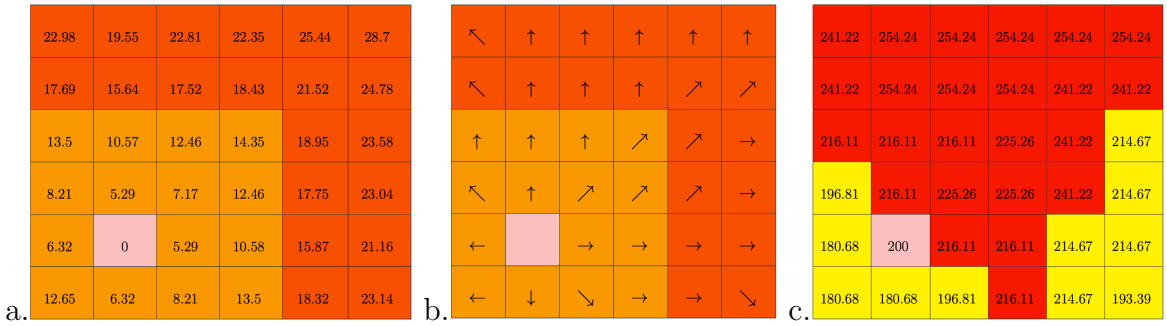

Figure 3.5: Fire arrival time (a), spread directions (b) and fireline intensities (c) for weather scenarios 1, 2, and 3 using the weather scenario tree shown in Figure 3.4.

The first and second test cases (Figures 3.5 and 3.7) use the simplest weather trees to demonstrate fire behavior responding to a weather change. These test cases are actually deterministic but with one weather change during the planning horizon: the weather trees consist of two sub scenarios that form one weather scenario (Figures 3.4 and 3.6). The two test cases have switched weather patterns: for the results shown in Figure 3.5 the weather

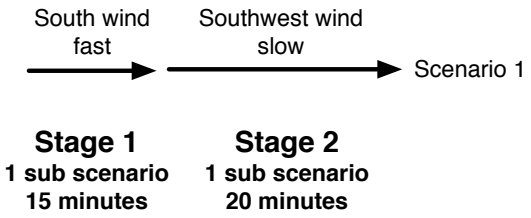

Figure 3.6: The weather scenario tree used to parameterize the results shown in Figure 3.7.

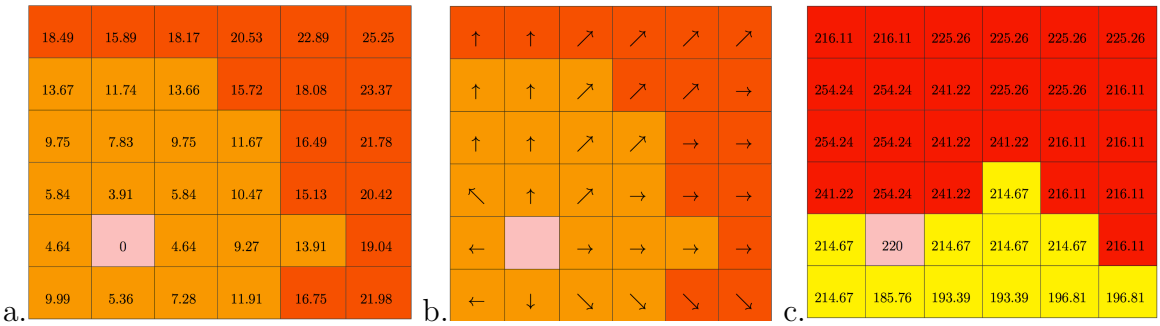

Legend for columns a and b:
- Fire arrived during sub scenario one
- Fire arrived during sub scenario two
- Fire never arrived in node
- Ignition occurred in node

Legend for column c:
- Fireline intensity under threshold
- Fireline intensity over threshold
- Fire never arrived in node

Figure 3.7: Fire arrival time (a), spread directions (b) and fireline intensities (c) for weather scenarios 1, 2, and 3 using the weather scenario tree shown in Figure 3.6.

is slow southwest winds for the first 15 minutes when it changes to the fast south winds for the last 20 minutes. The results in Figure 3.6 have flipped the sub scenarios: the weather is fast south winds for the first 15 minutes when it changes to slow southwest winds for the last 20 minutes.

The fire behavior in the first sub scenario of Figure 3.5 is the same as the fire behavior from the deterministic model with southwest slow winds (Figure 2.5.1). However, the behavior changes dramatically in the second sub scenario of Figure 3.5, arriving at the top edge much sooner than in Figure 2.5.1. The fireline intensity of the second sub scenario is also higher than the intensity from the deterministic model. In Figure 3.7, the first sub scenario shows a faster, more intense fire than the first sub scenario in Figure 3.5 and the nodes burned in the second sub scenario show a slower burning, less intense fire.

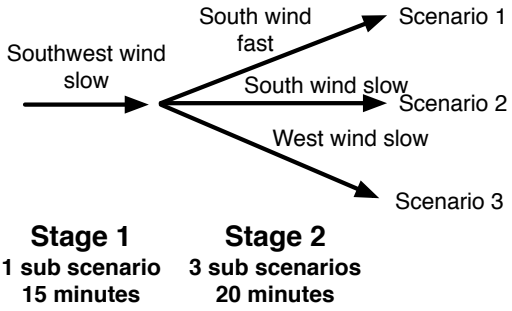

Figure 3.8: The weather scenario tree used to parameterize the results shown in Figure 3.9.

Figure 3.9 show the results from a more sophisticated weather tree, with three possible scenarios (Figure 3.8). Weather is now truly stochastic. Because all the scenarios share their first sub scenario, the fire behavior is identical in the first 15 minutes for all three weather scenarios. In the second sub scenario, the weather changes are clearly reflected by the fire behavior. Fire reaches all nodes that burn during the second sub scenario faster in Figure 3.9.1 than in Figures 3.9.2 or 3.9.3. Figures 3.9.2 and 3.9.3 mirror each other accross the northeast-southwest diagonal in the second sub scenario: for example, after 23.31 minutes, fire arrives at the northwest corner in Figure 3.9 and at the southeast corner of Figure 3.9.3. Given that fire spread in the northeast direction in the first sub scenario and

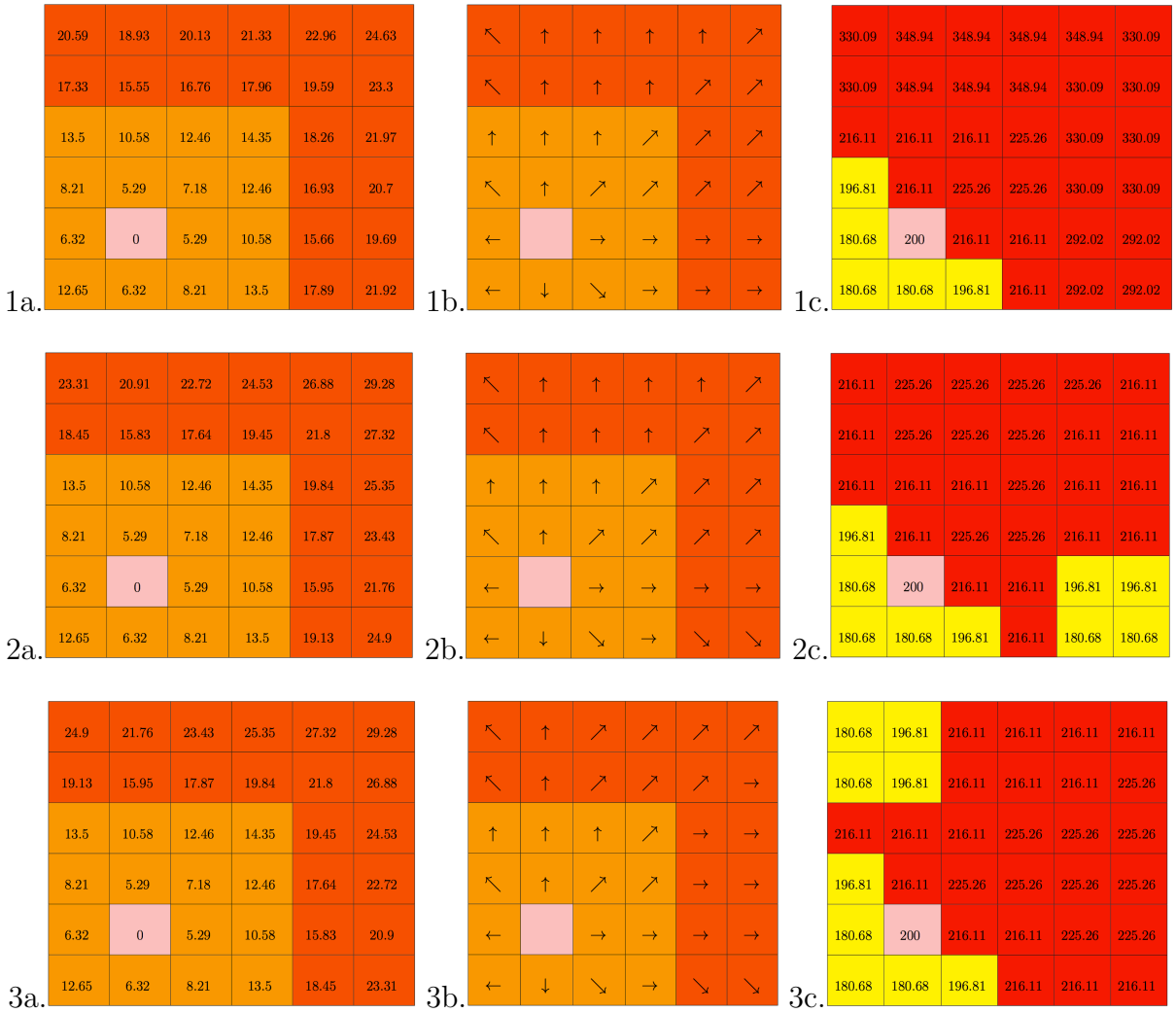

Legend for columns a and b:

- Fire arrived during sub scenario one
- Fire arrived during sub scenario two
- Fire never arrived in node
- Ignition occurred in node

Legend for column c:

- Fireline intensity under threshold
- Fireline intensity over threshold
- Fire never arrived in node

Figure 3.9: Fire arrival time (a), spread directions (b) and fireline intensities (c) for weather scenarios 1, 2, and 3 using the weather scenario tree shown in Figure 3.8.

then the winds changed to come from the south (Figure 3.9.2) and the west (Figure 3.9.3) we expect to see these two scenarios mirroring each other.

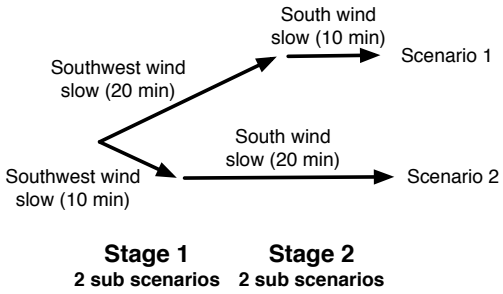

Figure 3.10: The weather scenario tree used to parameterize the results shown in Figure 3.11.

The results in Figure 3.9 shows an example of how the model can be used when there is uncertainty in the weather parameters themselves. Figure 3.10 presents a weather tree that reflects uncertainty in when the weather changes rather than how the parameters will change. This weather tree consists of two scenarios; in the first scenario the winds are slow and from the southwest for the first twenty minutes and then change to southerly winds at the same speed for the last ten minutes, conversely, in the second scenario the southwest winds last for only the first ten minutes and the south winds show up in the last twenty minutes of the scenario. The fire arrives slightly earlier in the southeast corner of the first scenario (Figure 3.11.1a) where the southwest wind lasts longer than in the second scenario (Figure 3.11.2a). The fireline intensities (Figures 3.11.1c and 3.11.2c) change as well, mostly due to how the wind aligns with the spread directions as many spread directions stay the same (Figure 3.11.1b and 3.11.2b), although a few MTT paths on the second column from the west and the second column from the south do change. The intensity threshold was changed to 220 BTU/ft/sec here to ensure that the model was indeed keeping track of beneficial and harmful fire designations properly and Figure 3.11c shows this is the case.

The test case in Figure 3.13 shows sub scenarios with varying lengths and a non-symmetrical tree structure (Figure 3.12). The intensity threshold was again set to 220 BTU/ft/sec. Scenarios 1 and 2 are exactly the same as in Figure 3.10; a slower southwest wind for the first ten minutes changing to a slow south wind for the last ten minutes for the first scenario with

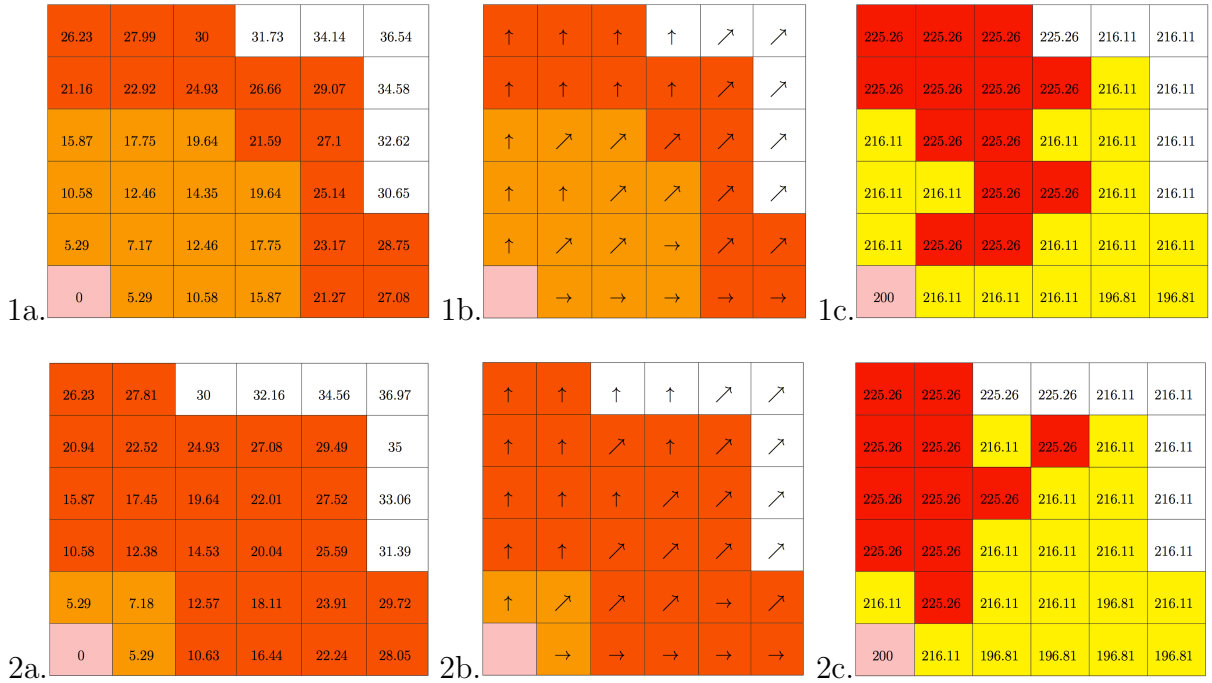

Legend for columns a and b:

- Fire arrived during sub scenario one
- Fire arrived during sub scenario two
- Fire never arrived in node
- Ignition occurred in node

Legend for column c:

- Fireline intensity under threshold
- Fireline intensity over threshold
- Fire never arrived in node

Figure 3.11: Fire arrival time (a), spread directions (b) and fireline intensities (c) for weather scenarios 1, 2, and 3 using the weather scenario tree shown in Figure 3.10.

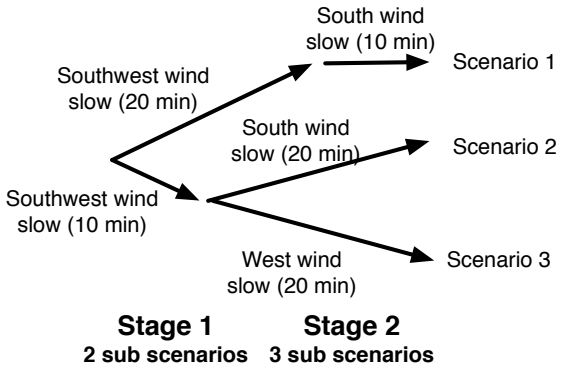

Figure 3.12: The weather scenario tree used to parameterize the results shown in Figure 3.13.

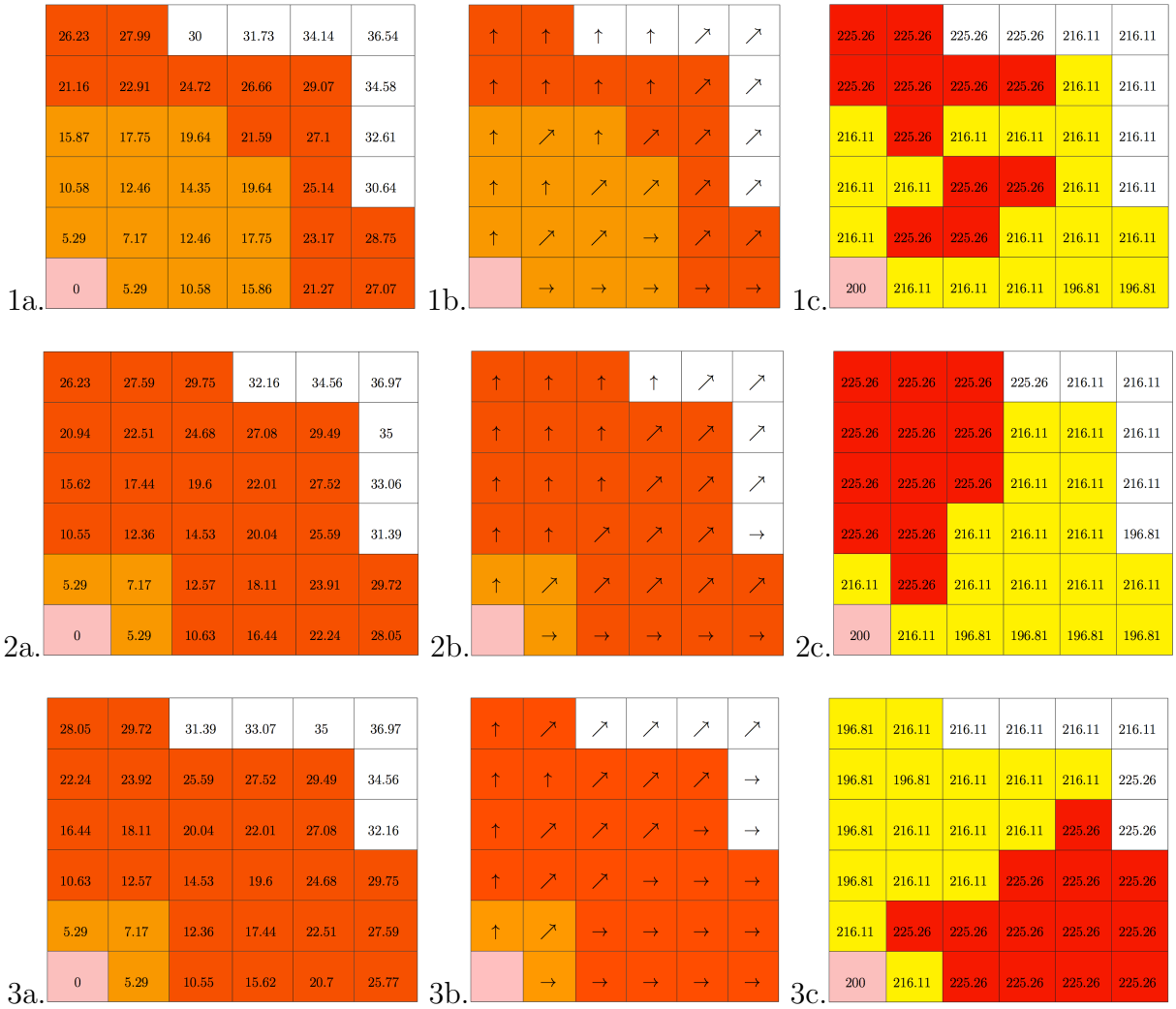

Figure 3.13: Fire arrival time (a), spread directions (b) and fireline intensities (c) for weather scenarios 1, 2, and 3 using the weather scenario tree shown in Figure 3.12.

the second scenario weather exactly the same but changing after only ten minutes. Scenario 3 shares its first sub scenario with scenario 2, but the winds change to come from the west rather than the south. Scenarios 1 and 2 (Figure 3.13.1 and Figure 3.13.2) exhibit the same fire behavior as the results in Figure 3.11. In Figure 3.13.3, the fire behavior mirrors the behavior shown in Figure 3.13.2 across the northeast-southwest diagonal.

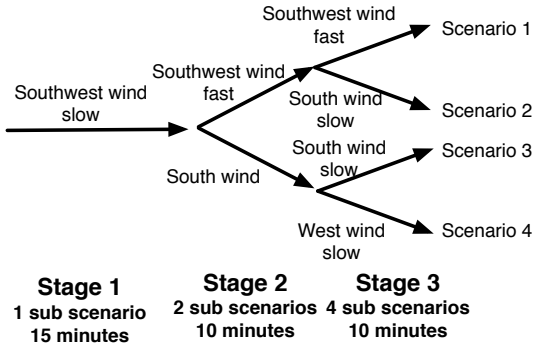

Figure 3.14: The weather scenario tree used to parameterize the results shown in Figure 3.15.

Figure 3.15 shows the results from a three sub scenario model with four weather scenarios (Figure 3.14). All four scenarios share the same first sub scenario and consequently, all four scenarios have exactly the same first sub scenario fire behavior. Similarly, the first and second scenario share a second sub scenario and exhibit the same fire behavior and the third and fourth scenarios also share their second sub scenarios and also show the same fire behavior. None of the four scenarios share a third sub scenario and all four scenarios have unique third sub scenario fire behavior. The intensity threshold was 220 BTU/ft/sec in these results, which help the fireline intensity maps highlight the differences and similarities between scenarios (Figure 3.15c)

The model can accommodate any number of sub scenarios, as demonstrated by the results in Figure 3.17. The corresponding weather tree is pictured in Figure 3.16 and is comprised of two scenarios that are each six sub scenarios long. The beginning of each sub scenario represents a decision point, as the weather stays constant for the last five stages in each weather scenario. The results show the same symmetry that numerous previous cases have shown: the fire behavior is symmetrical across the southwest-northeast diagonal due to the

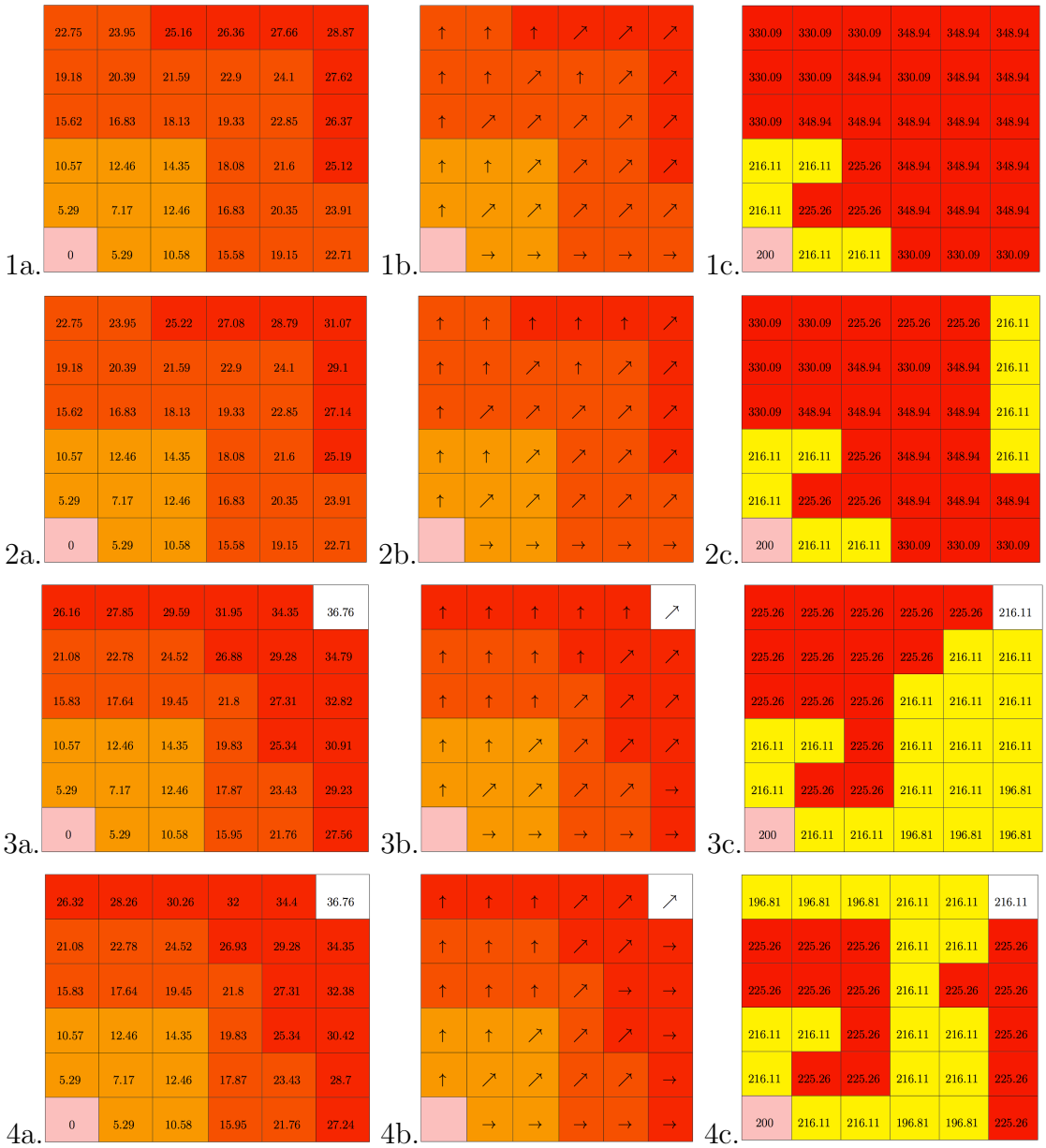

Legend for columns a and b:

- Fire arrived during sub scenario one
- Fire arrived during sub scenario two
- Fire arrived during sub scenario three
- Fire never arrived in node
- Ignition occurred in node

Legend for column c:

- Fireline intensity under threshold
- Fireline intensity over threshold
- Fire never arrived in node

Figure 3.15: Fire arrival time (a), spread directions (b) and fireline intensities (c) for weather scenarios 1, 2, 3 and 4 using the weather scenario tree shown in Figure 3.14.

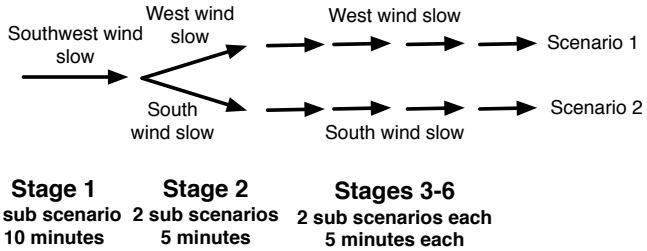

Figure 3.16: The weather scenario tree used to parameterize the results shown in Figure 3.17.

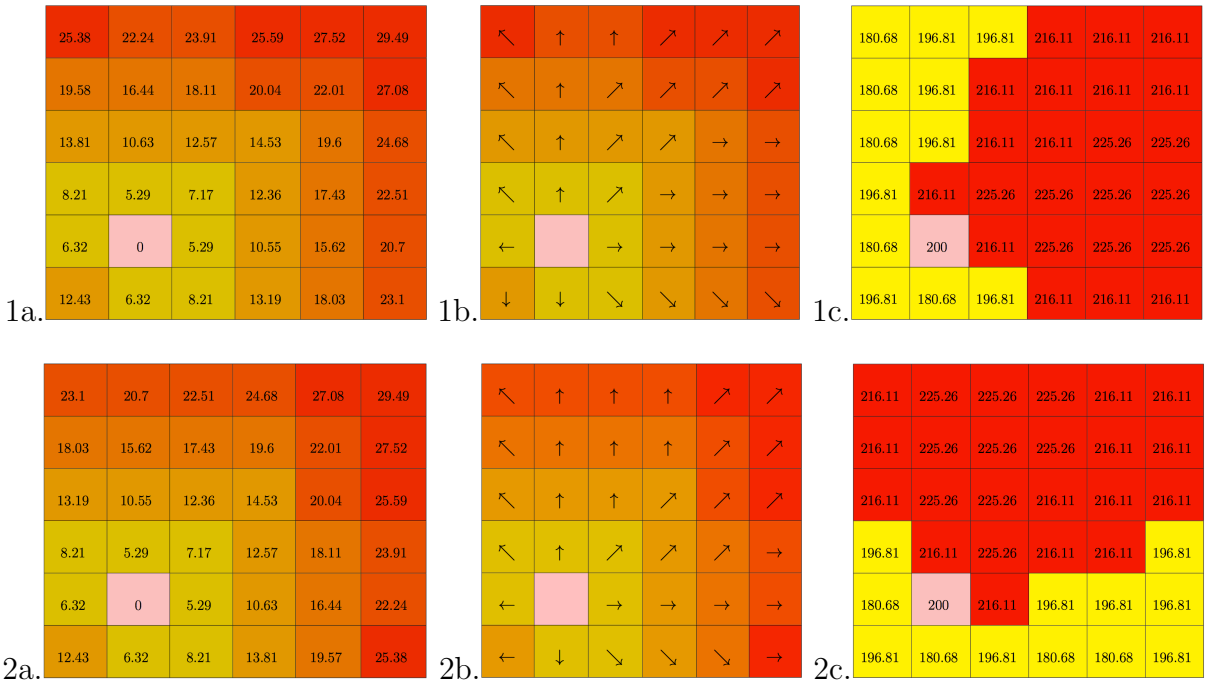

Legend for columns a and b:
- Fire arrived in node during stage one
- Fire arrived in node during stage two
- Fire arrived in node during stage three
- Fire arrived in node during stage four
- Fire arrived in node during stage five
- Fire never arrived in node
- Ignition occurred in node

Legend for column c:
- Fireline intensity under threshold
- Fireline intensity over threshold
- Fire never arrived in node

Figure 3.17: Fire arrival time (a), spread directions (b) and fireline intensities (c) for weather scenarios 1 and 2 using the weather scenario tree shown in Figure 3.16.

south winds in the first scenario (Figure 3.17.1) and the west winds in the second scenario (Figure 3.17.2).

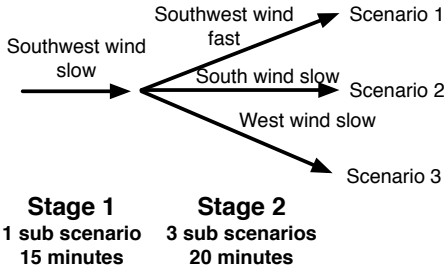

Figure 3.18: The weather scenario tree used to parameterize the results shown in Figure 3.19.

The previous results show the model successfully predicting fire spread for numerous weather trees. The following examples will show the model both predicting stochastic fire spread and optimizing control point placement given the different spread scenarios. The weather tree used for the next three test cases is shown in Figure 3.18. While nonanticipativity is implicit in the first stage of this tree (because all the scenarios share the first stage, the control decisions must be identical) the second stage requires explicit nonanticipativity constraints to force the model to make second stage decisions that do not anticipate which weather scenario will occur. However, the goal of these test cases is to show the model placing optimal suppression in response to differing weather scenarios. Therefore, nonanticipativity is not enforced for the second stage of results using this weather tree.

Figure 3.19 is the first test case to incorporate control points into the stochastic model. Two control points were allowed to be placed on the landscape at the beginning of the first stage and seven control points could be placed on the landscape in the second stage. Because the objective function minimized all fire on the landscape, all scenarios shared a sub scenario in the first stage, and because there were enough control points to keep any nodes from burning in the second stage, all three scenarios had the same suppression assignments regardless of second stage weather. The model used both control points in the first stage and needed six in the second stage. Although minimizing use of the control points was not included in the objective function, the model did not choose to place the extra control node

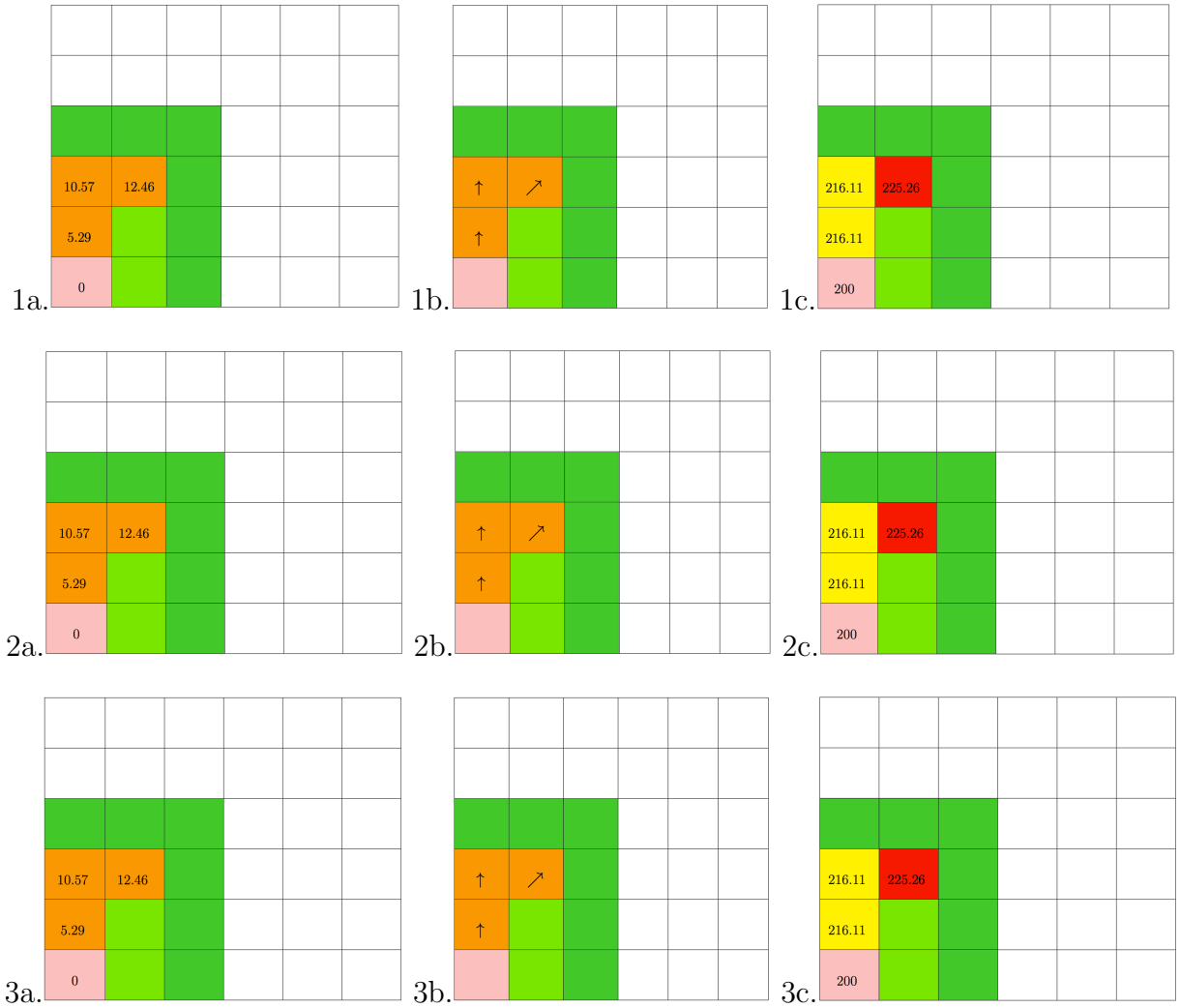

Legend for columns a and b:

- Fire arrived during sub scenario one
- Fire arrived during sub scenario two
- Fire never arrived in node
- Ignition occurred in node
- Control placed in node during stage one
- Control placed in node during stage two

Legend for column c:

- Fireline intensity under threshold
- Fireline intensity over threshold
- Fire never arrived in node

Figure 3.19: Fire arrival time (a), spread directions (b) and fireline intensities (c) for weather scenarios 1, 2, and 3 using the weather scenario tree shown in Figure 3.18.

on the landscape.

To give the model more suppression choices, I moved the ignition point into the center of the landscape. The fire behavior without any suppression is shown in Figure 3.20, which, like the previous example, uses the weather tree in Figure 3.18. The three scenarios share the first stage sub scenario, but have unique weather parameters in the second stage.

Figure 3.21 shows the results from allowing the model to place five control points in the first stage and ten control points in the second stage with everything else held constant from Figure 3.20 (using weather tree Figure 3.18). The objective function minimized the nodes that burned above the intensity threshold (Equation 3.28). In the first scenario (Figure 3.21.1), the control points fully controlled the fire, allowing only one node to burn above the intensity threshold. The control points could have been placed in this same pattern for the other two scenarios as well. However, since the only goal of the program was to minimize the nodes burned above the intensity threshold, the other two scenarios each have unique suppression patterns that both achieve just one node that burns at a harmful fireline intensity. In the second scenario (Figure 3.21.2), the fire is slowed such that two of the three nodes that burn above the intensity threshold do not burn until after the end of the planning horizon, therefore they do not get counted as either above or below. The third scenario allows the most fire on the landscape, but all of it is below the intensity threshold (Figure 3.21.3). Because all nodes share the same first stage, the decisions in the first stage are the same for all three scenarios.

The results in Figure 3.22 are also based upon the weather tree shown in Figure 3.18 and also were allowed five control points in the first stage and ten control points in the second stage. The only difference between Figures 3.21 and 3.22 is the objective function: in Figure 3.22 uses the objective function shown in Equation 3.28 instead of Equation 3.27, which maximizes the nodes that burn below the intensity threshold and minimizes the number of nodes that burn above the intensity threshold. The nodes that burn above the intensity threshold are weighted to be 1.75 times more important than the nodes that burn below the

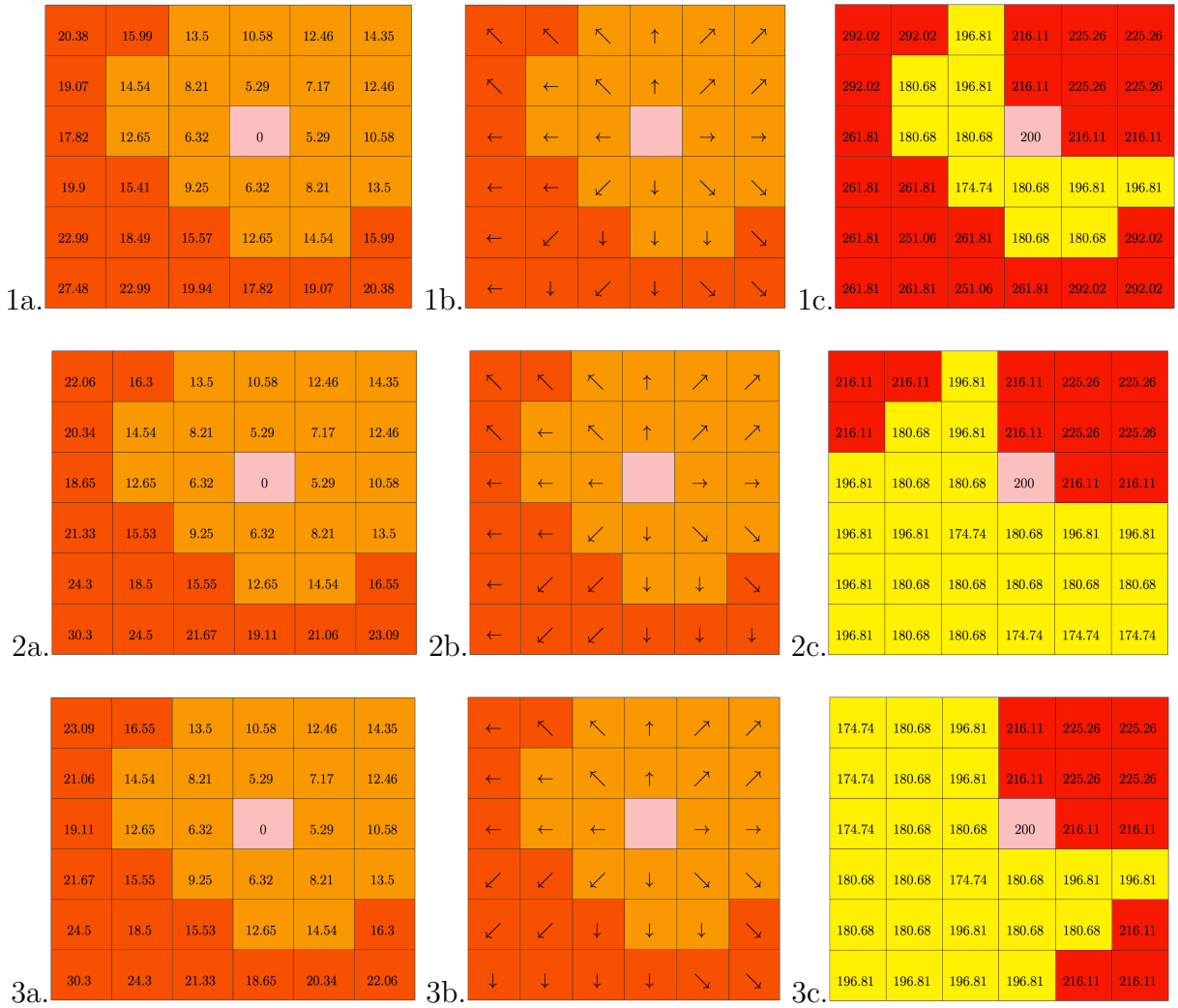

Legend for columns a and b:

- Fire arrived in node during stage one
- Fire arrived in node during stage two
- Fire never arrived in node
- Ignition occurred in node

Legend for column c:

- Fireline intensity under threshold
- Fireline intensity over threshold
- Fire never arrived in node

Figure 3.20: Fire arrival time (a), spread directions (b) and fireline intensities (c) for weather scenarios 1, 2, and 3 using the weather scenario tree shown in Figure 3.18.

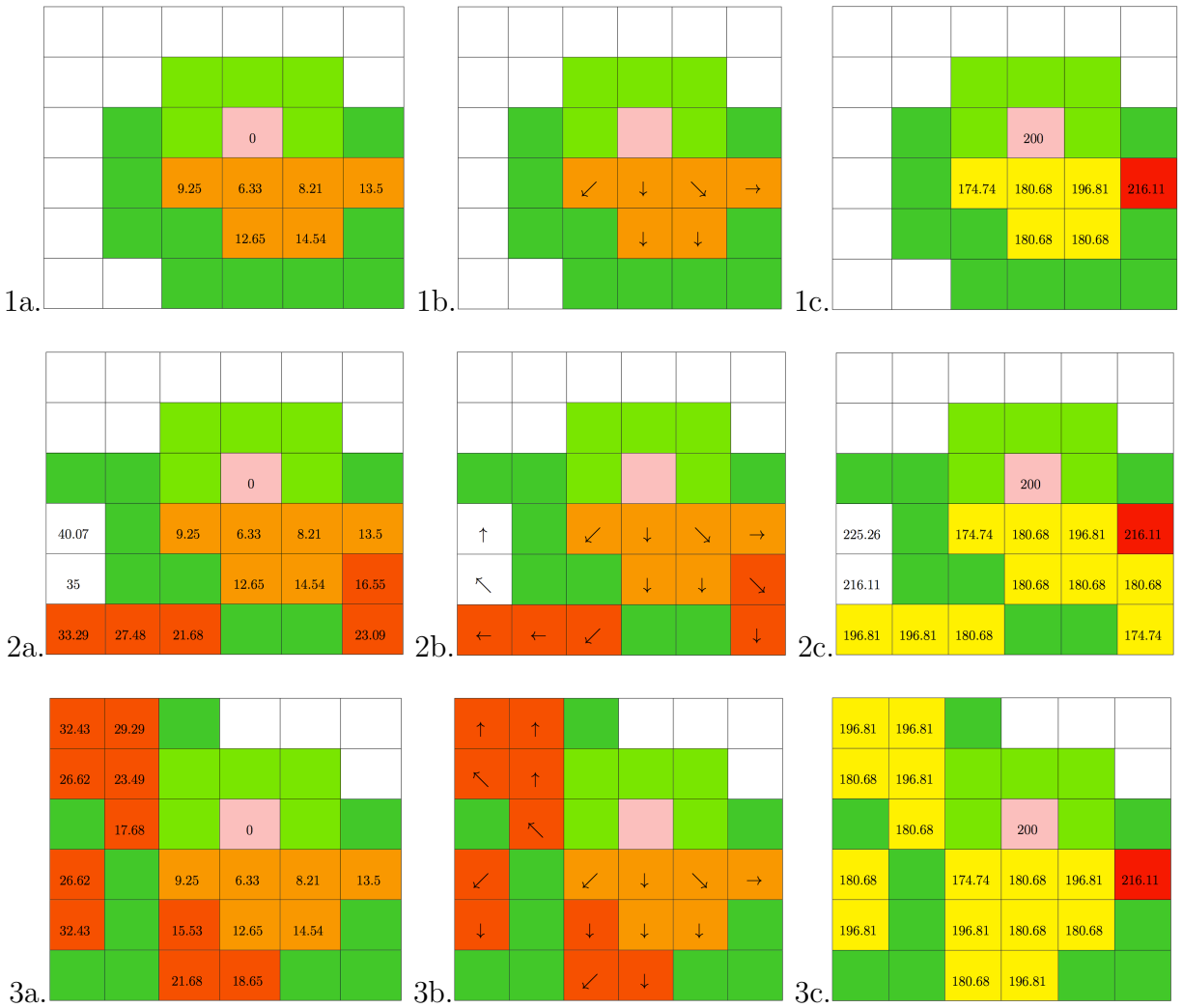

Legend for columns a and b:

- Fire arrived in node during stage one
- Fire arrived in node during stage two
- Fire never arrived in node
- Ignition occurred in node
- Control placed in node during stage one
- Control placed in node during stage two

Legend for column c:

- Fireline intensity under threshold
- Fireline intensity over threshold
- Fire never arrived in node

Figure 3.21: Fire arrival time (a), spread directions (b) and fireline intensities (c) for weather scenarios 1, 2, and 3 using the weather scenario tree shown in Figure 3.18.

intensity threshold. One important aspect of Equation 3.28 is that it does not weight the nodes by which stage they burn in. The node directly north of the ignition point (node n) and the node directly south of the ignition point (node s) count as six nodes that burned below the intensity threshold rather than just two. Although these nodes could have been successfully suppressed, allowing them to burn allowed at least eleven other nodes to burn under the intensity threshold where they otherwise would have either required suppression or burned above the threshold. For example, in Figure 3.22.2, if node n had not burned, then the node directly west of node n and the node northwest of node n would have received fire from the nodes directly south, and would have burned above the intensity threshold. The same reasoning holds for node s in Figure 3.22.3; the nodes to the south and southwest would have received fire from the nodes directly east and would have burned at above the intensity threshold. This is the first result presented that did not run to absolute optimality. While I cannot find any option that would be better than the best integer solution found by CPLEX, there was still a 40% gap after running for over 12 hours. I found that most results that used an objective function minimizing nodes burned above the intensity threshold and maximizing those that burned below were very difficult to solve. I will address this further in Chapter 5.

The maps in Figure 3.23 are another result from the weather tree pictured in 3.18. Note that in Figure 3.21, where Equation 3.28 was used to minimize the number of nodes burned above the intensity threshold, the control placement resulted in one node burned above the intensity threshold per scenario, just as the control point placement does in these results. The results in Figure 3.23 are therefore an alternative optima for the results in Figure 3.21 if Equation 3.28 is the objective function, but not for Equation 3.26.

Two more important aspects of the model have not yet been tested: unequal weather scenarios and nonanticipativity. In all of the previous results, I assumed that the weather scenarios were equally probable. However, this is not likely to be the case with real weather forecasts. Figures 3.26 and 3.27 are the first examples of weather scenarios with unequal

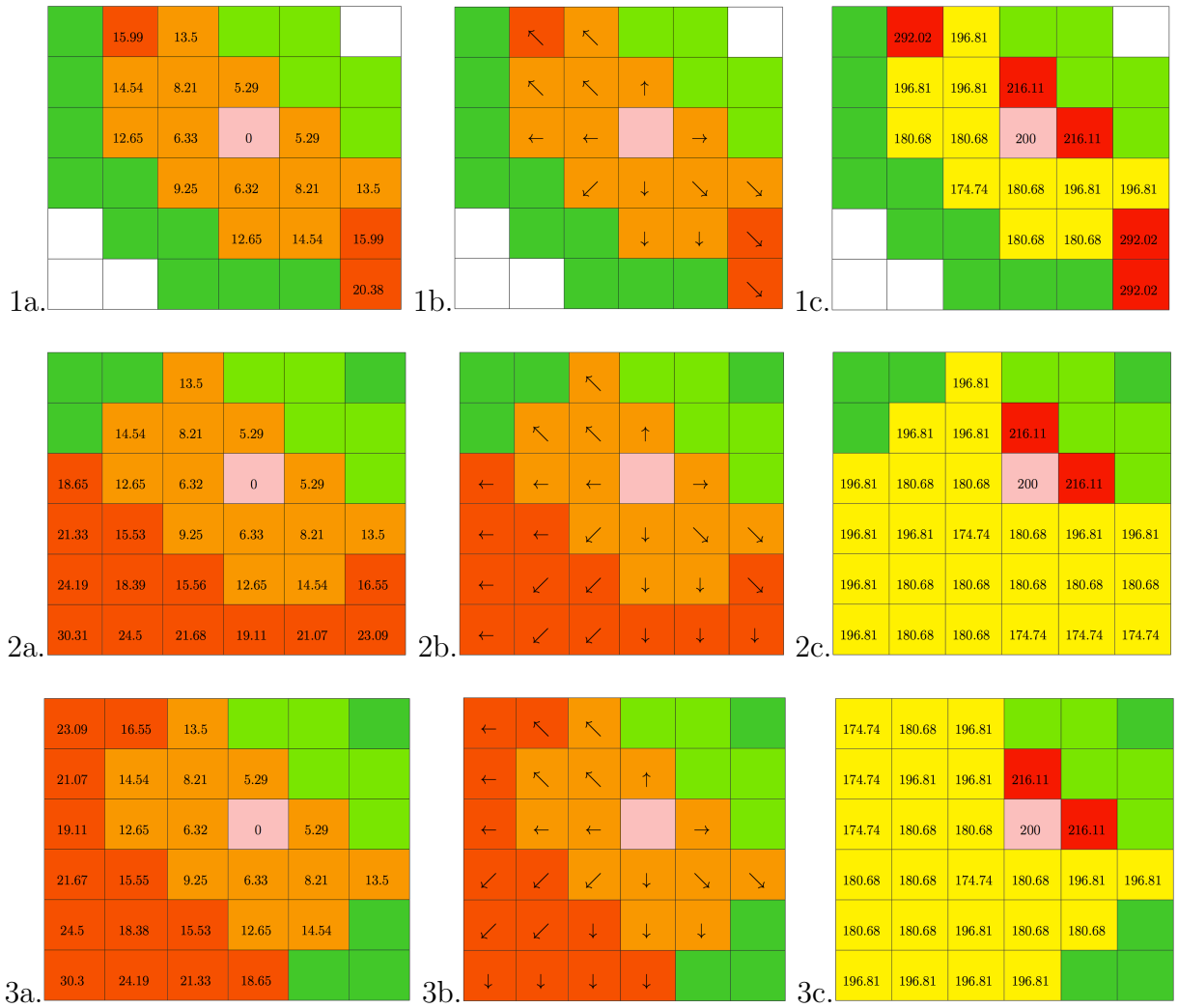

Legend for columns a and b:

- Fire arrived in node during stage one
- Fire arrived in node during stage two
- Fire never arrived in node
- Ignition occurred in node
- Control placed in node during stage one
- Control placed in node during stage two

Legend for column c:

- Fireline intensity under threshold
- Fireline intensity over threshold
- Fire never arrived in node

Figure 3.22: Fire arrival time (a), spread directions (b) and fireline intensities (c) for weather scenarios 1, 2, and 3 using the weather scenario tree shown in Figure 3.18.

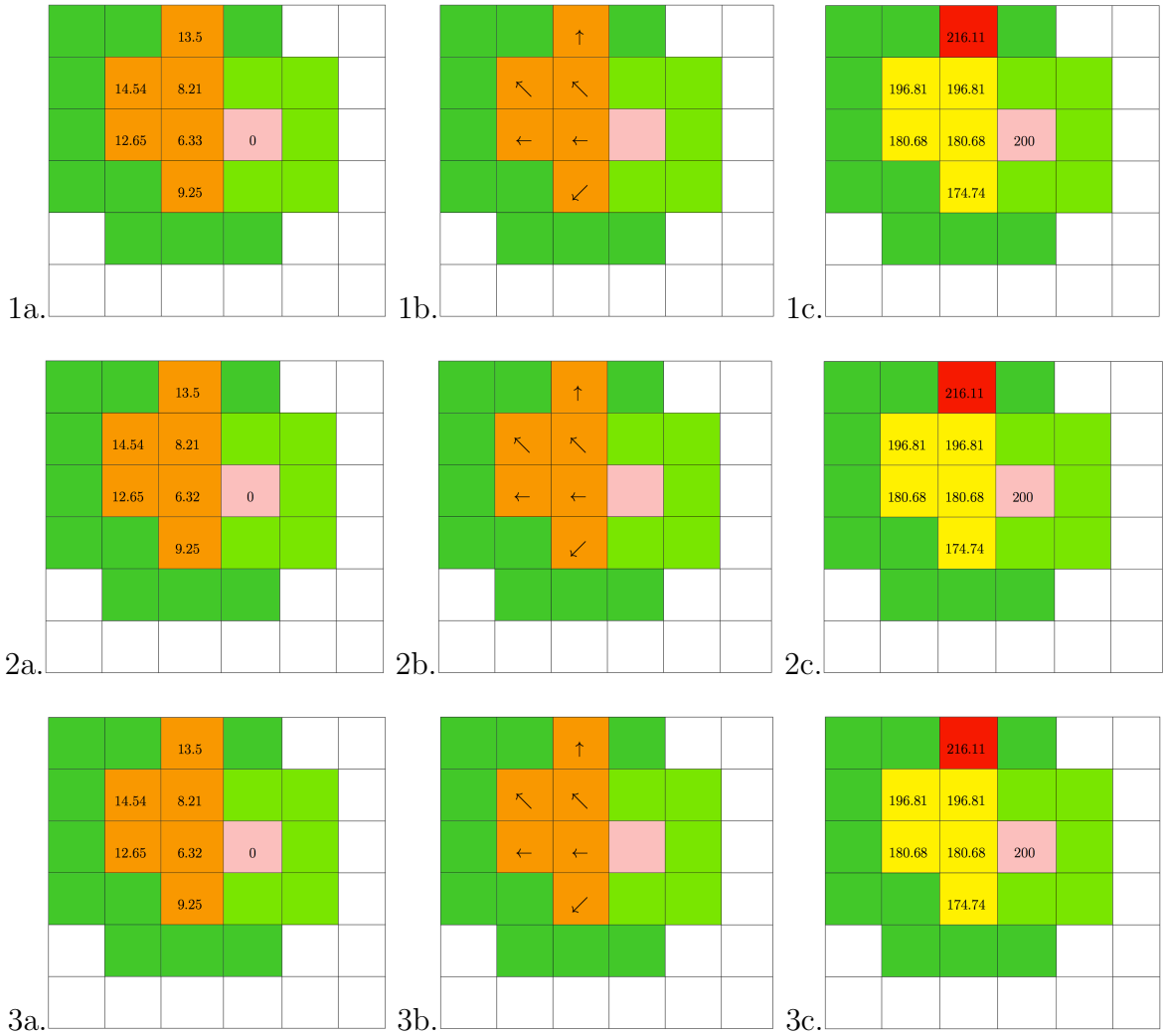

Legend for columns a and b:

- Fire arrived in node during stage one
- Fire arrived in node during stage two
- Fire never arrived in node
- Ignition occurred in node
- Control placed in node during stage one
- Control placed in node during stage two

Legend for column c:

- Fireline intensity under threshold
- Fireline intensity over threshold
- Fire never arrived in node

Figure 3.23: Fire arrival time (a), spread directions (b) and fireline intensities (c) for weather scenarios 1, 2, and 3 using the weather scenario tree shown in Figure 3.8.

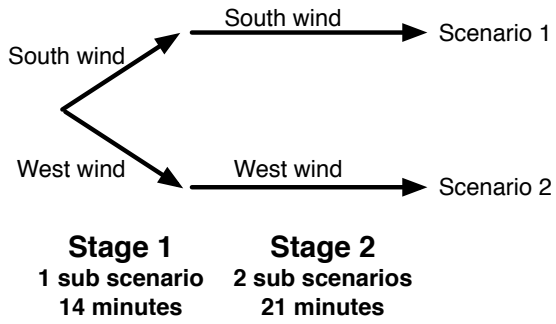

Figure 3.24: The weather tree for the test cases in Figures 3.25-3.27.

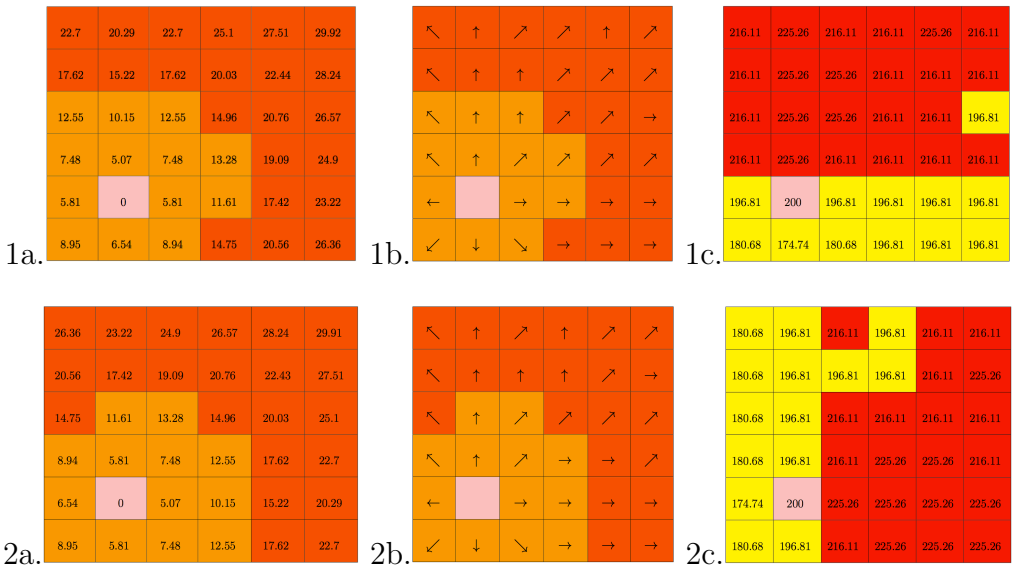

Legend for columns a and b:
- Fire arrived in node during stage one
- Fire arrived in node during stage two
- Fire never arrived in node
- Ignition occurred in node
- Control placed in node during stage one
- Control placed in node during stage two

Legend for column c:
- Fireline intensity under threshold
- Fireline intensity over threshold
- Fire never arrived in node

Figure 3.25: Fire arrival time (a), spread directions (b), fireline intensities (c), crew travel paths (d) and crew completion times (e) for weather scenarios 1 and 2 using the weather scenario tree shown in Figure 3.24.

probabilities. These results use the weather tree in Figure 3.24 and Equation 3.26 as the objective function. The fire behavior with no suppression can be seen in Figure 3.25. The results in Figure 3.26 show the model results when the first scenario with southerly winds is three times as likely as the second scenario with westerly winds. When the probabilities are swapped and the second scenario is three times as likely to happen as the first, the optimal control placement changes (Figure 3.27). The two optimal solutions are similar: in Figure 3.26.1, the control placement is symmetrical across the southwest-northeast diagonal with the control placement in Figure 3.27.2 and the control placement has the same symmetry for Figures 3.26.2 and 3.27.1. This symmetry is expected, as the weather driving the fire behavior is symmetrical across the southwest-northeast diagonal. The change in optimal control placement is driven by the weather scenario probabilities: the model saves more nodes in the scenarios which are more likely to happen (Figures 3.26.1 and 3.27.2) and fewer nodes in the scenarios less likely to occur (Figures 3.26.2 and 3.27.1). These optimal solutions do minimize the expected value of nodes burned.

The results in Figures 3.26 and 3.27 also show the model producing nonanticipative and recourse decisions. Explicit nonanticipativity constraints were enforced in the first stage for both test cases, which results in the same first stage decisions for both two scenarios of each test case (Figures 3.26.1 and 3.26.2 have identical first stage decisions as do Figures 3.27.1 and 3.27.2). However, the recourse decisions in the second stage are different depending on the outcome of the first stage scenario. Because the model would like to save more nodes from burning in the most probable scenario, the first stage decisions set up control points such that the recourse decisions in the second stage save two more nodes in the more probable scenarios than in the less probable scenarios.

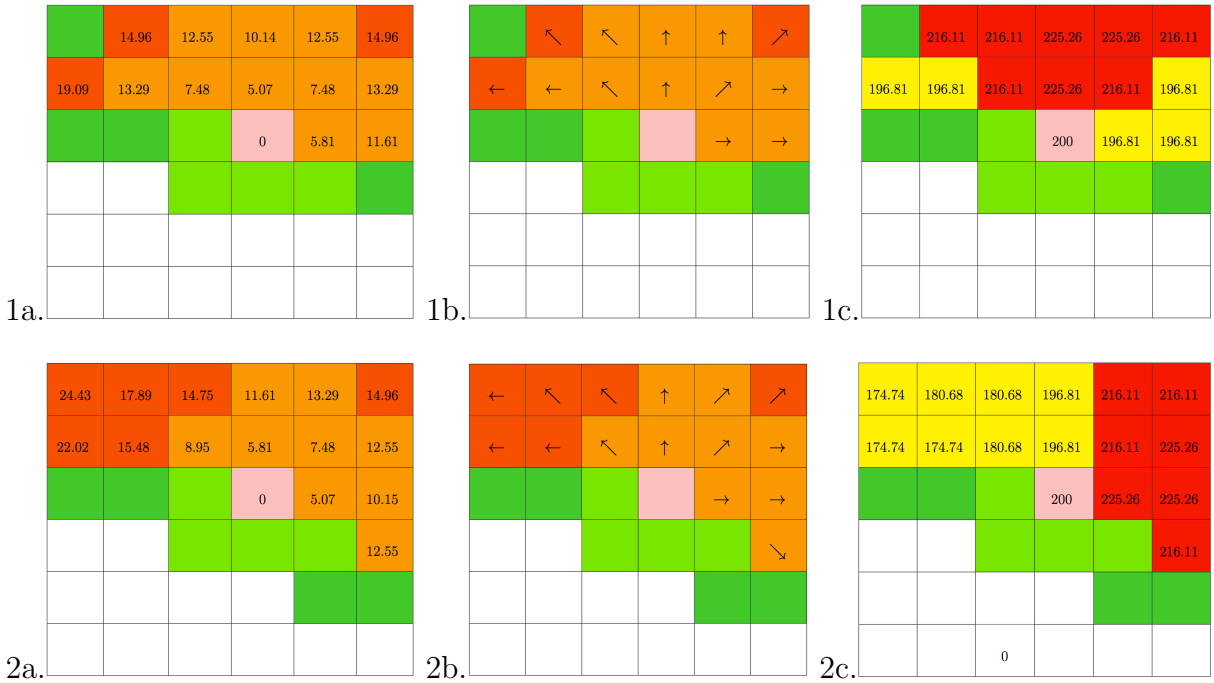

Legend for columns a and b:

- Fire arrived in node during stage one
- Fire arrived in node during stage two
- Fire never arrived in node
- Ignition occurred in node
- Control placed in node during stage one
- Control placed in node during stage two

Legend for column c:

- Fireline intensity under threshold
- Fireline intensity over threshold
- Fire never arrived in node

Figure 3.26: Fire arrival time (a), spread directions (b) and fireline intensities (c) for weather scenarios 1, 2, and 3 using the weather scenario tree shown in Figure 3.24.

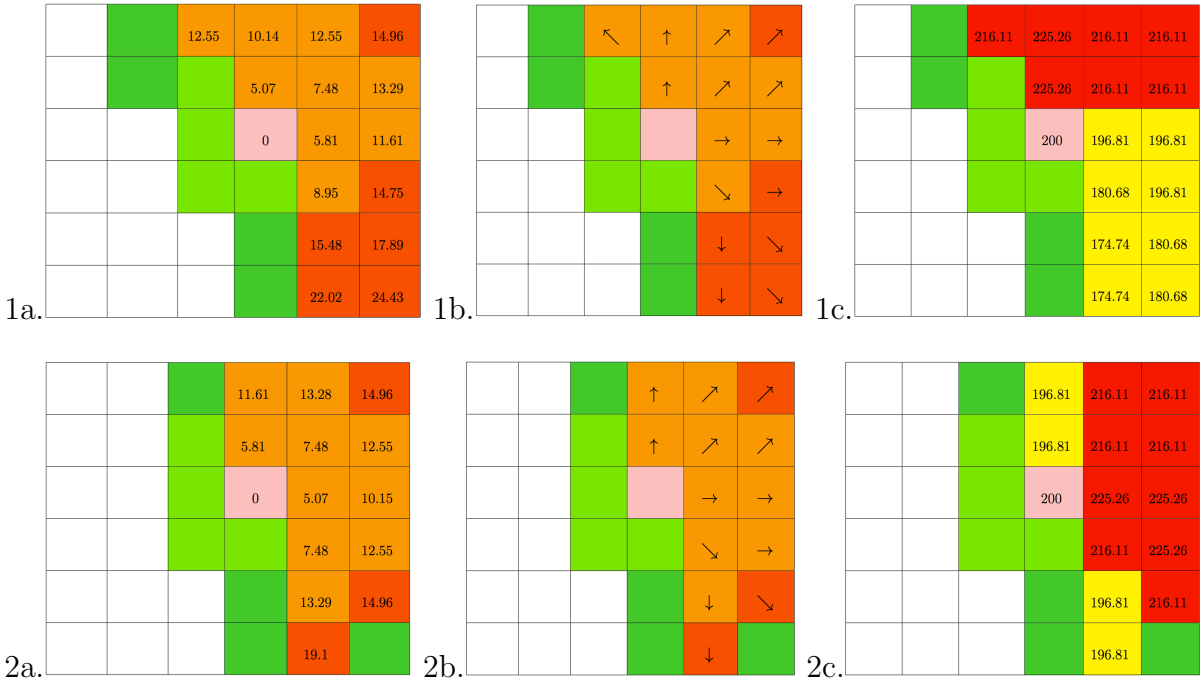

Legend for columns a and b:

- Fire arrived in node during stage one
- Fire arrived in node during stage two
- Fire never arrived in node
- Ignition occurred in node
- Control placed in node during stage one
- Control placed in node during stage two

Legend for column c:

- Fireline intensity under threshold
- Fireline intensity over threshold
- Fire never arrived in node

Figure 3.27: Fire arrival time (a), spread directions (b) and fireline intensities (c) for weather scenarios 1, 2, and 3 using the weather scenario tree shown in Figure 3.24.

3.4 Discussion

This chapter introduces a stochastic mixed integer programming model that predicts fire behavior for a raster grid given a stochastic weather tree and optimizes the placement of control points. Results were presented that showed fire behavior reacting to differing weather trees including weather trees with unequally likely scenarios, differing ignition points, differing control scenarios, and nonanticipativity constraints. The mathematical program explicitly models fireline intensity and classifies it as harmful or beneficial depending on a fireline intensity threshold. While the model presented in this chapter eliminates some weaknesses of the model from Chapter 2 (stochastic weather and multiple objectives have been added) some of the weaknesses identified in Chapter 2 still remain.

The suppression decisions made by this model are still simplistic. They are more nuanced than the control points used in Chapter 2 because the model can control the location of the control point in specific stages, they still do not account for many important facets of suppression. They do not acknowledge the spatial restrictions of crew movements, i.e., that crews' travel and suppression actions must be spatially continuous. Safety concerns for fire crews are also not addressed in this model. The control points used in this chapter still assume that if control is placed in a node, then the node becomes a barrier to fire. However, if fireline is not robust enough, then fire may jump the line. Therefore, this definition of control may not reflect actual fireline quality issues accurately.

Because the integer programming model built in this chapter is much more complex than the deterministic model in Chapter 2, large landscapes present an even harder problem to solve. Again, the solution algorithms have a much larger decision space to cover; therefore the algorithms run much slower on a large landscape. Additionally, because changing a fire spread path can change the fireline intensity at a node, objective functions that minimize nodes burned at a harmful intensity and maximize nodes burned at a beneficial intensity have particular problems running to optimality. Work on scaling the model up and providing incentives so that the model can handle a large landscape with more nuanced objectives is

discussed in Chapter 5.

Despite the weaknesses in solution complexity and suppression constraints identified above, the stochastic model is a step forward in modeling fire spread and suppression. This model incorporated stochastic, explicitly spatial, dynamic fire spread into an mathematical program. The inclusion of fireline intensity and fireline intensity thresholds to distinguish between harmful and beneficial fire provides many options for further extensions of the model and could allow for examining tradeoffs between different policy objectives.

In the next chapter I will introduce an enhanced model that introduces a control network to address crew behavior and fireline quality.

4 Fire Suppression Constraints for a Stochastic Programming Framework

4.1 Introduction

Chapter 3 developed a stochastic program which predicts spatially explicit fire behavior that dynamically interacts with suppression actions on the landscape. The suppression actions consisted of decisions about where to place control points on the landscape and in what stage to place them. However, two of the main assumptions underlying the control point model of suppression are quite problematic. First, suppression actions as modeled using standard production rates would not always be effective at containing a fire. For example, if a high intensity fire hits a fireline that was designed to hold a low intensity fire, then the fireline will likely fail. Second, suppression resources cannot just be placed in nodes arbitrarily. To model suppression more realistically, the spatial and temporal restrictions on the fire crews must be taken into account. In this chapter a set of constraints is developed to model a control network that allows for more realistic simulation of crew tactics. In this proof of concept study, I will focus specifically on teams of people who are creating fireline using a fire engine.

There are two main types of fireline construction: direct attack and indirect attack. If a crew is building fireline through direct attack, then they are creating fireline directly on the edge of the fire, with "one foot in the black." Indirect attack, in comparison, has the crews put fireline in place with a buffer zone between the crews and the fire so that the firefighters are never too close to the flames. Direct attack typically requires less fireline than indirect attack; however, if a fire is high intensity then direct attack may be unsafe and indirect tactics are used. The change from direct tactics to indirect tactics is not modeled as binary in this model. Rather, the safety constraints determine what size buffer the crews must keep between themselves and the fire based on the predicted fireline intensities at each node. Larger buffer zones indicate that direct attack is unsafe.

Crews begin work at one or more predetermined access points specified in the model and travel from these access points into neighboring nodes. Figure 4.1 shows a visualization of possible crew movements. As crews move from node to node, they can choose to build fireline. The length of time a crew works on each node is determined by the optimal solution. "Control line capacity" is determined by node and dictates how high the fireline intensity of the fire must be at that node in order for the fireline to fail. The control line capacity at each node will be proportional to the amount of time that the crews work on the node. If the final control line capacity completed at any given node exceeds the fireline intensity in that node then the suppression effort for that node is sufficient, i.e., the suppression actions at that node prevent the node from spreading fire to any of its neighbors. However, if the fire arrives with a fireline intensity higher than the control line capacity then the node will still be capable of spreading fire to its neighbors.

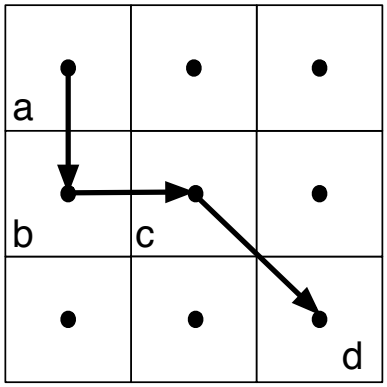

Figure 4.1: This is an example of a set of crew movements. Node a is the access point for this crew. Note that even if nodes c and d were both successfully suppressed, fire could still pass through the vertex that connects them.

The constraints developed in this chapter directly integrate with the constraints developed in Chapter 3, producing a stochastic mixed integer program with spatially explicit fire behavior that dynamically interacts with the suppression tactics.

4.2 Methods

4.2.1 Notation

As in the previous chapters, lower case arabic and greek letters represent parameters, upper case greek letters represent sets, and upper case arabic letters represent decision variables. The parameters and decision variables from the stochastic fire spread model are not repeated here, although some of them do appear in the suppression equations.

Parameters:

c = index for the crew of interest

j' = the node from which a crew enters node i

j = the node to which a crew moves to when leaving node i

$trt_{c,i,j}$ = the travel time required for crew c to travel from node i to node j

sm = amount of time needed between the fire and the crew per unit intensity if the fire is not safe for direct attack

$a_{c,i}$ = the first sub scenario at which crew c can arrive at access point i

α_i = the standardized rate at which an average crew can produce fireline in node i (for example, for every 10 minutes a crew works it can builds 10 ft of line that will holds a fire of 5 BTU/(ft-s))

Decision Variables:

$Y_{i,q}$ = indicates if suppression holds in node i during scenario q

$P_{c,i}$ = binary variable indicating if crew c choose to use node i as an access point from which to start

C_{c,j',i,q_m} = indicates if a crew moved from node j' to node i during sub scenario q_m

C_{c,i,q_m} = indicates if a crew was working in i for both sub scenarios $m-1$ and m in scenario q

$CT_{c,i,q}$ = time crew c finishes work in node i for scenario q

WT_{c,j',i,q_m} = amount of time crew c works on node i (after leaving node j') in sub scenario q_m

WT_{c,i,q_m} = amount of time crew c works on node i in sub scenario q_m (used if the crew is in node i during more than one sub scenario)

$W_{i,q}$ = total effective work on node i done during scenario q

$LC_{i,q}$ = the control line capacity in node i for scenario q

$SM_{i,q}$ = the amount of time required between a crew's departure from node i and the fire arrival (safety margin) in scenario q

$WC_{i,q}$ = the time at which all crews have completed their work on node i in scenario q

Sets:

$\mathscr{A}_c$ = the set of nodes that can be used as access points by crew c

Λ_p = the set of sub scenarios which must be non-anticipative with respect to decision point p

4.2.2 Constraints

Modifications to the Stochastic Fire Growth Equations

In order to model direct attack, suppression resources must be able to coexist with fire at each node. The spatial relationship equations that were developed in Chapter 3 only allow for either suppression or fire to take place at a node, but not both. Therefore, in order to model direct attack tactics Equations 3.2 and 3.4 must be slightly altered as shown below.

$$\sum_{m \in \Phi_q} D_{i,q_m} + \xi_i \geq \sum_{m \in \Phi_q} \left(D_{j,q_k} - Y_{j,q} \right) \quad \forall i, j \in \Omega_i, q \tag{4.1}$$

$$B_{i,j,q_m} \leq \sum_{k=1}^{m} \left(D_{i,q_k} - Y_{i,q} \right) \quad \forall i, j \in \Omega_i, q, m \in \Phi_q \tag{4.2}$$

Equation 3.2 is replaced by Equation 4.1. The new set of constraints shown in Equation 4.1 works in a similar fashion to Equation 3.2, but instead of one constraint that requires each node i to burn if at least one of its neighbors burn, a constraint is created for each neighbor j, such that if node j burns then node i must burn as well. This change allows suppression and fire to coexist in node j without forcing node i to burn (i.e, this change allows the model to simulate direct attack). Equation 4.2 replaces Equation 3.4 to reflect this change; if a cell burns but has sufficient suppression in it, then the cell can no longer spread fire to its neighbors.

Equations 4.1 and 4.2 only allow suppression in each node to be sufficient ($Y_{i,q}$=1) once per scenario. Thus, $Y_{i,q}$ only indicates whether or not the fireline created going into a node was sufficient to hold the fire in the sub scenario that the fire arrived at the node. It does not indicate anything about what sub scenario the fireline was completed.

One of the MTT constraints must also be modified.

$$TL_{j,i,q_m} \leq d_{j,i} + M \sum_{k=1}^{m} (A_{j,i,q_m} + Y_{j,q} + \xi) \quad \forall i, j \in \Omega_i, q, m \in \Phi_q \tag{4.3}$$

If node j has sufficient suppression then Equation 4.3 allows the travel time and length from node j to i to be non-binding in the other two MTT equations (Equations 3.15 and 3.16).

Spatial Crew Path Constraints

The spatial limitations to which the crews are subject are enforced by Equations 4.4-4.13. One integral assumption to the constraints presented below is that each crew is only allowed into each node once. This model could be modified to include a second arrival in each node. Adding a second arrival would allow the crews more flexibility, especially in their recourse decisions, but it would increase the model size and complexity. I also assumed that once a crew has completed their assignment (i.e., their shift is over or the fire is controlled), then they can walk out along the fireline that they created.

The equations that govern crews' spatial movements can be split into two groups: constraints that cover how a crew accesses the landscape and constraints that control how a crew moves once they are on the landscape. I will present the latter equations first.

$$\sum_{i \in \mathscr{A}_c} P_{c,i} \leq 1 \quad \forall c \tag{4.4}$$

$$\sum_{j \in \Omega_i} C_{c,i,j,q_m} + C_{c,i,q_{m+1}} \geq P_{c,i} \quad \forall c, i \in \mathscr{A}_c, q, m = a_{c,i} \tag{4.5}$$

$$\sum_{k \geq m} \sum_{j \in \Omega_i} C_{c,i,j,q_k} \geq P_{c,i} \quad \forall c, i \in \mathscr{A}_c, q, m = a_{c,i} \tag{4.6}$$

$$\sum_{k < m} \sum_{j \in \Omega_i} C_{c,i,j,q_k} + C_{c,i,q_{k+1}} \leq 0 \quad \forall c, i \in \mathscr{A}_c, q, m = a_{c,i} \tag{4.7}$$

$$\sum_{k \geq m} \sum_{j \in \Omega_i} C_{c,i,j,q_k} \leq 1 \quad \forall c, i \in \mathscr{A}_c, q, m = a_{c,i} \tag{4.8}$$

I assume that both the possible access points and the time at which each crew can arrive at the access points is predetermined. Equations 4.4-4.8 deal only with the crews' behavior at access points. Crew c may only use one access point $P_{c,i}$ (Equation 4.4). If a crew c chooses to use an access point i in sub scenario q_m then Equation 4.5 forces the crew to either stay in node i for the whole sub scenario or leave node i before sub scenario q_m ends. Similarly, if crew c decides to use an access point i, then Equation 4.6 ensures that crew c can only leave node i once in each scenario q and crew c must leave node i at some point during every scenario q. Crew c cannot be in an access point node i or leave node i in any sub scenario before crew c arrives at node i (Equation 4.7). Equation 4.8 ensures that crew c is only allowed to leave access node i once.

Once a crew leaves an access point, then their spatial behavior is restricted by Equations 4.9-4.13. I assume crews are on foot or in an engine, so they must travel in a continuous path. A crew may continue to work on a node as long as the model deems necessary, which may be for less than a sub scenario or may be for multiple sub scenarios.

$$C_{c,i,q_m} \leq 1 - \sum_{k=1}^{m-1} \sum_{j \in \Omega_i} C_{c,i,j,q_{k-1}} \quad \forall c, i, q, m > 1 \tag{4.9}$$

$$P_{c,i} + \sum_{k=1}^{\tilde{m_q}-1} \sum_{j' \in \Omega_i} C_{c,j',i,q_k} \leq 1 \quad \forall c, i, q \tag{4.10}$$

$$\sum_{i} C_{c,i,q_m} \leq 1 \quad \forall c, i, q, m > 1 \tag{4.11}$$

$$C_{c,i,q_m+1} \leq \sum_{j \in \Omega_i} C_{c,j',i,q_m} + C_{c,i,m} \quad \forall c, i \notin \mathscr{A}_c, q, m \leq \tilde{m}_q \tag{4.12}$$

$$C_{c,i,q_m} + \sum_{j' \in \Omega_i} C_{c,j',i,q_m} = C_{c,i,q_{m+1}} + \sum_{j \in \Omega_i} C_{c,i,j,q_m} \quad \forall c, i \notin \mathscr{A}_c, q_m, m \leq \tilde{m}_q \tag{4.13}$$

If crew c leaves node i, crew c cannot come back to node i in a future sub scenario (Equation 4.9). Equation 4.10 ensures that crew c is only allowed to enter node i once, including using node i as an access point. If crew c is in node i in both sub scenario q_m and q_{m+1}, then Equation 4.11 forces crew c to be only in node i during the transition between sub scenarios. Equation 4.12 allows crew c to be in node i during the transition between sub scenario q_m and sub scenario q_{m+1} only if crew c moved into node i during sub scenario q_m or if crew c started sub scenario q_m in node i. To guarantee that crews travel in a continuous path, if crew c starts sub scenario q_m in node i, then Equation 4.13 requires that crew c must either leave node i for some node j during sub scenario q_m or stay in node i until after sub scenario q_{m+1} has started.

Crew Work and Arrival Times

The timing of suppression actions is an important aspect of the suppression decisions. Suppression actions at each node must happen prior to the fire arriving at that node. The work produced at each node can only occur when a crew is actually in that node and must occur before fire arrives at the node.

$$WT_{c,j',i,q_m} \leq t_{q_m} C_{c,j',i,q_m} \quad \forall c, i, j' \in \Omega_i, q, m \tag{4.14}$$

$$WT_{c,i,q_m} \leq t_{q_m} C_{c,i,q_m} \quad \forall c, i, q, m \tag{4.15}$$

$$WT_{c,i,q_m} \leq (\sum_{k=1}^{m} t_{q_m} - a_{c,i}) P_{c,i} \quad \forall c, i \in \mathscr{A}_c, q, m \tag{4.16}$$

$$\sum_{i} \left(WT_{c,i,q_m} \sum_{j \in \Omega_i} WT_{c,i,j,q_m} \right) \leq t_{q_m} \quad \forall c, q, m \in \{1, ..., \tilde{m}_q - 1\} \tag{4.17}$$

A crew may spend up to the entire sub scenario working on a node if they are leaving node j' for node i in sub scenario m (Equation 4.14) or if they started the sub scenario in node i (Equation 4.15 and 4.16). However, the total work they do on all nodes in a single sub scenario must be less than or equal to the amount of time the sub scenario lasts (Equation 4.17).

$$CT_{c,i,q} \geq a'_{c,i} P_{c,i} + \sum_{k=m}^{\tilde{m}_q - 1} WT_{c,i,q_k} \quad \forall c, i \in \mathscr{A}_c, q, m = a_{c,i} \tag{4.18}$$

$$CT_{c,i,q} \geq \left(CT_{c,j',q} + trt_{c,j',i} + \sum_{k=1}^{\tilde{m}_q - 1} WT_{c,j',i,q_m} + WT_{c,i,q_m} \right) - M(1 - \sum_{k=1}^{\tilde{m}_q - 1} C_{c,j',i,q_m}) \quad \forall c, i \notin \mathscr{A}_c, j \in \Omega_i, q \tag{4.19}$$

A crew must finish any work on the access point before they leave it (Equation 4.18). The time that a crew can leave any node that is not an access point is determined by the path the crew took to get to the node and the amount of work the crew did on the node. Equation 4.19 is only binding when crew c leaves node j' for node i and given that, then the time at which crew c can leave node i is the time that crew c left node j' plus any work time spent on node i. The spatial constraints outlined in Section 4.2.2 actually need Equations 4.18 and 4.19 in order to work properly.

$$CT_{c,i,q} \geq \sum_{k=1}^{m-1} t_{q_k} - M \left(1 - \sum_{j \in \Omega_i} C_{c,i,j,q_m} \right) \quad \forall i, j \in \Omega_i, q, m \leq \tilde{m} \tag{4.20}$$

$$CT_{c,i,q} \leq \sum_{k=1}^{m} t_{q_k} + M\left(1 - \sum_{j \in \Omega_i} C_{c,i,j,q_m}\right) \quad \forall i, j \in \Omega_i, q, m \leq \tilde{m} \tag{4.21}$$

The sub scenario during which a crew leaves a node must be connected with the actual time that the crew leaves the node. This condition is enforced by Equations 4.20 and 4.21. Without these constraints, the model will allow crews to work on nodes in sub scenarios when the crew has either left the node already or before the crew gets to the node.

Control Line Capacity

Most models that simulate fireline containment assume that once the amount of fireline produced exceeds the length of the fire perimeter, then the fire is contained, which implicitly implies that fireline always holds. Unfortunately fireline does not always hold. The quality of the fireline is essential to determining if fireline holds or not. If the control line can withstand the intensity of the fire, then the fireline holds. However, if the control line cannot withstand the intensity of the fire, then the fire jumps the control line and the fire is not controlled. The following equations relate crew work times to control line capacity and determine if the control line capacity is sufficient for suppression to be successful.

$$WC_{i,q} \geq CT_{c,i,q} \quad \forall c, i, q \quad \forall i, q \tag{4.22}$$

$$W_{i,q} = \sum_{c} \sum_{k=1}^{\tilde{m}_q - 1} l_{c,i,q_k} \left(\sum_{j' \in \Omega_i} WT_{c,j',i,q_k} + WT_{c,i,q_k}\right) \quad \forall i, q \tag{4.23}$$

$$LC_{i,q} = f_{LI}(W_{i,q}) \quad \forall i, q \tag{4.24}$$

$$LC_{i,q} = \alpha_i W_{i,q} \tag{4.25}$$

If multiple crews are working on a landscape, then multiple crews may end up working on a single node. I designate a work completion time for each node ($WC_{i,q}$), which, at smallest, must equal the time that the last crew c finishes their work on the node i in scenario q (Equation 4.22). Since crews may work at different rates, the work time from all crews needs

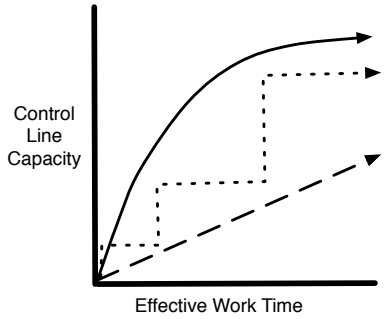

Figure 4.2: Three possible relationships between control line capacity and effective work time.

to be combined and translated into a control line capacity. I chose to combine the work times by adjusting work times for crew productivity (Equation 4.23) instead of modeling an individual rate for each crew.

Crew productivity rates are difficult to quantify. Previous research has determined direct attack and indirect line production rates for different types of crews by fuel type, but does not quantify a relationship between line quality and work time. The most recent update of the standard crew production rates used by the Forest Service was provided by Broyles (2011). Broyles (2011) directly observed fire crews to obtain new estimates of fireline production rates. Nine of the of the thirteen fuel models were assigned a value for the production of fireline in direct attack and indirect attack, including 95% confidence intervals. These production rates and time estimates are only for day shifts; this study did not look at night shift rates. Other research to quantify fireline productions rates include Fried and Gilless (1989) and Hirsch et al. (1998), who used expert option surveys to determine fireline production rates. Recently, Holmes and Calkin (2013) attempted to quantify econometric relationships between fireline production rates with the level of suppression input using data gathered from large wildland fires in the US in 2008. Based on their results, I hypothesize that the relationship between control line capacity and work time will either concave and therefore relatively easy to represent using a linear function, either using a linear transformation or a piecewise function (see Equation 4.24 and Figure 4.2). For testing purposes, I have assumed it takes the form shown in Equation 4.25.

$$LC_{i,q} \geq I_{i,q} - M(1 - Y_{i,q}) \quad \forall i, q \tag{4.26}$$

$$Y_{i,q} \geq \frac{1}{M} W_{i,q} \quad \forall i, q \tag{4.27}$$

$$LC_{i,q} \leq I_{i,q} + M Y_{i,q} \quad \forall i, q \tag{4.28}$$

Equation 4.26 allows suppression to be successful in a node only if the control line capacity is greater than the fireline intensity. I included Equation 4.27 so that if a crew begins working on a node, then they must create enough fireline capacity such that the line holds in all future weather scenarios. This equation could be replaced with Equation 4.28 which will ensure that if the fireline intensity is less than the control line capacity, then the line must hold (even if there is a benefit to allowing the fire to burn through). However, in order to use the safety margin constraints presented in the next section, Equation 4.27 is important.

Safety Constraints

One of the most important functions of any fire manager is to keep crews safe. Unless the fireline intensity is low enough for direct attack to be safe, crews need to have a buffer between themselves and the fire. In this model, the safety buffer is an amount of time between when the crews finish their work on the node and when fire arrives at the node. The safety margin is controlled here by the fireline intensity: the more intense the fire is then the larger the safety margin must be. I hypothesize that a fire manager could come up with a relationship between safety margin and fireline intensity that would be easy to represent with a linear equation. The crew has no control over the fireline intensity. They do, however, have control over the control line capacity. Because Equation 4.27 requires that all fireline built must have a high enough capacity to hold against the highest intensity, line capacity can be used as a proxy for fireline intensity (Equation 4.29 and Figure 4.3).

$$SM_{i,q} = f_{SM}(LC_{i,q}) \quad \forall i, q \tag{4.29}$$

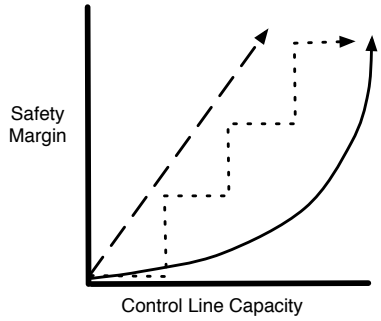

Figure 4.3: Three possible relationships between the fireline intensity and the safety margin between the crew and the fire.

$$SM_{i,q} = sm_i LC_{i,q} \quad \forall i, q \tag{4.30}$$

$$WC_{i,q} + SM_{i,q} \leq F_{i,q} \quad \forall i, q \tag{4.31}$$

For testing, I assume that the function relating safety margin and control line capacity is linear (Equation 4.30). Once the safety margin is determined, Equation 4.31 ensures that crews finish their work within the safety margin required.

Nonanticipativity and Decision Timing

Because the variables determining if control line capacity is sufficient are determined by scenario in this model rather than by sub scenario, the nonanticipativity constraints must use significantly different decision variables here than were used in Chapter 3. The decisions that must be nonanticipative address what the crew does: where they travel and what work they produce during each stage.

$$WT_{c,i,j,q_m} = WT_{c,i,j,q_k} \forall c, i, j, q_m \text{ and } q_k \in \Lambda_p, p \tag{4.32}$$

$$WT_{c,i,q_m} = WT_{c,i,q_k} \forall c, i, j, q_m \text{ and } q_k \in \Lambda_p, p \tag{4.33}$$

$$C_{c,i,j,q_m} = C_{c,i,j,q_k} \forall c, i, j, q_m \text{ and } q_k \in \Lambda_p, p \tag{4.34}$$

$$C_{c,i,q_m} = C_{c,i,q_k} \forall c, i, j, q_m \text{ and } q_k \in \Lambda_p, p \tag{4.35}$$

Equations 4.32 and 4.33 ensure that any work that a crew produces must be nonanticipative and Equations 4.34 and 4.35 ensure that the crew movements are nonanticipative. The work completion times and crew completion times are set by scenario and cannot be nonanticipative without introducing several logic constraints. If there is any slack in the system, the crew work completion times and node work completion times may not be correct. However, a post-solution processing can quickly remove the slack by recalculating completion times based on the amount of time worked, with no loss of optimality.

4.2.3 Objective function

While the fire behavior constraints perform consistently regardless of the objective function, the objective function drives the suppression constraints. Given unlimited suppression resources, there must be a cost to building fireline in the objective function, otherwise the program has no incentive to send crews along the most efficient route. In fact, without a cost to build fireline, the model may send the crew zig-zagging all over the landscape. One solution to this is to simply add the total distance the crew travels to the objective function but weight it very lightly (i.e., use 0.0001). If crews are expensive or scarce, the model is likely to use resources efficiently, but minimizing travel distance can help when resources are not scarce. Also, having line length in the objective function tends to speed up the solution time. Let $LL_{c,q}$ be the distance traveled by crew c in scenario q. Equation 4.36 is a bookkeeping constraint that tracks the total distance traveled by each crew and $LL_{c,q}$ can be included in the objective function.

$$LL_{c,q} = \sum_{i} \sum_{j \in \Omega_i} d_{i,j} C_{c,j',i,q} \quad \forall c, q \tag{4.36}$$

For testing, I assume all fire is harmful and the goal is simply to contain the fire at least cost. Using distance traveled as a proxy for cost, Equation 4.37 reflects minimizing expected area burned at least cost.

$$\text{Min } Z = \sum_{q} \left(\sum_{k \in \Phi_q} \sum_{i} D_{i,q_m} + \sum_{c} 0.0001 LL_{c,q} \right) \tag{4.37}$$

4.3 Results

The results presented in this chapter use the same parameters as the results in Chapter 3, which can be found in Tables 3.2 and 3.1. Because the landscapes are small and the time periods are relatively short, the crews I model are able to travel and produce line quickly, i.e., every minute each crew works they can produce 100 ft of fireline that holds a fire between 250BTU/ft/sec and 400 BTU/ft/sec. For visualization purposes, fireline intensities of 175 BTU/ft/sec, 250 BTU/ft/sec, and 400 BTU/ft/sec correspond roughly to 4-5 ft, 6-7 ft, and 10-12 ft flame lengths, respectively. Because the landscape is composed of flat grass-shrub cells, the crews I model in the test cases are analogous to a fire crew working out of engine and spraying water directly on the flame front. These work rates may be a bit high, however, the crews modeled in this chapter needed to work this fast in order to demonstrate interesting results on the 6x6 landscape. Crew work rates could be adjusted to use the constraints presented in this chapter to model hand crews.

The first set of results (Figures 4.5-4.7) use the weather tree pictured in Figure 4.4. I do not enforce any nonanticipativity constraints in the second stage, although because all three scenarios share a first stage sub scenario the results end up looking like they are nonanticipative. These results are presented to show the suppression model working on several different weather scenarios and some interesting results of optimal solutions. The second set of results (Figures 4.9-4.13) use the weather tree from Figure 4.8 and demonstrate how including nonanticipativity constraints changes the solutions.

Figure 4.4 shows the weather scenarios associated with Figures 4.5, 4.6, and 4.7. Figure 4.5 shows fire behavior in the absence of suppression. The first stage fire behavior is identical for all three scenarios, while the second stage fire behavior varies depending on the weather conditions. Figure 4.6 shows the results when one crew that works very quickly is

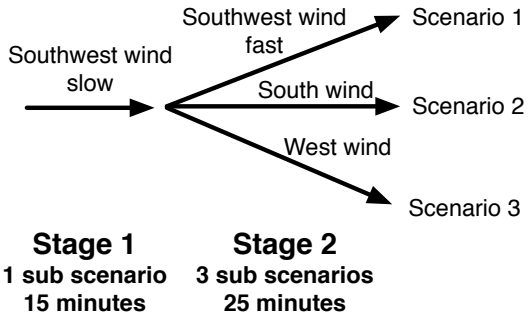

Figure 4.4: The weather tree for the test cases in Figures 4.5=4.7.

allowed on the landscape; this crew can build 100ft of fireline that holds a 400 BTU/ft/sec fire every minute. The crew can work fast enough to finish controlling the fire within the first stage. Since the first stage is identical for all scenarios, the crews take exactly the same actions in all three scenarios.

Figure 4.7 shows the results of one crew working at a slower rate than the crew in Figure 4.6; this crew can build 100ft of fireline that holds a 250 BTU/ft/sec fire every minute. The solution produces unintuitive results. Upon initial examination, the crew travels in a circuitous route that looks to be much less efficient than the route taken in Figure 4.6. However, the crew is forced to cut across the node directly north of the ignition point in order reach the node two rows north of the ignition point in time. Because the node two rows north and one row west of the ignition burns at a lower intensity than the node two rows north and one row east of the ignition, the crew is able to reach the node two rows directly above the ignition more quickly going the circuitous route. Without going the circuitous route, the crew would not reach the node two rows north of the ignition before the safety margin required them to be out of that node and the crew would lose an extra node or two to the fire.

In both Figures 4.6 and 4.7, the crew travels in a continuous fashion leaving from an access point, i.e., the spatial restrictions of the crews are modeled correctly. The crews spend enough time in each node to build a fireline to withstand the intensity of the fire, so line quality is accounted for correctly. The crews leave each node in time for the safety

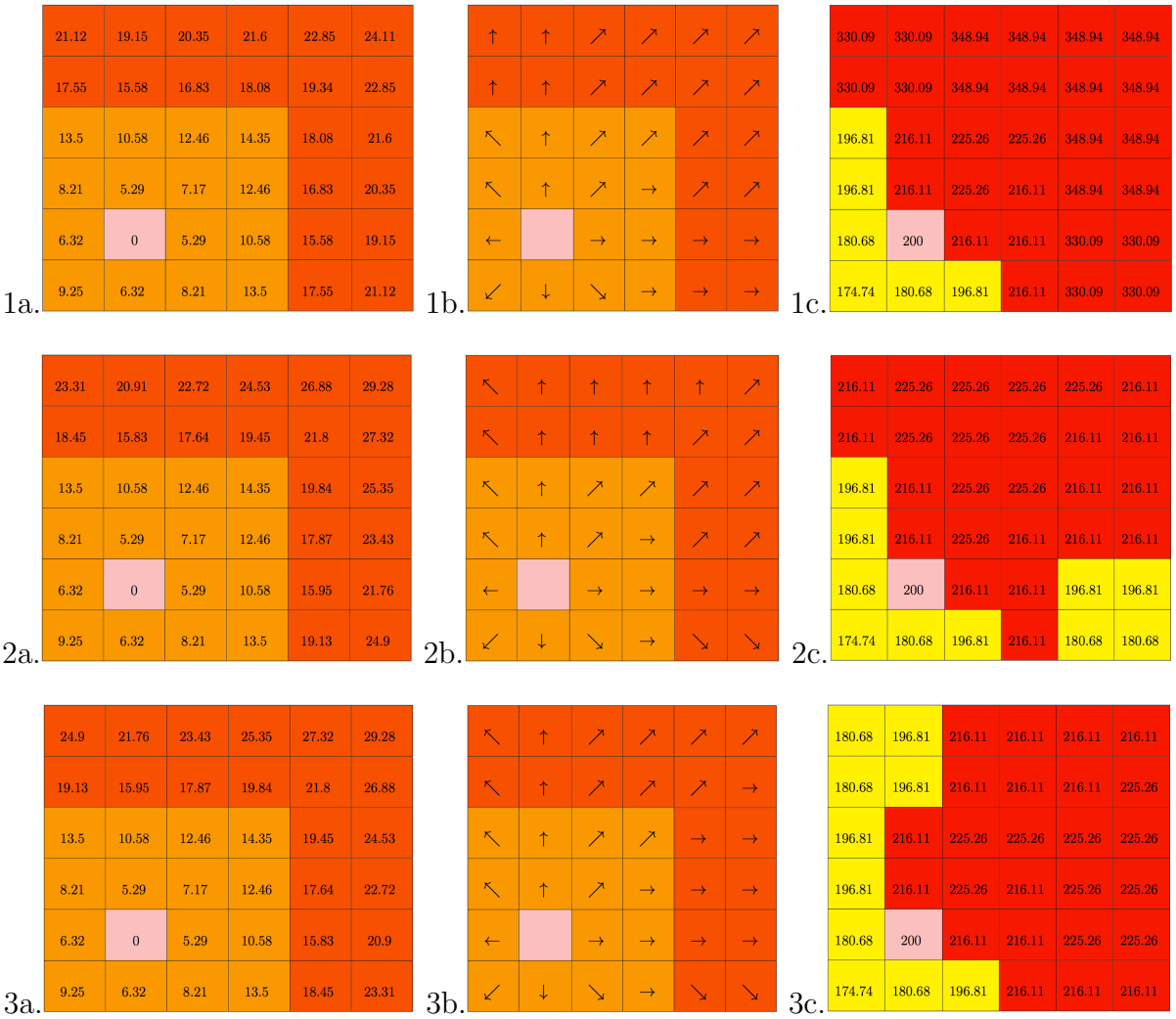

Legend for columns a and b:

- Fire arrived in node during stage one
- Fire arrived in node during stage two
- Fire never arrived in node
- Ignition occurred in node
- Control placed in node during stage one
- Control placed in node during stage two

Legend for column c:

- Fireline intensity under threshold
- Fireline intensity over threshold
- Fire never arrived in node

Figure 4.5: Fire arrival time (a), spread directions (b) and fireline intensities (c) for weather scenarios 1, 2, and 3 using the weather scenario tree shown in Figure 4.4.

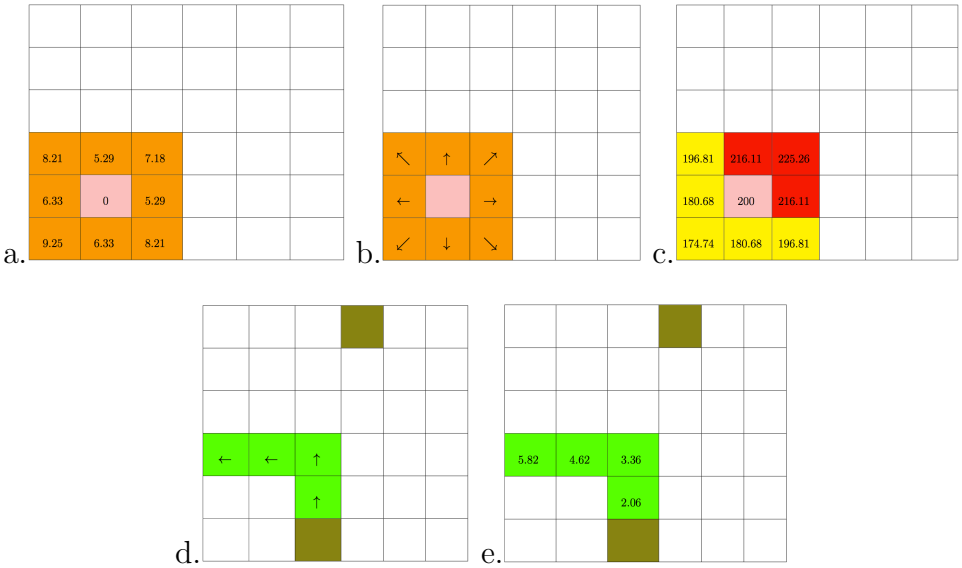

Figure 4.6: Fire arrival time (a), spread directions (b), fireline intensities (c), crew travel paths (d) and crew completion times (e) for weather scenarios 1, 2, and 3 using the weather scenario tree shown in Figure 4.4. The results for all three scenarios are the same.

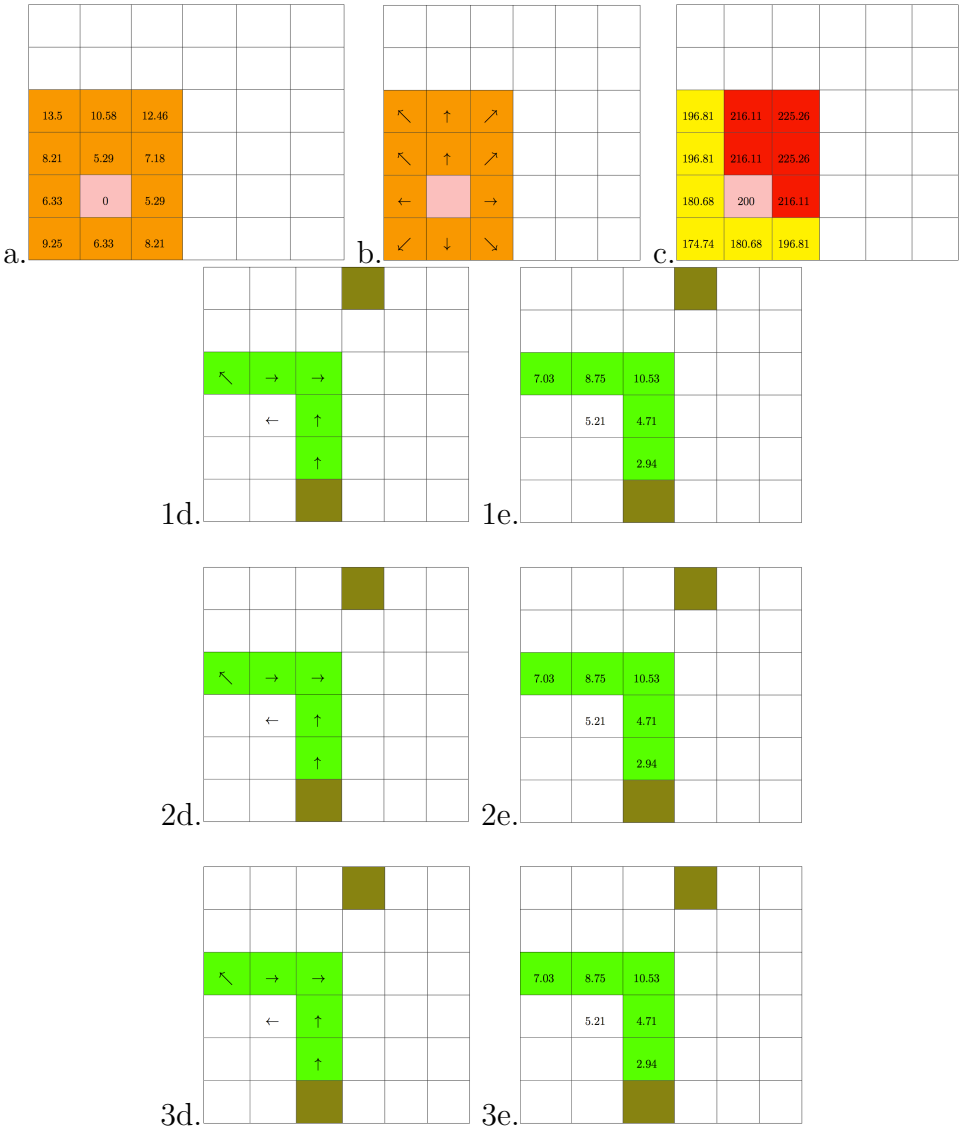

Figure 4.7: Fire arrival time (a), spread directions (b), fireline intensities (c), crew travel paths (d) and crew completion times (e) for weather scenarios 1, 2, and 3 using the weather scenario tree shown in Figure 4.4. Fire arrival times, spread paths, and fireline intensities are the same for all three scenarios and so are only shown once.

margin to be enforced, and so the results are consistent with the safety constraints. In short, these results demonstrate that the suppression constraints are capable of modeling crew tactics. However, when the crew is slowed any further than being able to produce 100 ft of line to withstand a 250 BTU/ft/sec fire per minute, the model has a very difficult time even getting a feasible solution. This issue will be further addressed in Chapter 5.

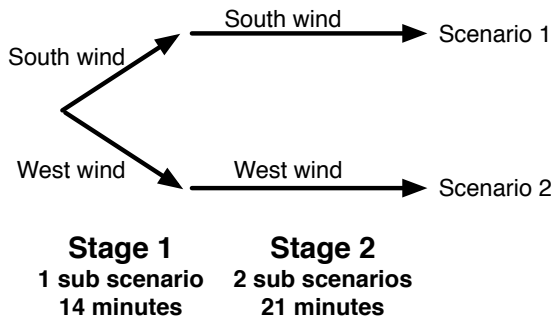

Figure 4.8: The weather tree for the test cases in Figures 4.9-4.13.

Figure 4.8, shows the weather scenarios for Figures 4.9-4.13. This weather scenario is particularly apt for examining nonanticipativity as it features breaks in the scenarios where decisions are to be made. For the decisions to be nonanticipative, the first stage decisions need to be the same and the second stage decisions are recourse decisions. Figure 4.9 shows fire behavior with no suppression. Figure 4.10 shows a case of fast suppression (the crew can produce 100 ft of fireline that holds a fire of 350 BTU/ft/sec) with no nonanticipativity constraints. The crew is able to control the fire within the first stage and follows the same path in both scenarios, but chooses to go in opposite directions in each scenario. When nonanticipativity constraints are added (Figure 4.11), the model forces the crews to work the same route in both scenarios. The solutions shown in Figures 4.10 and 4.11 are alternative optima for the test case which did not enforce nonanticipativity, but the solution in Figure 4.10 is not feasible when anticipativity constraints are added.

In the results shown in Figure 4.12, the weather tree is still shown in Figure 4.8 but the crew has been slowed down a bit; this crew can produce 100 ft of fireline that holds a fire with a fireline intensity of 320 BTU/ft/sec. The solution again shows the crew traveling

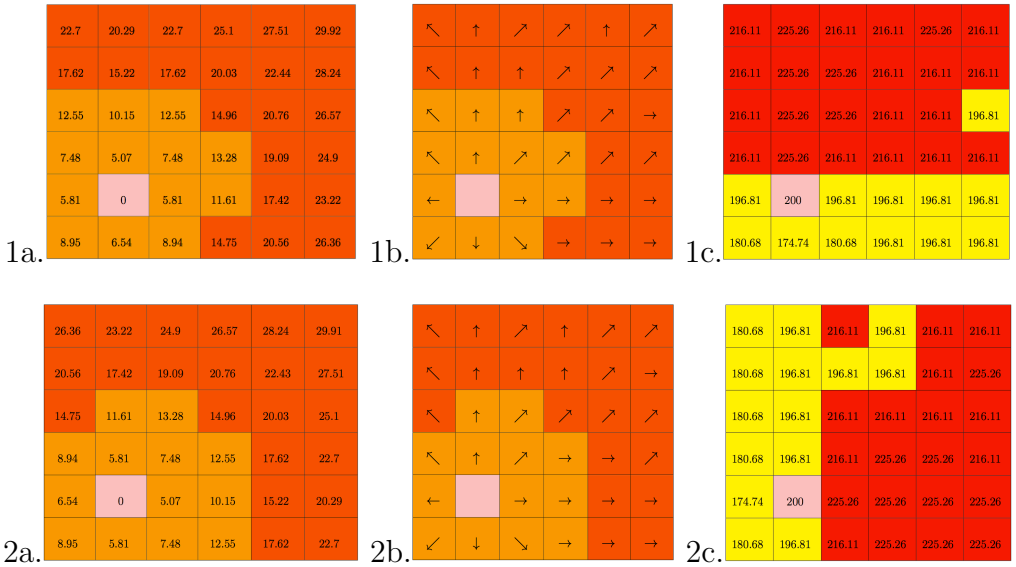

Legend for columns a and b:

- Fire arrived in node during stage one
- Fire arrived in node during stage two
- Fire never arrived in node
- Ignition occurred in node
- Control placed in node during stage one
- Control placed in node during stage two

Legend for column c:

- Fireline intensity under threshold
- Fireline intensity over threshold
- Fire never arrived in node

Figure 4.9: Fire arrival time (a), spread directions (b), fireline intensities (c), crew travel paths (d) and crew completion times (e) for weather scenarios 1 and 2 using the weather scenario tree shown in Figure 4.8.

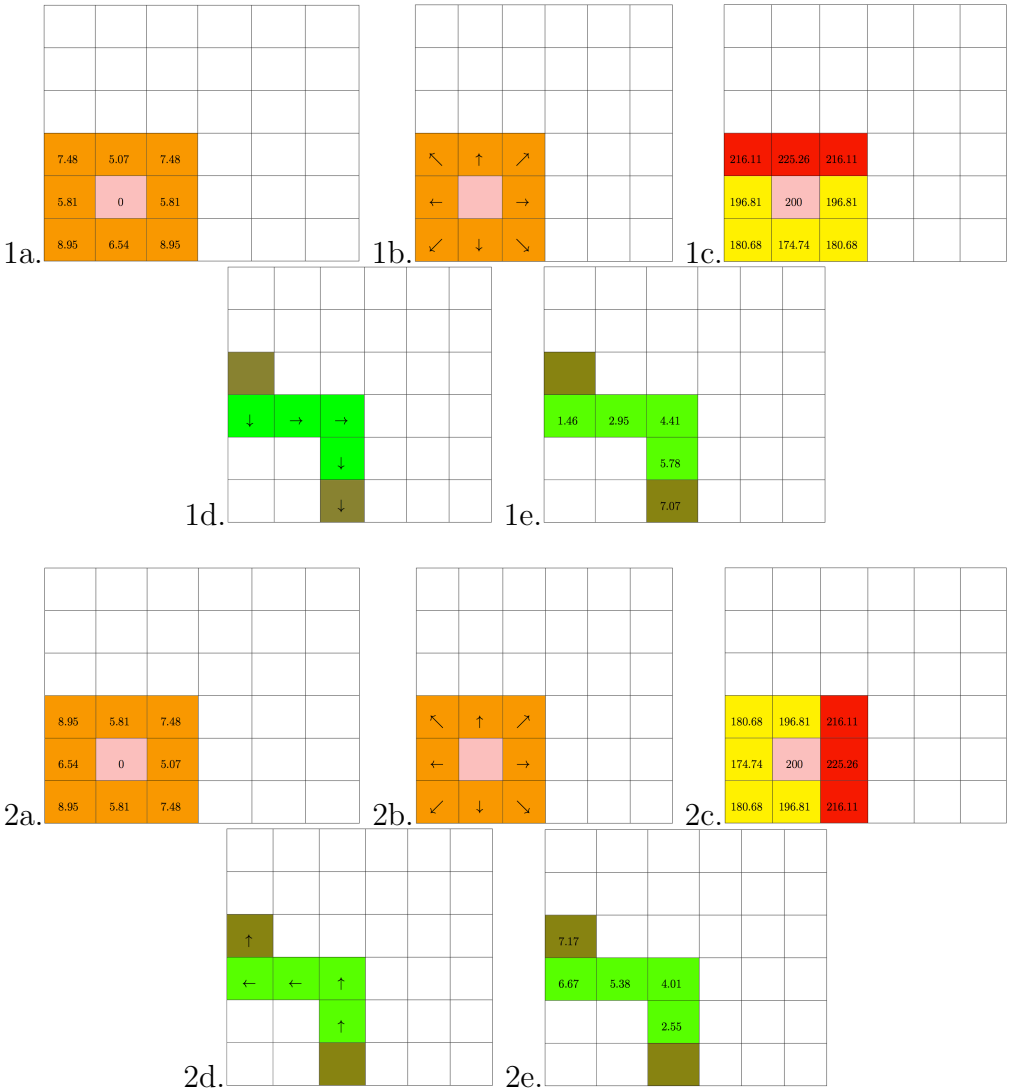

Legend:

- Igntion occurred in node
- Fire arrived during stage one
- Access point
- Fireline intensity under threshold
- Fireline intensity over threshold
- Crew arrived during stage one

Figure 4.10: Fire arrival time (a), spread directions (b), fireline intensities (c), crew travel paths (d) and crew completion times (e) for weather scenarios 1 and 2 using the weather scenario tree shown in Figure 4.8.

in a circuitous route in order to reach a node in time. Like in Figure 4.10, the crews go in opposite directions to reach the nodes in time. When nonanticipativity constraints are added to the model (Figure 4.13), the crew can no longer just take the same path as it did in Figure 4.11. Instead, the crew must take a longer path in order to satisfy nonanticipativity and contain the fire. The new suppression activities take more work for the crew and lose an extra seven nodes to the fire (as compared to the anticipative case), but it contains the fire and keeps the crews safe for both scenarios. The only difference between the two crew paths is the crew work completion time on the final node. This is just slack: the crew actually does the same amount of work on that node in both scenarios but is able to stay longer in the node in the first scenario.

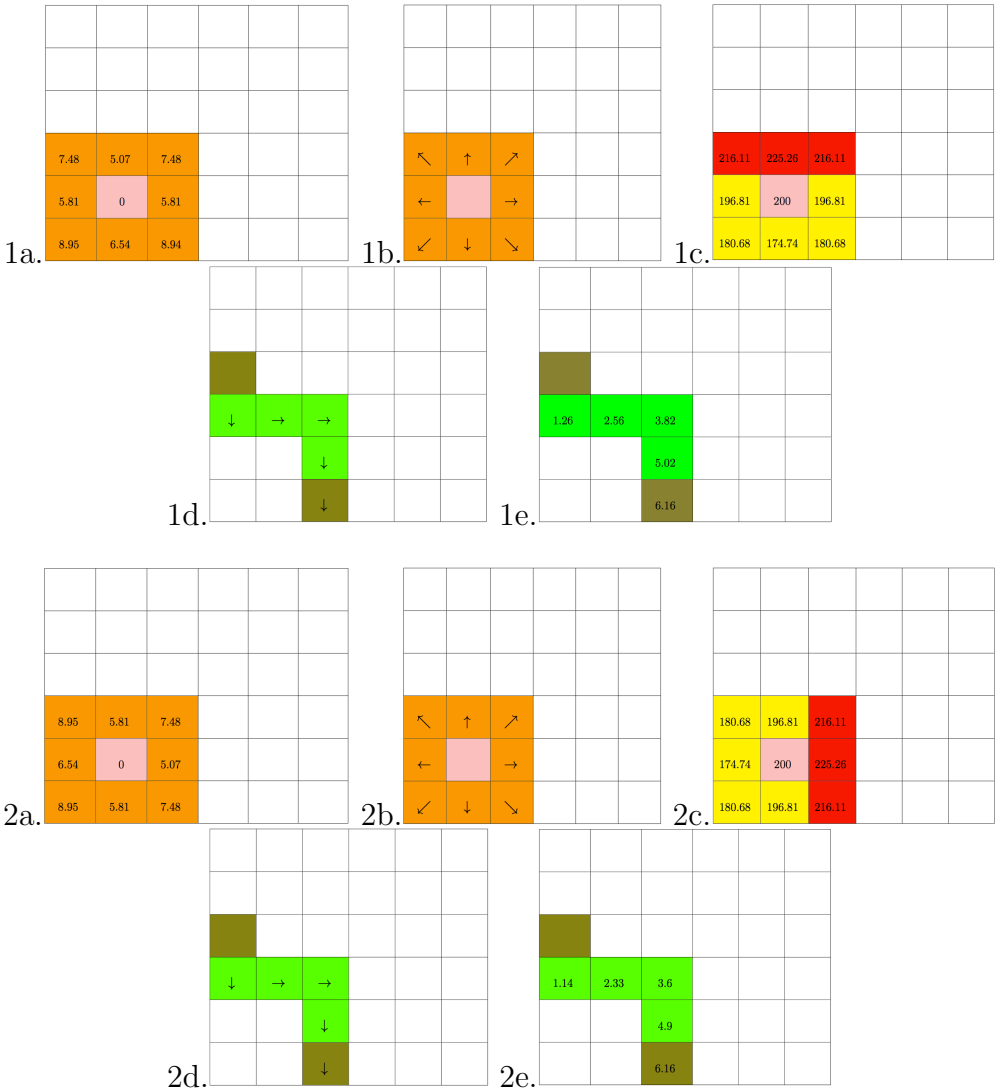

Legend:

- Igntion occurred in node
- Fire arrived during stage one
- Access point
- Fireline intensity under threshold
- Fireline intensity over threshold
- Crew arrived during stage one

Figure 4.11: Fire arrival time (a), spread directions (b), fireline intensities (c), crew travel paths (d) and crew completion times (e) for weather scenarios 1 and 2 using the weather scenario tree shown in Figure 4.8.

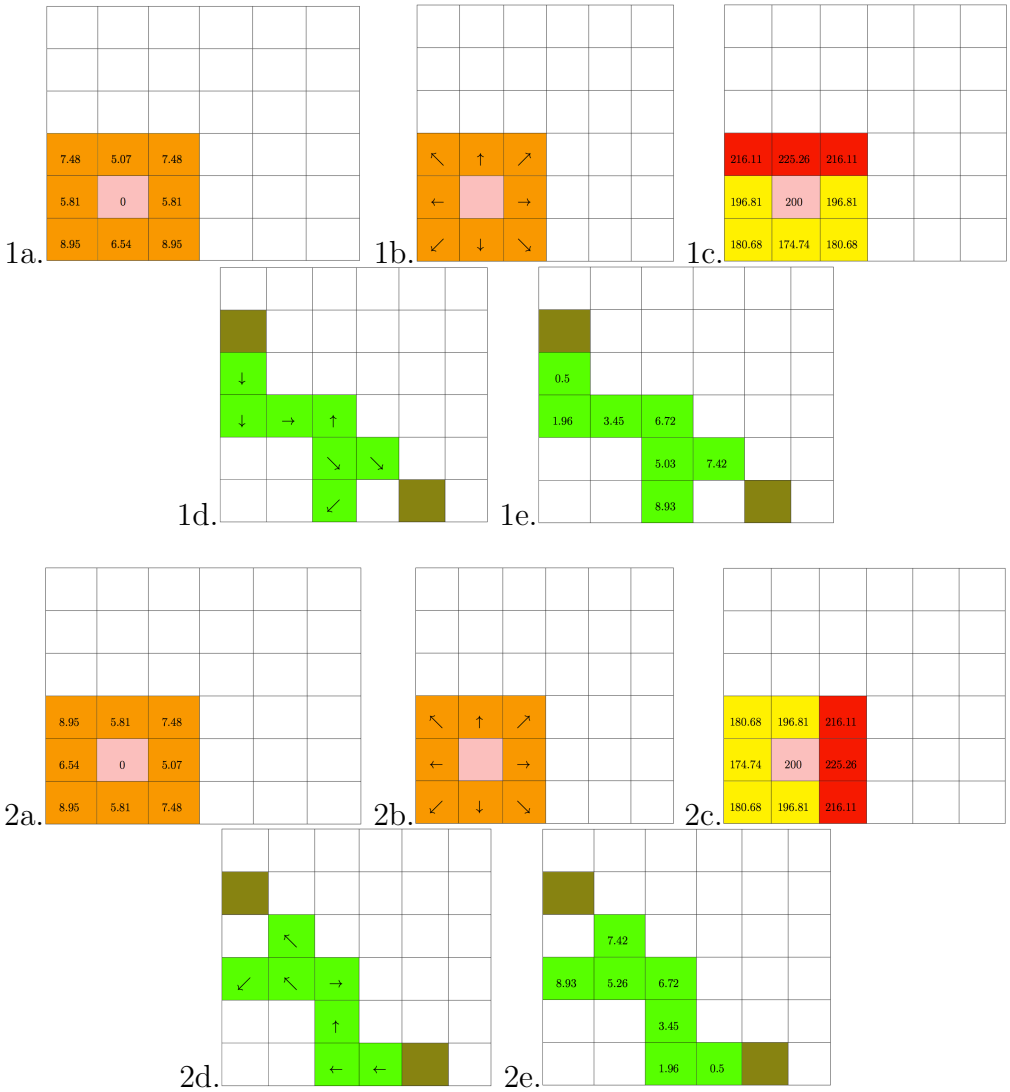

Legend:

- Igntion occurred in node
- Fire arrived during stage one
- Access point
- Fireline intensity under threshold
- Fireline intensity over threshold
- Crew arrived during stage one

Figure 4.12: Fire arrival time (a), spread directions (b), fireline intensities (c), crew travel paths (d) and crew completion times (e) for weather scenarios 1 and 2 using the weather scenario tree shown in Figure 4.8.

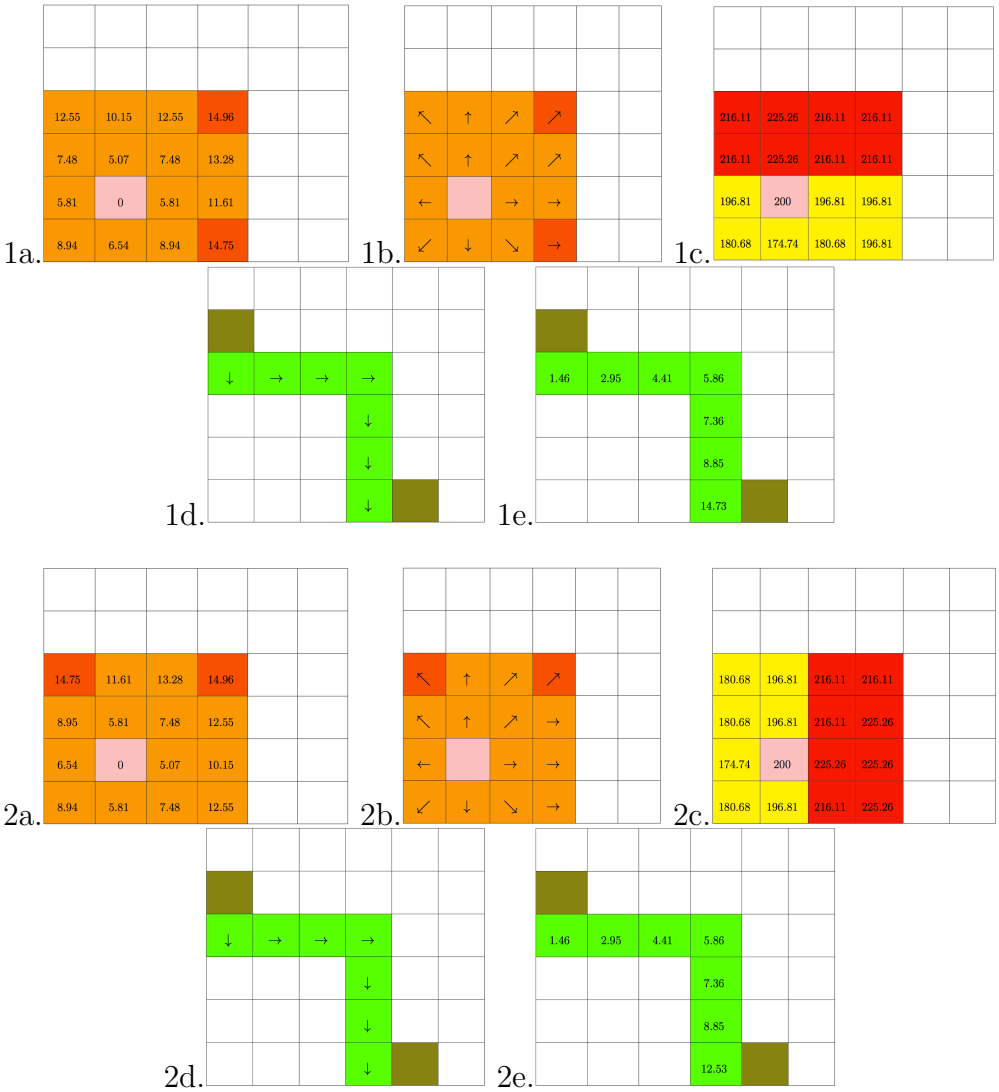

Legend:

- Igntion occurred in node
- Fire arrived during stage one
- Access point
- Fireline intensity under threshold
- Fireline intensity over threshold
- Crew arrived during stage one

Figure 4.13: Fire arrival time (a), spread directions (b), fireline intensities (c), crew travel paths (d) and crew completion times (e) for weather scenarios 1 and 2 using the weather scenario tree shown in Figure 4.8.

4.4 Discussion

The stochastic control network presented in this chapter incorporates detailed suppression decisions with stochastic fire behavior to create a framework from which fire suppression decisions can be modeled. Spatial restrictions on crew movements were enforced as were safety restrictions for fire crews. Fireline quality was accounted for both using variable crew productivity and constraints to determine if the control line capacity was sufficient for the line to hold. The solutions to the model provide a map of the optimal path for each crew and determine the amount of work that needs to be done on each node. The control network provides much more useful information to a manager than the control points did. Incorporating explicit nonanticipativity constraints in the model produces solutions that are both efficient and robust to weather uncertainties.

There are still many ways in which this suppression model could be improved. For example, if fireline does not stop a fire, it may still slow the fire down. A delay time could be incorporated into the fire behavior for fires that cross a fireline. Another example is cost. In the results presented here, I used line length as a proxy for costs. However, explicit costs could be added; both fixed costs for calling a crew and the variable costs of the work the crew produces could be added to the model.

One of the major weakness of the model is solution time. Even on some of the small 6x6 landscapes, CPLEX had trouble finding feasible solutions. For example, one model run of a 6x6 landscape with three weather scenarios and two stages ran for over 12 hours on a workstation with 32 GB of RAM without finding a single feasible solution. In order for the program to be used operationally, the landscape needs to be scaled up and the solution times need to be fast. Scaling and solution time issues are addressed in Chapter 5.

5 Future Work and Summary of Contributions

While the stochastic, spatially explicit, dynamic fire behavior model and integrated control network developed in this dissertation provide a solid basis for further work on the optimization of suppression resource assignments, much work remains unfinished. Weather scenario tree generation, objective function testing, simulation of additional fire behavior and suppression actions, and model size issues and solution times are all discussed below, as they are some of the issues most integral to using this model operationally. The final section of this chapter summarizes the major contributions of this dissertation.

Weather Scenario Tree Generation

Constructing statistically sound probabilistic weather scenarios based on accurate weather forecasting is a complex and challenging task, which is beyond the scope of this dissertation. However, as the results in Figures 3.26 and 3.27 demonstrated, fire weather drives stochastic fire spread patterns and fire suppression decisions. Synthesizing future weather forecasts into weather trees to guide suppression decisions requires a significant amount of work that may rely on support from expertise beyond the field of fire behavior and operations research.

Objective Function Testing

The test cases in this dissertation were focused on lowering total expected area burned or lowering the expected area burned at a harmful fire intensity and improving the expected area burned at a beneficial fire intensity. However, fire management is a risk adverse field (Canton-Thompson et al. 2008). Future research may investigate objectives to minimize the fire damage caused by the worst case scenario. One possible method of minimizing the damage from the worst case scenario is to use chance constraints in the model, which could be used to optimize suppression decisions by maximizing the percentage of scenarios in which the fire is controlled at a certain time or size limit. Because there are so many possible

objective functions, examining which objective functions best reflect current fire policy and management is crucial.

The objective function is not only the key component of modeling different suppression policies; it can also influence the computer solution times. In general, objective functions focusing on minimizing the total expected area burned tended to run faster than those minimizing the expected area burned at a harmful fireline intensity level, and these both ran much faster than a model considering both the beneficial and detrimental effects of fire. One reason for the differences in solution times may be because suppression actions can impact fire behavior. For example, if a node receives fire from the south this fire may be detrimental, but if it receives fire from the southeast it becomes beneficial due to lower intensity of the fire. When suppression changes the fire spread path to come from the southeast rather than from north it improves the objective function value. However, the same suppression action may cause fire in a different cell to change from beneficial to harmful. Due to these tradeoffs, the multiple objective problem is more difficult to solve than the simpler problem of containment only.

Fire Behavior and Suppression Actions

The model presented in this study is the first instance where spatially explicit fire behavior (beyond fire arrival time) is modeled in a mixed integer program. However, the current model does not capture all fire behavior that is important to fire managers. For example, reburn and spotfires can both dramatically affect suppression actions, but those behaviors are not built in this model. Chapter 4 is the first mixed integer program to simulate crew actions that account for the spatial and safety restrictions on the crews and line quality. The current system does not model helicopters or air tankers, although both of those are commonly used in fire suppression. Including all the possible suppression resources is an important step towards integrated aerial and group fire suppression; however, it will require a significant amount of future work.

Size Issues and Solution Times

Problem size and model solution times are challenging problems that are intrinsically linked in this model. As landscapes scale up, the model size increases exponentially. It is a challenge to run the deterministic fire behavior model for a 20x20 cell landscape. Based on the test cases I examined, if CPLEX is given a feasible solution from which to start, the optimization process often speeds up. For example, CPLEX has run for three weeks without finding a feasible solution for some problems, but when provided with a feasible or near feasible (but not optimal) start, the same problem ran to optimality in less than five minutes. I developed three pre-processing procedures that could potentially help find feasible starts to speed up the solution process using CPLEX.

The first method for finding near feasible mixed integer program starts is an iterative process of running the model with no suppression on a small landscape, then using the values from that optimal solution as a mixed integer program start for a landscape that was just one row (or column) larger. The second method was also iterative. For this method, the landscape was sliced up into smaller sub-landscapes. An example is shown in Figure 5.1, where a 21x21 landscape is divided up into sub-landscapes that are each 5x5 cells, with the edge cells of each landscape overlapping with their neighbors. The model (with no suppression) was run for the sub-landscape that contained the initial ignition. The sub-landscapes that share an edge with the first landscape were then parameterized by assuming that the fire arrival times of their shared edges could be assigned using the solution from the first landscape. The model was run iteratively by adding new sub-landscapes until solution values for the whole landscape had been determined. These solution values were organized to create a starting solution for the entire landscape. While the solution was not always feasible due to minimum travel time spread paths that were not accounted for at the edges of the landscape, it was always close to feasible and could be used as the starting point for the CPLEX run on the entire landscape. The fewer sub-landscapes created, the more likely the starting solution will be a true feasible solution.

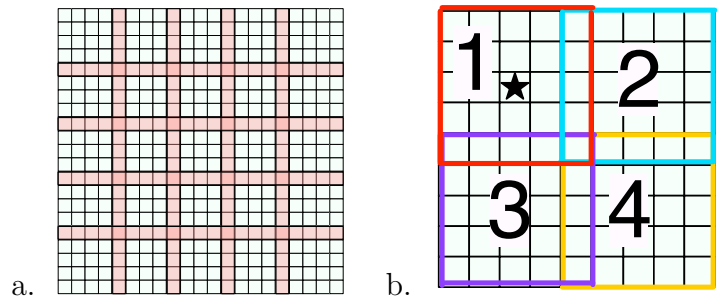

Figure 5.1: (a) A 21x21 landscape divided up in to 25 smaller (5x5) overlapping landscapes. The pink cells are in more than one of the smaller sub landscapes. (b) An example of an ignition point (the star) in a landscape and a possible order to run the smaller landscapes.

Both of these iterative processes created near feasible starts, but neither guaranteed a feasible start. A simulation program could be built to determine a true feasible start with no suppression by first determining the fire arrival times of the nodes directly touching the ignition point, then moving out one row and one column to determine the next set of arrival times and so forth. The largest landscape I was able to run using the stochastic fire behavior model from Chapter 3 was a 17x17 cell heterogeneous landscape from the Black Hills of South Dakota, with a deterministic weather tree (only one scenario) that had two sub scenarios. The fire spread paths from this run are shown in Figure 5.2. If the standard 30m by 30m raster cells are used, a 17x17 landscape covers 900m^2 (64 acres). The fire spread in this landscape was first estimated using the iterative procedure demonstrated in Figure 5.1.

Adding the decisions that construct a control network into the fire behavior model significant increased the model complexity. This model could not be solved for the 6x6 landscape with the control network in place and the weather tree shown in Figure 4.8 without a near feasible start. I developed the following heuristic to address this solution problem: I examined the landscape, found what I believed to be a good control point solution and hardwired it into the program (i.e., I manually fixed the values for $Y_{i,q}$ using bounds). With the control solution set, the program ran to optimality in a few minutes. I then used that optimal solution as an mixed integer program start and the unconstrained full problem solved within minutes. This only worked when no recourse decisions were necessary.

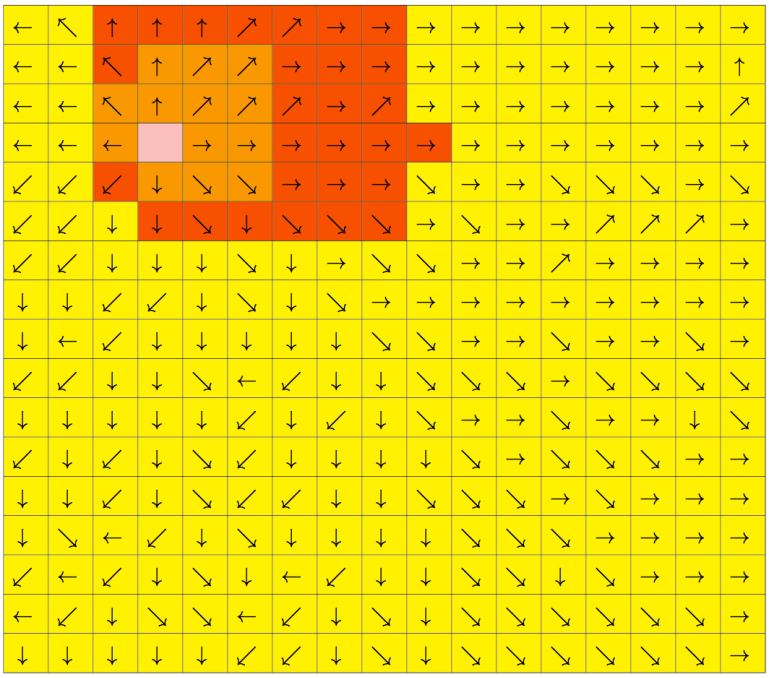

Figure 5.2: The fire spread paths from largest landscape I was able to run using the stochastic fire spread model presented in Chapter 3. The lighter orange cells indicate fire arrived in the first stage, the darker orange cells indicate that fire arrived in the second stage, and yellow cells indicated fire arrived after the end of the planning horizon.

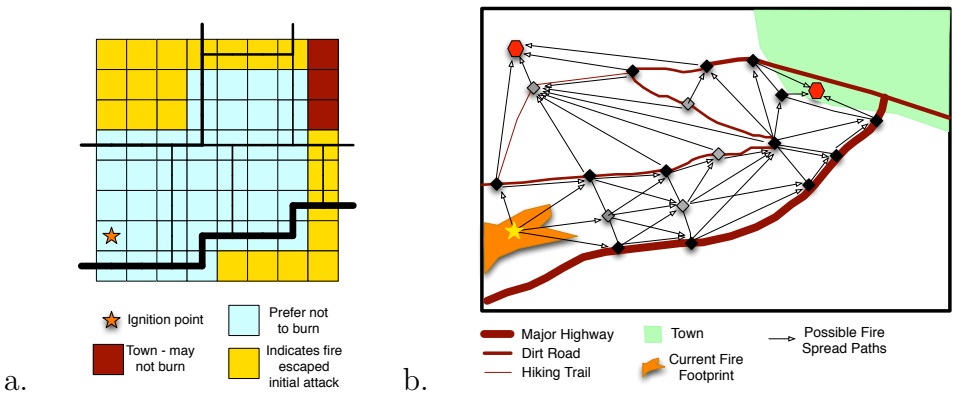

Figure 5.3: a)An example of a landscape where crew paths have been reduced to the black lines connecting nodes. b) A possible simplification of the landscape using a vector landscape instead of a raster landscape.

Preprocessing the landscape to limit crew paths is another promising alternative to speed up solution times. For example, Figure 5.3a shows an example of a landscape where the crew paths are limited to the black lines. The thicker the line, the less work needed for the path to hold as a fireline. Having these predetermined crew paths would greatly reduce model complexity and size and is likely to better represent possible fire crew movements.

Another possibility for scaling the model up is to move from a raster view of the landscape to a vector view. An example is shown in Figure 5.3b. However, the vector landscape provides unique fire behavior modeling challenges, as MTT paths may not be well represented.

Summary of Completed Work

The models presented in this dissertation provide a new framework for integrating spatially explicit, stochastic, dynamic fire behavior with a control network in order to optimize fire suppression decisions. The deterministic mixed integer programming model presented here integrated explicitly spatial fire behavior with suppression actions into a mathematical programming framework and provided a basis for the stochastic fire behavior model. Fire behavior simulated by the deterministic model included fire arrival times and fireline intensities at each node and the minimum travel time path by which fire reached the node. The fire behavior dynamically interacted with simple suppression decisions of where to place control points on the landscape. The test cases for the deterministic model provided examples of spatially explicit fire behavior and corresponding optimal suppression placement for a variety of suppression levels.

A stochastic mixed integer program represents a substantial extension and improvement on the deterministic model. The stochastic model allowed fire behavior to react to weather changes and weather uncertainty, both of which were represented using probabilistic weather decision trees. Constraints were included that characterized fire as ecologically beneficial or harmful based upon the fireline intensity. Several alternative policy objectives were modeled in the test cases, including minimizing the total expected area burned, minimizing the

expected area burned at an ecologically harmful fireline intensity, maximizing the expected area burned at an ecologically beneficial fireline intensity, and minimizing expected fireline production. Explicit nonanticipativity constraints are included to make sure the model produced suppression decisions that accounted for uncertainty in weather forecasts. Recourse decisions allowed the model to create optimal suppression decisions for each possible weather scenario that followed up the robust first stage suppression actions after the outcome of the weather uncertainty was determined.

Detailed fire control networks were incorporated into the stochastic mixed integer fire growth and behavior program to model more realistic suppression decisions. These constraints accounted for fire crew spatial restrictions; for example, a crew's travel path was required to be continuous. Crew safety was also addressed; crews had to keep a safety buffer zone between themselves and the fire. Fireline quality was accounted for by calculating the control line capacity. Crew production rates can be varied to allow the model the flexibility to fit work assignments to the predicted fire behavior.

There is still much work to be done before this model can be used operationally. Size and solution time issues, the generation of weather decision trees, testing of objective functions, and adding additional fire behavior and suppression options all provide rich and difficult problems for future research to address. Despite these issues, the model presented in this dissertation does integrate stochastic, spatially explicit, dynamic fire behavior with realistic optimal suppression decisions. Hopefully resources exist to allow researchers to continue working on the important task of providing fire managers with improved decision support tools which allow tradeoffs of different policy objectives and suppression strategies to be examined.

References

M.E. Alexander. Estimating the length-to-breadth ratio of elliptical forest fire patterns. In *Proceedings of the Eighth Conference on Fire and Forest Meteorology*, pages 287–304, Bethesda, MD, 1985. Society of American Foresters.

A. Alexandridis, L. Russo, D. Vakalis, G.V. Bafas, and C.I. Siettos. Wildland fire spread modelling using cellular automata: evlolution n large-scale spatially heterogeneous environments under fire suppression tactics. *International Journal of Wildland Fire*, 20: 633–647, 2011.

Patricia L. Andrews. Behaveplus fire modeling system: past, present, and future. In *Proceedings of 7th Symposium on Fire and Forest Meteorology*. American Meteorological Society, 23-25 October 2007.

John R. Birge and Francois Louveaux. *Introduction to Stochastic Programming*. Springer, 1997.

Den Boychuk, W. John Braun, Reg J. Kelperger, Zinovi L. Krougly, and David A. Stanford. A stochastic forest fire growth model. *Environmental and Ecological Statistics*, 16:133–151, 2009.

George Broyles. Fireline production rates. Technical Report 5100-Fire Management, 1151 1805-SDTDC, US Department of Agriculture Forest Service, April 2011.

David E Calkin, Mark A. Finney, Alan A. Agar, Matthwe P. Thompson, and Krista M. Gerbert. Progress towards and barriers to implementation of a risk framework for us federal wild land fire policy and decision making. *Forest Policy and Economics*, 13:378–389, 2011.

Janie Canton-Thompson, Krista M. Gebert, Brooke Thompson, Greg Jones, David Calkin, and Geoff Donovan. External human factors in incident management team decisionmaking and their effect on large fire suppression expenditures. *Journal of Forestry*, pages 416–424, December 2008.

Joseph Y.J. Chow and Amelia C. Regan. Resource location and relocation models with rolling horizon forecasting for wildland fire planning. *Information Systems and Operational Research*, 49(1):31–43, February 2011.

George B. Dantzig. Linear programming. *Operations Research*, 50(1):42–47, January-February 2002.

Geoffrey H. Donovan and Douglas B. Rideout. An integer programming model to optimize resource allocation for wildfire containment. *Forest Science*, 49(2):331–335, 2003.

Mark A. Finney. Fire growth using minimum travel time methods. *Canadian Journal of Forest Research*, 32:1420–1424, 2002.

Mark A. Finney. Farsite: Fire area simulator - model development and evaluation. *USDA Forest Service Research Paper RMRS-RP-4 Revised*, February 2004.

Mark A. Finney. An overview of flammap fire modeling capabilities. *USDA Forest Service Proceedings RMRS-P-41*, 2006.

Mark A. Finney, Isaac C. Grenfell, Charles W. McHugh, Robert C. Seli, Diane Trethewey, Richard D. Stratton, and Stuart Brittain. A method for ensemble wildland fire simulation. *Environ Model Assess*, 16:153–167, 2011.

Jeremy S. Fried and Burton D. Fried. Simulating wildfire containment with realistic tactics. *Forest Science*, 42(3):267–281, 1996.

Jeremy S. Fried and Burton D. Fried. A foundation for initial attack simulation: The fried and fried fire containment. *Fire Management Today*, 70(2):44–47, 2010.

Jeremy S. Fried and J. Keith Gilless. Expert opinion estimation of fireline production rates. *Forest Science*, 35(3):870–877, September 1989.

Robert G. Haight and Jeremy S. Fried. Deploying wild land fire suppression resources with a scenario-based standard response model. *Information Systems and Operational Research*, 45(1):31–39, 2007.

Lisa Haven, T. Parkin Hunter, and Theodore G. Storey. Production rates for crews using hand tools on firelines. Technical Report PSW-62, US Department of Agriculture Forest Service, Pacific Southwest Forest and Range Experiment Station, December 1982.

Kelvin G. Hirsch, Paul N. Corey, and David L. Martell. Using expert judgment to model initial attack fire crew effectiveness. *Forest Science*, 44(4):539–549, 1998.

M. J. Hodgson and R. G. Newstead. Location-allocation models for one-strike initial attack of forest fires by airtankers. *Canadian Journal of Forest Research*, 8(2):145–154, June 1978.

John Hof, Philip N. Omi, Michael Bevers, and Richard D. Laven. A timing- oriented approach to spatial allocation of fire management effort. *Forest Science*, 46(3):442–451, 2000 2000.

Thomas P. Holmes and David E. Calkin. Econometric analysis of fire suppression production functions for large wildland fires. *International Journal of Wildland Fire*, 22:246–255, 2013.

Baisravan HomChaudhuri, Manish Kumar, and Kelly Cohen. Optimal fireline generation for wildfire fighting in uncertain and heterogeneous environment. In *2010 American Control Conference*, June 30-July 02 2010.

Xiaolin Hu and Lewis Ntaimo. Integrated simulation and optimization for wildfire containmentl. *ACM Transactions on Modeling and Computer Simulation*, 19(4), 2009.

Andrew G. Kirsch and Douglas B. Rideout. Optimizing initial attack effectiveness by uisng performance measures. In *Systems Analysis in Forest Resources: Proceedings of the 2003 Symposium*. USDA Forest Service, October 7-9 2003.

P.H. Kourtz and W.G. O'Regan. A model for a small forest fire ... to simulate burned and burning areas for use in a detection model. *Forest Science*, 17(2):163–169, 1971.

Jan Mandel, Lynn S. Bennethum, Jonathan D. Beezley, Janice L. Coen, Craig C. Douglas, Minjeong Kim, and Anthony Vodacek. A wildland fire model with data assimilation. *University of Colorado at Denver and Health Sciences Center: Center for Computational Mathematics*, Report No 233, 2006.

Lewis Ntaimo, Bernard P. Seigler, Maria J. Vasconcelos, and Bithika Khargharia. Forest fire spread and suppression in devs. *Simulation: Transactions of the Society for Modeling and Simulation International*, 80(10):479–500, 2004.

Lewis Ntaimo, Julian A. Gallego-Arrubla, Jianbang Gan, Curt Stripling, Joshua Young, and Thomas Spencer. A simulation and stochastic integer programming approach to wildfire initial attack planning. *Forest Science*, 59(1):105–117, 2013.

William G. O'Regan, Peter Kourtz, and Shirley Nozaki. Bias in the contagion analog to fire spread. *Forest Science*, 22(1):61–68, 1976.

George M. Parks. Development and application of a model for suppression of forest fires. *Management Science*, 10(4):760–766, 1964.

Richard C. Rothermel. A mathematical model for predicting fire spread in wildland fuels. Research Paper INT-115, US Department of Agriculture Forest Servcie, Intermountain Forest and Range Experiment Station, January 1972.

Joe H. Scott and Robert E. Burgan. Standard fire behavior fuel models: A comprehensive set for use with rothermel's surface fire spread model. General Technical Report RMRS-GTR-153, United States Department of Agriculture, Forest Service, Rocky Mountain Research Station, Fort Collins, CO, June 2005.

US GAO. Emerging issues highlight the need to address persistent management challenges. Technical Report GAO-09-443T, United States Government Accountability Office, Washington, DC, 2009a.

US GAO. Federal agencies have taken important steps forward, but additional, strategic action is needed to capitalize on those steps. Technical Report GAO-09-887, United States Government Accountability Office, Washington, DC, 2009b.

Yu Wei, Douglas B. Rideout, and Thomas B. Hall. Toward efficient management of large fires: A mixed integer programming model and two interative approaches. *Forest Science*, 57(5):435–447, October 2011.

Mark Wiitala. A dynamic programming approach to determining optimal forest wildfire initial attack responses. Technical Report PSW-GTR-173, USDA Forest Service, 1999.